# *MSH2*, APOPTOSIS, AND CARCINOGENESIS

**Neil John Toft**

**Submitted for the degree of Doctor of Medicine**

**The University of Edinburgh**

**1998**

# CONTENTS

## DECLARATION

I declare that this thesis and the work contained in it is all my own, except where specifically acknowledged.

Neil John Toft

1998

# ACKNOWLEDGEMENTS

I wish to thank the Faculty of Medicine for awarding me the Leckie-Mactier Research Fellowship to allow me to study for an MD; to Professor Andrew Wyllie for a post in the Department of Pathology and for his enthusiasm and help over the two years; and Dr Mark Arends and Dr Alan Clarke for their guidance, knowledge, and encouragement throughout. I am also grateful to Hein te Riele for supplying the *MSH2*-targeted mice and plasmid pHA224; Doug Winton for his help with the *Dlb-1* assay and counting the villi; Geoff Margison for supplying Benzylguanine and assaying AGT activity; Malcolm Stevens for supplying Temozolomide; Jennifer Doig and John Verth for their help with the mouse tails and looking after the numerous mouse colonies; Andrea Leitch and Sarah Howie for performing the immunophenotyping; Melanie McMillan for staining so many tissue sections; John Quinn for arranging the automatic sequencing; and the Medical Statistics Department for their help with calculating the log rank test statistics. The comparative genomic hybridisation was kindly performed by Lucy Curtis. Finally, I am particularly indebted to all those other people who made life enjoyable in the face of disasters in the laboratory.

# ABBREVIATIONS

| | |
|---|---|
| AGT | $O^6$-Alkylguanine-DNA-alkyltransferase |
| *APC* | Adenomatous Polyposis Coli |
| BeG | $O^6$-Benzylguanine |
| bp | base pairs |
| CGH | Comparative Genomic Hybridisation |
| DDW | Deionised Distilled Water |
| *Dlb-1* | *Dolichos biflorus*-1 |
| DMSO | Dimethyl Sulfoxide |
| FAP | Familial Adenomatous Polyposis |
| H&E | Haematoxylin and Eosin |
| HNPCC | Hereditary Nonpolyposis Colorectal Cancer |
| i.p. | intra-peritoneal |
| *Min* | Multiple intestinal neoplasia |
| *MLH1* | *Mut L* Homologue 1 |
| MMR | Mismatch Repair |
| MNNG | N-methyl-N'-nitro-N-nitrosoguanidine |
| *MSH2* | *Mut S* Homologue 2 |
| *MSH2* +/+ | Wild-type for *MSH2* |
| *MSH2* +/- | Heterozygous for *MSH2* |
| *MSH2* -/- | Homozygous null for *MSH2* |
| *p53* +/+ | Wild-type for *p53* |
| *p53* +/- | Heterozygous for *p53* |
| *p53* -/- | Homozygous null for *p53* |
| PBS | Phosphate Buffered Saline |
| PCR | Polymerase Chain Reaction |
| $RER^+$ | Replication Error Positive |
| sem | standard error of the mean |
| TBE | Tris/Borate/EDTA |
| TE | Tris/EDTA |

# ABSTRACT

**Epidemiological studies have suggested that at least 15% of colorectal cancers occur in dominantly inherited patterns. Hereditary Nonpolyposis Colorectal Cancer (HNPCC) is an autosomal dominant disorder characterised by the early onset of colorectal cancer and is linked to germline mutations in any one of several genes involved in DNA mismatch repair. Defects in *MSH2* account for at least 50% of cases of HNPCC with loss of DNA mismatch repair resulting in microsatellite instability which occurs in the majority of tumours from patients with HNPCC and also in approximately 13-17% of sporadic colorectal cancers. Hence, the normal function of *MSH2* in repairing incorrectly paired nucleotides following DNA replication is essential to the maintenance of genomic integrity and prevention of tumourigenesis. To investigate further the role of *MSH2* in these processes mice carrying a null mutation in the *MSH2* gene were studied. Several different endpoints associated with carcinogenesis were addressed including apoptosis, mutation frequency, and genomic instability.**

**Tumour cells which lack DNA mismatch repair are resistant to the cytotoxic effects of DNA methylating agents and Cisplatin. To address whether this resistance is mediated through loss of an *MSH2*-dependent apoptotic pathway, the apoptotic response of the murine small intestine to DNA methylating agents and Cisplatin was studied. *MSH2* was found to play a significant role in the initiation of apoptosis *in vivo*. The immediate apoptotic response to these agents was *p53*-dependent in the first 24 hours, however a smaller *p53*-independent apoptotic response was observed beyond this point. Mice doubly null for both *MSH2* and *p53* revealed that this delayed *p53*-independent response was entirely *MSH2*-dependent. These results demonstrate the existence of a pathway to apoptosis following DNA methylation which is dependent upon both *MSH2* and *p53*.**

**The DNA repair enzyme $O^6$-Alkylguanine-DNA-alkyltransferase (AGT), which removes potentially mutagenic methyl groups from guanine residues, appeared to play no significant role in modulating the *MSH2*-dependent apoptotic**

**response of intestinal cells to methylating agents or Cisplatin. $O^6$-Benzylguanine, a competitive inhibitor of AGT, prevented the metabolic activation of Dacarbazine probably through the inhibition of cytochrome P450 enzymes. This novel finding has adverse implications towards the potential clinical use of $O^6$-Benzylguanine.**

**The consequences of *MSH2* loss upon *in vivo* mutation frequency, either through loss of an apoptotic pathway or through failed DNA repair was investigated. A six-fold elevation in the spontaneous mutation frequency at the *Dlb-1* locus within cells of the intestinal epithelium was observed in *MSH2* null mice compared to wild-type controls. *MSH2*-deficiency also resulted in 13.8 and 5.0-fold elevations in mutation frequency following exposure to the methylating agents Temozolomide and N-methyl-N'-nitro-N-nitrosoguanidine (MNNG) respectively. In contrast, a minor 1.7-fold increase in mutation frequency was observed for Cisplatin. These results highlight the capacity for *MSH2*-deficiency to serve as a potent driving force during the multi-step evolution of colon tumours, especially following exposure to methylating type DNA damage.**

**Genomic instability is an integral component of colorectal neoplasia and can occur through mismatch repair deficiency and instability at the nucleotide sequence level. Alternatively chromosomal instability and the development of aneuploidy may occur which are strongly associated with *p53* deficiency. The contribution of these two forms of instability in murine tumourigenesis was addressed in an inter-cross of *MSH2* null and *p53* null mice. *MSH2* -/- *p53* -/- mice were viable but rapidly succumbed to tumours. Combined ablation of *MSH2* and *p53* in mice accelerated tumourigenesis significantly earlier than deficiency of *MSH2* or *p53* alone. Furthermore, absence of *MSH2* function greatly accelerated the rate of tumour development in *p53* heterozygote mice. Analysis of the tumours, arising in mice segregating for *MSH2* and *p53* deficiency, by flow cytometry and comparative genomic hybridisation suggested that *MSH2*-driven genomic instability was the predominant pathway.**

**The data presented in this thesis demonstrate that *MSH2* plays a pivotal role in determining both the apoptotic response and mutation frequency of the murine**

**intestine to methylating DNA damage and suggests that the consequences of *MSH2*-deficiency may be more significant to the initial stages of carcinogenesis than loss of *p53*.**

# GENERAL INTRODUCTION

## INTRODUCTION

Neoplasia is the abnormal proliferation of cells within a tissue. Cancer is a malignant form of neoplasia characterised by its ability to invade surrounding structures and spread throughout the body in the form of metastasis. In the United Kingdom, over 250 000 new cases of cancer are recorded each year, and from such a statistic it is estimated that 1 in 3 people are at risk of developing cancer at sometime during their life. Over 30 000 new cases of colorectal cancer are diagnosed each year which have a 5 year survival of only 37% (Cancer Research Campaign, 1997). Despite lifestyle changes and intensive research, neither the incidence, nor the 5 year survival, has altered materially over the past 20 years. Research into the pathogenesis of this disease is needed to understand the critical events in its evolution. Armed with this knowledge measures to decrease its incidence and increase the effectiveness of therapy can be implemented.

## COLORECTAL CANCER

Carcinogenesis within the colon is a multi-step process which involves the transition from normal epithelium sequentially through a hyperproliferative state, then adenomatous changes with increasing dysplasia, and finally frank malignancy with metastasis. This sequence is known as the adenoma-carcinoma sequence and the evolution of each well defined morphological stage is associated with progressive genetic changes (Fearon & Vogelstein, 1990) (Figure A). The transition from normal epithelium to adenoma is very strongly associated with loss of Adenomatous Polyposis Coli (*APC*) gene product function (Groden *et al.*, 1991). Mutations in a number of genes including K-*ras*, Deleted in Colorectal Cancer (*DCC*), and *DPC4* may then occur in one of these benign tumour cells leading to further clonal expansion (Vogelstein & Kinzler, 1993; MacGrogan *et al.*, 1997). Finally, mutations in the *p53* gene are thought to drive the change from benign tumourigenesis to malignancy. This process of sequential mutations can be accelerated by the phenomenon of genomic instability which occurs following mutations in one of the DNA mismatch repair enzymes, for example *MSH2*. Our understanding of the adenoma-carcinoma sequence

## Figure A

Adenoma-carcinoma sequence of colorectal epithelium. The genetic changes driving normal epithelium to carcinoma formation are shown. Genomic instability resulting from mismatch repair deficiency can accelerate the transition from one stage to the next.

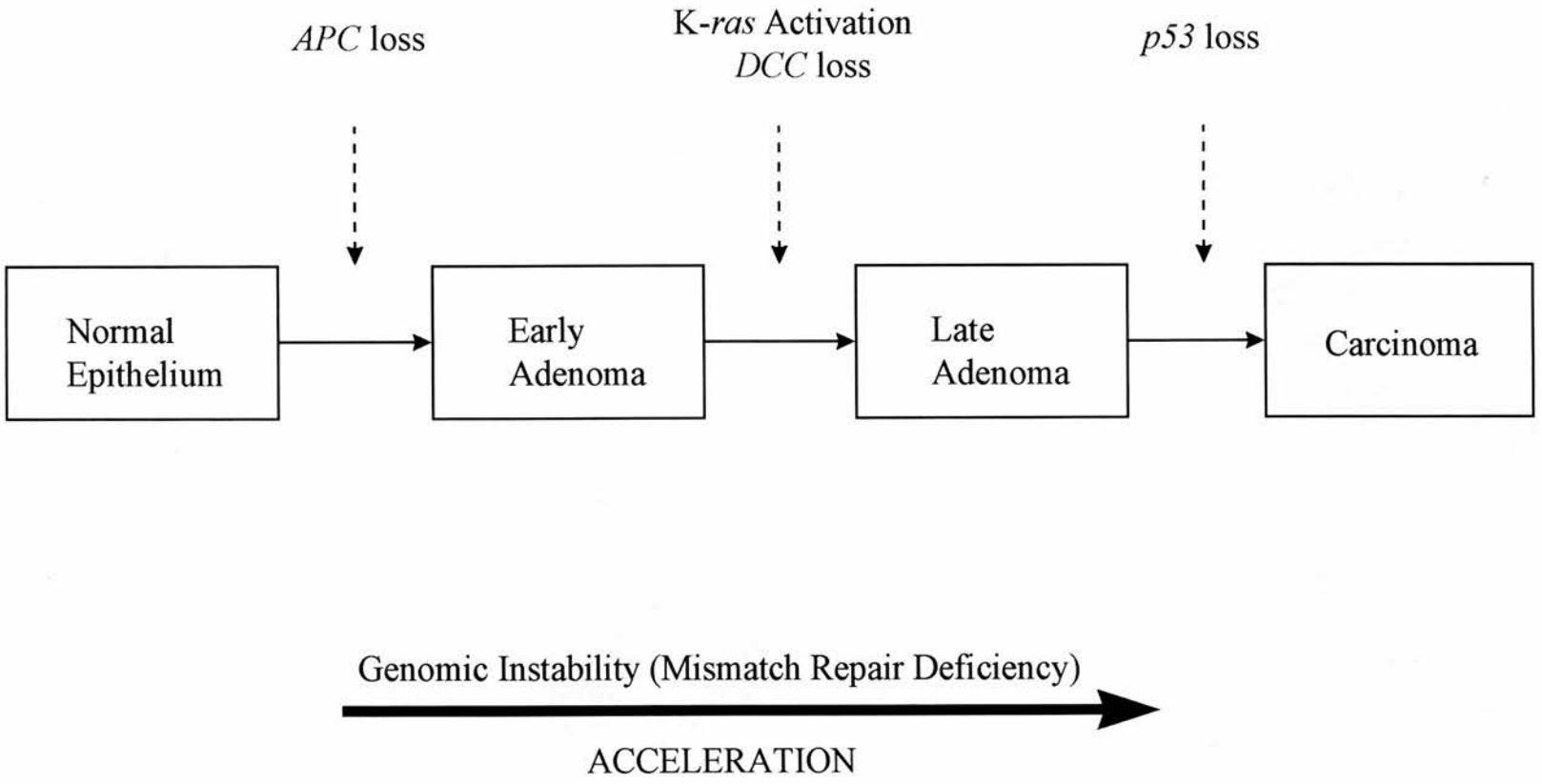
*APC* loss
K-*ras* Activation
*DCC* loss
*p53* loss
Normal Epithelium
Early Adenoma
Late Adenoma
Carcinoma
Genomic Instability (Mismatch Repair Deficiency)
ACCELERATION

has been greatly facilitated through the study of inherited forms of colorectal cancer and murine models.

**Familial Adenomatous Polyposis Coli**

Familial Adenomatous Polyposis Coli (FAP) is a dominantly inherited syndrome in which affected individuals are predisposed to develop numerous intestinal adenomas. It accounts for less than 1% of colorectal cancer with an incidence of 1 in 7000 (Kinzler & Vogelstein, 1996). Patients with FAP have many hundreds to thousands of polyps scattered throughout the gastrointestinal tract but mainly located in the colon. They appear between the ages of 10 and 35 and without surgical treatment, the presentation of malignant tumour invariably follows leaving FAP patients with a mean life expectancy of 40 years (Bussey, 1978). In addition to the colonic polyposis some individuals also develop extra-colonic manifestations including multiple osteomas, exostoses of the skeleton, desmoid tumours, and congenital hypertrophic retinal pigment epithelium (CHRPE) (Gorlin & Chaudry, 1960; Lewis, *et al.*, 1984).

Mutations in the Adenomatous Polyposis Coli (*APC*) gene are responsible for FAP. Individuals with FAP carry a germline mutation in one copy of *APC* (Groden *et al.*, 1991; Kinzler *et al.*, 1991). Somatic mutations in the remaining allele lead to defective *APC* function and the development of adenomas. Inactivation of *APC* has also been shown to occur in the majority of sporadic colorectal adenomas and carcinomas (Cottrell *et al.*, 1992). Most mutations identified create premature stop codons, 60% of which are in exon 15 and result in truncation of the *APC* protein (Nagase & Nakamura, 1993; Polakis, 1995). Furthermore, the exact location of the mutation within the *APC* gene can determine the number of polyps and whether extra-colonic features are present (Cunningham & Dunlop, 1996).

At a biochemical level *APC* protein binds β-catenin through two binding repeat motifs located in the central third of the protein, promoting β-catenin destruction (Rubinfeld *et al.*,1993; Iylas & Tomlinson, 1997). The *APC*/β-catenin complex regulates cell adhesion and migration through its interaction with the cell surface molecule E-cadherin and its contol over microtubule formation (Kemler, 1993; Gumbiner, 1995; Smith *et al.*, 1994; Munemitsu *et al.*, 1994). Virtually all mutant *APC* proteins lack at

least one type of β-catenin repeat, and fail to bind β-catenin resulting in a rise of free β-catenin within the cell (Rubinfeld *et al.*, 1996; Peifer, 1997). An increase of free β-catenin within the cell activates transcription factors of the T-cell factor-lymphoid enhancer family (Tcf-Lef), modifying gene expression. The genes activated are thought to promote cell proliferation and antagonise apoptosis (Peifer, 1997).

**Hereditary Nonpolyposis Colorectal Cancer**

Approximately 15% of all colorectal cancers occur in dominantly inherited patterns (Cannon-Albright *et al.*, 1988). Hereditary Nonpolyposis Colorectal Cancer (HNPCC) accounts for about 5% of all colorectal cancers with estimates of the incidence of HNPCC varying from 1 in 200 to 1 in 500, making it one of the commonest inherited diseases (Kinzler & Vogelstein, 1996). This figure is likely to be an underestimate as the International Collaborative Group on HNPCC has set stringent criteria (primarily for research purposes) for the diagnosis of HNPCC (Vasen *et al.*, 1991). The criteria are as follows: (1) three or more relatives with histologically proven colorectal cancer, one of whom is a first degree relative of the other two; (2) colorectal cancer involving at least two generations; and (3) at least one family member affected before the age of 50 years. In a clinical setting HNPCC is characterised by an autosomal dominant mode of inheritance with high penetrance, and the development of colorectal cancers which show a preponderance for the proximal colon (before the splenic flexure), in the absence of multiple polyps (Lynch *et al.*, 1993; Thibodeau *et al.*, 1993). In contrast to sporadic colorectal cancer which affects patients with an average age of 67, HNPCC patients with colorectal cancer have a mean age of 42 years at diagnosis (Kinzler & Vogelstein, 1996). Colon carcinomas arising in HNPCC patients often show different clinical and pathological features from non-HNPCC related cancers, tending to be larger with a near-diploid DNA content, confer a more favourable prognosis, display microsatellite instability and demonstrate a lower frequency of *p53* protein immunoreactivity (Kouri *et al.*, 1990; Lothe *et al.*, 1993). Histologically, the HNPCC colon cancers include higher proportions of mucinous, poorly differentiated carcinomas and tend to show more prominent lymphocytic infiltration (Kim *et al.*, 1994). There is a tendency for HNPCC

individuals to develop multiple colorectal cancers. Indeed, if patients do not receive a subtotal colectomy following initial diagnosis, 40% develop a second carcinoma within 10 years (Lynch *et al.*, 1996). Individuals with HNPCC may develop colorectal cancer alone (Lynch type I syndrome) or may develop additional tumours throughout the body, particularly cancers of the endometrium (the most prevalent extra-colonic tumour), ovary, stomach, upper urinary tract, pancreas, small bowel and skin (Lynch type II syndrome) (Lynch *et al.*, 1996). The Muir-Torre syndrome is considered to be a subset of HNPCC and is characterised by the association of colon cancers and skin tumours, especially sebaceous gland neoplasms and keratoacanthomas (Cohen *et al.*, 1991; Kolodner *et al.*, 1994).

**DNA mismatch repair and HNPCC**

Insights into the cause of HNPCC came from three related areas of research. First, using linkage analysis to study large kindreds affected by the disease some of the genes responsible were found to map to either chromosome 2p16 or 3p21 and be transmitted by a pattern of autosomal dominant inheritance (Peltomaki *et al.*, 1993a; Lindblom *et al.*, 1993). Second, analysis of oncosuppressor gene changes in tumours from these patients, by loss of heterozygosity at numerous microsatellite loci throughout the genome, showed regions of expanded microsatellites rather than evidence of loss as predicted [microsatellites are repetitive DNA sequences where the unit of repetition is often short, such as mono-, di-, or tri- nucleotide groups and these are scattered throughout the genome e.g. CACA(CA)n...] (Aaltonen *et al.*, 1993; Thibodeau *et al.*, 1993). Finally, similar patterns of change in microsatellites had already been observed in bacteria harbouring mutations in the bacterial DNA mismatch repair enzymes *mutS* and *mutL* (Levinson & Gutman, 1987). Tying all these lines of investigation together, it emerged that the human homologues of bacterial *mutS* and *mutL*, called *hMSH2* and *hMLH1*, were located on chromosomes 2p16 and 3p21 respectively, and were found to be mutated in different HNPCC kindreds (Leach *et al.*, 1993; Papadopoulos *et al.*, 1994).

The DNA mismatch repair (MMR) pathway is essential for the correct maintenance of genetic material (Fishel & Kolodner, 1995). It functions to remove misincorporated

single nucleotide bases following DNA replication or recombination, and also small loops of DNA which arise through slippage of the DNA polymerase on the template strand of DNA during DNA replication. This phenomenon of slippage is more likely to occur at sites of repetition of short units of DNA sequence, such as microsatellites. In addition, the DNA mismatch repair system has been shown to have an important role in the cytotoxicity of alkylating mutagens/carcinogens through the lethal processing of mispaired methylated guanine residues (Branch *et al.*, 1993; Karran & Bignami, 1994).

The MMR pathway consists of a number of enzymes beginning with a heterodimer (known as *mutSα*) of *hMSH2* protein and G/T mismatch-binding protein (*GTBP*/p160) that is capable of recognising and binding to DNA mismatches (Drummond *et al.*, 1995). Another *mutS* homologue, *hMSH3* may bind *hMSH2* replacing *GTBP*, forming a heterodimer (called *mutSβ*), which increases the specificity for loops of nucleotides (Risinger *et al.*, 1996; Palombo *et al.*, 1996). However, the majority of *hMSH2* is bound to *GTBP*. Subsequently, a second heterodimer consisting of *hMLH1* and *hPMS2* proteins (*mutL*) is recruited and binds to the *hMSH2/GTBP* dimer forming a large complex (Kolodner, 1995). Finally, the DNA mismatch is repaired by excision of the DNA strand containing the mismatch or modified base and synthesis of a correct complementary DNA strand through the actions of undefined helicase, nuclease, polymerase and ligase enzymes which use the intact DNA strand as a template. The role of *hPMS1* in this process is unknown. The specific components of the MMR are shown in Figure B.

HNPCC affected individuals are heterozygous for a germline mutation in one of at least four DNA mismatch repair enzymes *hMSH2*, *hMLH1*, *hPMS1*, *hPMS2* which are found on chromosomes 2p, 3p, 2q, and 7p respectively (Kinzler & Vogelstein, 1996). Mutations in *hMSH2* and *hMLH1* together account for approximately 95% of germline mutations reported (Wijnen *et al.*, 1998). However, only in one quarter of HNPCC cases can such mutations be identified (Wijnen *et al.*, 1998). Seventy percent of the germline mutations identified produce truncated forms of the protein with loss of function, with the remainder being missense mutations (Kinzler & Vogelstein, 1996). In addition, mutations in *GTBP* have been identified in cell lines with

## Figure B

Components of the DNA mismatch repair system and their mechanism of action.

a) Double-stranded DNA containing a single base mismatch or a loop of nucleotides due to strand slippage.
b) Mismatch recognised by a heterodimer of *hMSH2* and *GTBP* proteins with recruitment of *hMLH1* and *hPMS2* proteins.
c) Removal of the mismatch is effected by the excision of the altered DNA single strand by the action of undefined helicase and nuclease enzymes.
d) Repair is completed by synthesis of a new DNA strand complementary to the intact strand by undefined polymerase and ligase enzymes.

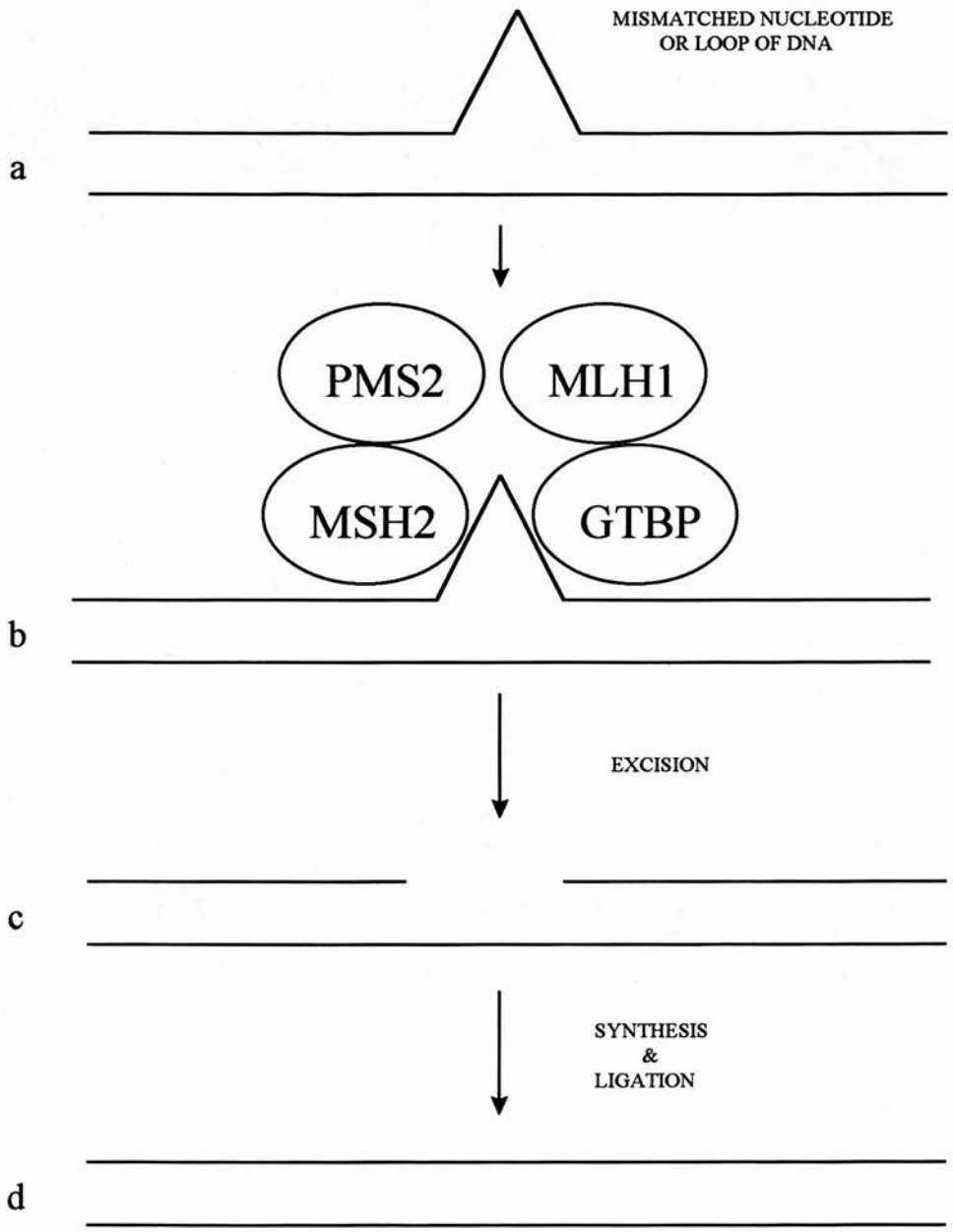
MISMATCHED NUCLEOTIDE
OR LOOP OF DNA
a
PMS2
MLH1
MSH2
GTBP
b
EXCISION
c
SYNTHESIS
&
LIGATION
d

microsatellite instability and a germline mutation of *GTBP* has been identified in a single HNPCC pedigree (Papadopoulos *et al.*, 1995; Miyaki *et al.*, 1997).

Tumour cells from HNPCC individuals harbour mutations or alterations in both alleles of a mismatch repair gene, with inheritance of one mutated allele and loss of function of the second allele occurring through somatic mutation or allele loss leading to reduction to homozygosity. Thus, MMR genes behave as true tumour suppressor genes in keeping with Knudson's two hit hypothesis (Knudson, 1985). This loss of post-replicative DNA mismatch repair increases mutation rates 100 to 600 fold above normal levels (Shibata *et al.*, 1993; Bhattacharyya *et al.*, 1994; Eshleman *et al.*, 1995). Such tumours may be described as possessing a "mutator phenotype" in the absence of effective DNA mismatch repair. This mutator phenotype has two consequences. First, the replication error phenotype ($RER^+$) described above is acquired leading to the appearance of microsatellite instabilty which were it restricted to nonexonic sequences would be in itself harmless to the cell.. Second, and more ominously, there is a susceptibility to rapid accumulation of mutations in many different genes including growth controlling genes anywhere in the genome, hence explaining the accelerated progression through the multi-step adenoma to carcinoma pathway. A prominent example is mutation in the TGFβII receptor gene which contains a stretch of repetitive dinucleotides within one of the exons that acts as a target for deficient DNA mismatch repair (Markowitz *et al.*, 1995). It is also possible that the $RER^+$ phenotype may produce mutations in the other components of the DNA repair systems accelerating tumourigenesis even further (Perucho, 1996).

**Sporadic colorectal cancer and microsatellite instability**

By the age of 70 years about half the population in industrialised nations have a benign adenoma in their colon but only one in ten develop an invasive carcinoma (Kinzler & Vogelstein, 1996). Such colon cancers arising in patients with a negative family history for colon cancer are termed "sporadic" carcinomas. Microsatellite instability can be shown in around 15% of all sporadic colorectal carcinomas (Aaltonen *et al.*, 1993; Lothe *et al.*, 1993). These sporadic colon cancers with microsatellite instability share similar characteristics to HNPCC tumours, tending to

be larger, located in the proximal colon, diploid, and poorly differentiated or mucinous (Chung & Rustgi, 1995). However, the role of the common DNA mismatch repair enzymes in their pathogenesis is less clear (Eshleman & Markowitz, 1996). Approximately 60% of sporadic tumours harbour mutations in the same DNA mismatch repair genes that cause HNPCC, whereas in other cancers no mutations in MMR genes can be identified (Liu *et al.*, 1995; Eshleman & Markowitz, 1996). However, mutations have been detected in other components of the mismatch repair system including *GTBP*, *MSH3*, and the proofreading domain of polymerase δ (da Costa *et al.*, 1995; Malkhosyan *et al.*, 1996). It is possible that uncharacterised DNA repair genes may be mutated or that inactivation of known MMR genes may involve subtle intronic lesions or transcriptional pathways (Bubb *et al.*, 1996). A comparison of the relative importance of each DNA mismatch repair enzyme to both HNPCC and sporadic colorectal carcinomas is shown in Table 1.

**Other cancers with microsatellite instability**

Cancers arising in other tissues of the body distinct from the colon have also been shown to have microsatellite instability and show a $RER^+$ phenotype (Eshleman & Markowitz, 1995). For example, endometrial carcinomas arising in both HNPCC patients and sporadic cases display microsatellite instability in 75% and 17% of cancers respectively (Risinger *et al.*, 1993). In contrast to colon cancers, endometrial carcinomas with microsatellite instability tend to be high grade and carry a poorer prognosis (Caduff *et al.*, 1996). Microsatellite instability can also be seen in 67% of pancreatic carcinomas, 25% of renal carcinomas, 56% of prostatic adenocarcinomas, 45% of small cell lung cancers, 18% of gastric carcinomas and in a small proportion of ovarian tumours, melanomas, and gliomas (Han *et al.*, 1993; Merlo *et al.*, 1994; Uchida *et al.*, 1994 & 1995). In contrast, tumours of the breast, testes and lung do not show a $RER^+$ phenotype (Peltomaki *et al.*, 1993b). Interestingly, those HNPCC patients with Lynch type II syndrome have an increased susceptibility to tumour types which, when sporadic, tend to display microsatellite instability (Lynch *et al.*, 1996). This could reflect tissue-specific differences in the susceptibility to the genome

## Table 1

Table comparing HNPCC-derived cancers and sporadic colon cancers outlining the relative contributions of MMR genes to each. *PMS1* mutations have only been identified in a single kindred.

**TABLE 1**

| | HNPCC | Sporadic Colon Cancer |
|---|---|---|
| Lifetime risk | 1 in 200 | 1 in 20 |
| Frequency of MMR deficiency / $RER^+$ | >90% | ~15% |
| Prevalence of MMR mutations in $RER^+$ tumours | 26-70%* | ~10% |
| Breakdown of MMR mutations in colorectal cancers with proven MMR mutations | | |
| *MSH2* | 45% | 60% |
| *MLH1* | 49% | 35% |
| *PMS2* | 6% | 5% |

[* Data from Liu *et al.*, 1996a & Wijnen *et al.*, 1998]

destabilising effects of defective mismatch repair. Mutations in *hMSH2* and *hMLH1* have been identified many $RER^+$ sporadic tumours although it is likely that other mismatch repair enzymes play an important role (Chung & Rustgi, 1995; Kobayashi *et al.*, 1996).

### *p53* and colorectal cancer

*p53* is the most commonly mutated gene in human malignancy and is mutated in 50% of all colorectal carcinomas (Hollstein *et al.*, 1991; Khine *et al.*, 1994). *p53* acts as a tumour suppressor gene with many cancers showing loss of one *p53* allele (loss of heterozygosity) and inactivation of the second allele by point mutation (Chang *et al.*, 1993). However, certain mutants may also bind to and inactivate the remaining wild-type allele by a dominant negative inhibition (Vogelstein & Kinzler, 1992). Furthermore, there is evidence that a cell with only one copy of functional wild-type *p53* is predisposed to malignancy (L. Donehower, personal communication). Loss of heterozygosity of chromosome 17p, where the *p53* gene is located, is infrequent in adenomas of any stage suggesting that loss of *p53* function is associated with the transition of a benign adenoma to a malignant carcinoma.

### *p53* structure and function

One of the many functions ascribed to *p53* is that it acts a transcription factor that enhances the rate of transcription of several genes which carry out the *p53*-dependent functions of a cell, including cell cycle arrest, DNA repair and apoptosis (Levine, 1997). *p53* exists as a tetramer (Jeffery *et al.*, 1995) and contains a sequence-specific DNA binding domain and also a transcriptional activation domain that interacts with the basal transcriptional machinery to both positively and negatively regulate gene expression (Haffner & Oren, 1995). More than 90% of the missense mutations identified localise to the sequence-specific DNA binding domain, thus abolishing its control over gene expression (Hollstein *et al.*, 1994).

In normal cells *p53* protein is maintained at low levels by its short half life of approximately 20 minutes (Maltzman & Czyzyk, 1984). Under conditions of cellular stress including DNA damage (e.g. γ-irrradiation, UV-irradiation, or chemical

damage), hypoxia or depletion of ribonucleotide triphosphate pools, *p53* is upregulated, stabilised and activated with engagement of transcription (Lane, 1992; Graeber *et al.*, 1996; Linke *et al.*, 1996). Genes known to be transactivated include *p21, MDM-2, GADD45, Bax,* and insulin-like growth factor-binding protein 3 (*IGF-BP3*) (Levine, 1997). Activation of *p21*, which inhibits cyclin-dependent kinases, results in cell cycle arrest at both $G_1$/S and $G_2$/M phases, preventing cells from both entering the cell cycle or completing mitosis (Cox & Lane, 1995). In addition, *p21* interacts with proliferating cell nuclear antigen (PCNA) blocking the role of PCNA as an auxillary DNA polymerase factor in DNA replication, but not its role in DNA repair (Cox & Lane, 1995). Those cells bearing excessive DNA damage or incomplete repair are thought to be deleted by apoptosis. Apoptosis can be initiated directly through *p53* in the absence of transcription or alternatively through the transcription of *Bax* (Miyashita & Reed, 1995). *Bax* dimers are thought to initiate apoptois by binding to and removing functional *Bcl-2*, a strong inhibitor of apoptosis (White, 1996). Thus, *p53* co-ordinates the cell cycle, and DNA repair mechanisms and can also initiate apoptosis to prevent the propagation of mutant daughter cells (Lane, 1992). Hence, in the absence of *p53*, it is predicted that DNA damage and ensuing mutations are passed on to daughter cells increasing the likelihood of conversion to malignancy.

### *p53* and genomic instability

By acting as a cellular gatekeeper for growth and division and thus controlling the cellular response to DNA damage, *p53* is responsible for maintaining the integrity of cellular DNA and has been dubbed "the guardian of the genome" (Lane, 1992). Hence, loss of *p53* results in increased genomic instability and is positively correlated with the development of aneuploidy within colorectal tumours (Livingstone *et al.*, 1992; Carder *et al.*, 1993; Wyllie *et al.*, 1994). Four pieces of evidence support *p53* as a key player in maintaining a stable genome. First, the C-terminal domain of *p53* itself is capable of recognising insertion/deletion DNA mismatches (Lee *et al.*, 1995). Second, absence of *p53* is correlated with gene amplification, thought to arise from non-homologous recombination in a bridge-breakage-fusion cycle (Yin *et al.*, 1992).

Third, when mitotic spindle inhibitors are added to wild-type *p53* cells, the cells are arrested in $G_2$. However, in the absence of *p53*, these cells reinitiate DNA synthesis increasing the ploidy of cells (Cross *et al.*, 1995). Finally, *p53* is essential to the regulation of centromere number and subsequent aneuploidy (Fukasawa *et al.*, 1996).

**Two pathways to colorectal tumourigenesis**

When comparing $RER^+$ colon cancers with microsatellite instability (both sporadic and HNPCC derived) to $RER^-$ colon tumours it is clear that they behave differently both in terms of their clinical features and their molecular pathogenesis. This suggests that at least two distinct pathways from premalignant cells to carcinoma may exist (Eshleman & Markowitz, 1996). The more prevalent $RER^-$ cancers tend to be aneuploid in nature and show loss or alteration of large regions of chromosomes either by mitotic recombination or incomplete segregation at mitosis. At a molecular level mutations in *APC*, K-*ras*, and *p53* are common (Kinzler & Vogelstein, 1996). Inactivation of the *p53* gene or the genes involved in chromosome segregation are thought to play a key role in the initiation this type of instability (Carder *et al.*, 1993 & 1995; Bouffler *et al.*, 1995; Tlsty, 1997).

$RER^+$ tumours on the other hand are diploid and do not tend to show random allelic loss or major chromosomal rearrangements (Schlegel *et al.*, 1995). Furthermore, they show a relative paucity of mutations in *APC*, K-*ras* and *p53* (Shibata, 1996). This alternative form of genomic instability produces more subtle genetic alterations throughout the genome perhaps at different growth controlling loci from $RER^-$ cancers (Konishi *et al.*, 1996). For example it is known that $RER^+$ cancers have a high incidence of TGF-β II receptor mutations of the type usually repaired by the MMR pathway compared to $RER^-$ cancers (Markowitz *et al.*, 1995). Thus, the development of colon cancers is strongly associated with the acquisition of genomic instability (Figure C). The mechanisms influencing whether instability arises through gross chromosomal aberrations, or through mismatch repair and minor DNA changes remain elusive.

## Figure C

At least two different pathways of genomic instability have been identified which associate with the transition of a premalignant cell to a cancer cell. Defects in *p53* or the controls over chromosomal stability are proposed to lead to gross chromosomal changes and the development of aneuploidy. In contrast, loss of DNA mismatch repair activity results in subtle changes throughout the genome in the form of point mutations and represents an alternative route to tumourigenesis.

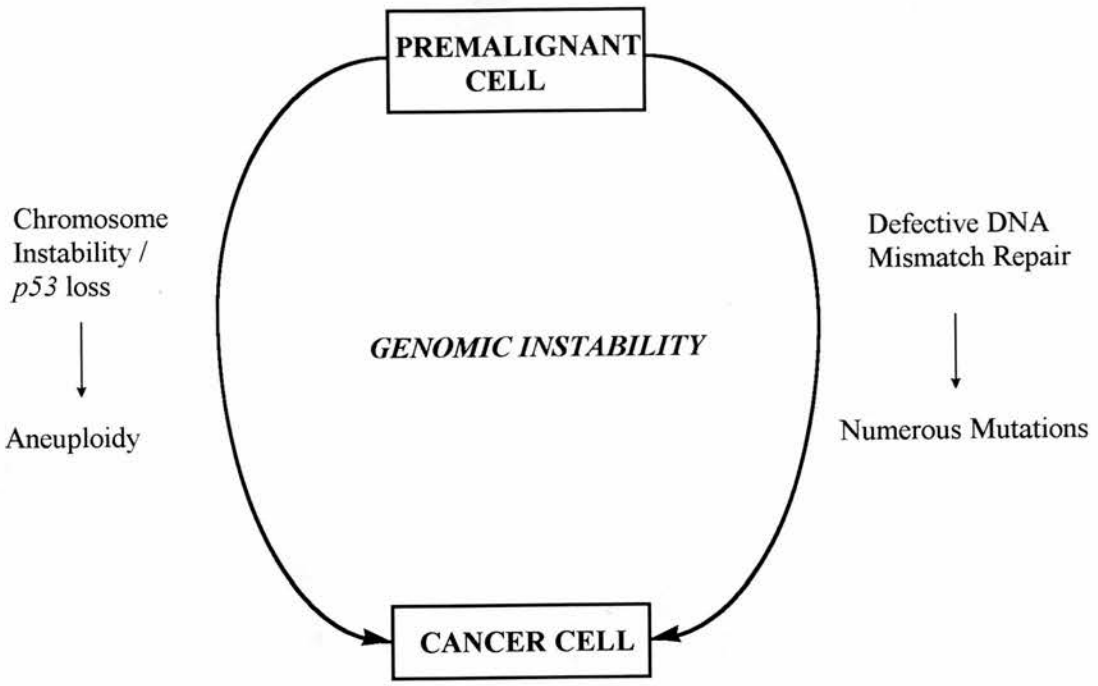
PREMALIGNANT CELL
Chromosome Instability / p53 loss
Aneuploidy
GENOMIC INSTABILITY
Defective DNA Mismatch Repair
Numerous Mutations
CANCER CELL

## APOPTOSIS

Apoptosis or programmed cell death is a genetically controlled response of cells to a variety of stimuli to commit suicide. It occurs in a wide variety of physiological and pathological conditions including tumours. The inhibition of apoptosis in cancers has been associated with tumour growth, neoplastic progression, and resistance to cytotoxic anticancer agents (Bellamy *et al.*, 1995; Lyons & Clarke, 1997).

### Cell death in tumours

Cell death is a critical determinant of tumour growth (Wyllie, 1985). The two patterns of cell death in tumours are apoptosis and necrosis and they differ in morphology, incidence, and regulation. Apoptosis usually affects single cells surrounded by viable neighbours. Apoptosis is a genetically programmed mode of cell death that is regulated by many genes, including oncogenes and oncosuppressor genes, which may be mutated, deleted or abnormally expressed in neoplasms, thus altering tumour cell susceptibility to apoptosis (Arends, 1995). In contrast, necrosis often occurs in confluent zones and results from severe non-physiological perturbation of the cellular environment, such as hypoxia due to inadequate blood flow in tumours (Wyllie, 1981). The topography of necrosis in tumours is a complex function, the major determinant of which is the rate of proliferation of tumour cells relative to the process of angiogenesis (Folkmann, 1995). Local regions of rapid tumour expansion may produce zones of relative hypoxia resulting in necrosis.

The growth rate of a tumour mass is often regarded as a key parameter that is of fundamental significance for tumour aggression, a major factor in determining the prognosis for a patient. Proliferation in tumours has been investigated extensively, but does not correlate well with overall growth. A major reason for this is that net tumour growth results from the balance of cell gain and cell loss. However, the contribution of cell loss to tumour growth and aggressiveness is less well understood. In the few instances where quantitative data are available tumour cell loss is considerable.

Cells may be lost from tumour cell populations by a variety of mechanisms. Cells may depart the primary tumour site by natural exfoliation or cell migration. They may leave the proliferating pool of cells by terminal differentiation, or they may die. Many

descriptions of tumour cell death have often focused on necrosis (Thomlinson & Gray, 1955; Steel, 1977; Moore, 1983 & 1987), with less extensive study of apoptosis in tumours (Kerr *et al.*, 1972; Wyllie, 1985). Quantitative estimates of net tumour cell loss have been made (Steel, 1977; Moore, 1983 & 1987). It is possible to calculate the potential doubling time (Tp) from estimates of tumour cell production rates (mitotic indices, nucleotide incorporation or fraction of cycling cells), and the actual doubling time (Td) from measurements of tumour volume, and so derive the cell loss factor (CLF = 1 - Tp/Td). The CLF approaches zero with no cell loss, and unity if extensive loss makes the actual doubling time unmeasurably large. In deriving CLFs, errors can arise from several inevitable assumptions, but in almost every tumour studied the CLF is large. In rodent sarcomas and carcinomas CLFs of 0.65 to 0.78, and in human bronchial and colorectal carcinomas and a malignant melanoma CLFs of 0.73 to 0.96 have been recorded (Steel, 1977; Moore, 1983 & 1987; Kerr & Lamb, 1984). The high level of tumour CLFs presumably explains the poor correlation between measures of cell proliferation, such as the thymidine labelling index, and the tumour volume doubling times for a whole range of human tumours and points to the considerable importance of tumour cell loss in determining tumour growth rate (Steel, 1977). Large cell loss factors are likely to act as major regulators of the rate of tumour expansion and probably determine the overall growth pattern in terms of tumour enlargement, stasis or regression.

It has been argued that cell death is numerically the most significant form of cell loss from a growing tumour (Kerr *et al.*, 1972, Wyllie, 1985; Bowen & Bowen, 1990). This may occur either by necrosis or apoptosis. However, despite the histologically conspicuous appearance of necrosis, it is by no means established that it can account for the high levels of cell loss observed in tumours. Apoptosis is less conspicuous histologically because it has a short timecourse, leaves no residual fingerprints, and occurs in a scattered distribution within tumours. It is readily calculated that a surprisingly small proportion of apoptotic cells visualised in a tissue section can represent very substantial cell loss, and there are increasing quantitative reports on apoptosis in tumours (Sarraf & Bowen, 1986 & 1988). Indeed the transformation of

colorectal epithelium to carcinomas has been associated with a progressive inhibition of apoptosis (Bedi *et al.*, 1995).

**Morphology of apoptosis**

The morphological changes of apoptosis can be divided into three overlapping phases (Wyllie *et al.*, 1980 & 1984; Wyllie, 1987; Arends & Wyllie, 1991). In the first, there is reduction in nuclear size with condensation of chromatin into crescentic caps or toroids at the periphery of the nucleus. There is a characteristic pattern of disintegration of the nucleolus, and early in apoptosis cells detach themselves from their viable neighbours. Associated with the loss of contact regions there is also loss of specialised surface structures, such as microvilli and the cell initially adopts a smooth contour. The sudden onset of cell shrinkage, with surface blebbing and bubbling, sometimes known as zeiosis, is known as phase 1 (Evan *et al.*, 1992). As the cell shrinks, cytoplasmic organelles become compacted and the smooth endoplasmic reticulum undergoes dilatation. These dilated cisternae fuse with the cell membrane, giving rise to a cratered appearance at the surface on scanning electron microscopy. Cytoskeletal filaments may be seen to aggregate in side-to-side bundles, parallel to the cell surface, and ribosomal particles are dispersed from the endoplasmic reticulum and may form semi-crystalline arrays, but otherwise the organelles remain intact.

In phase 2 apoptosis, there is blebbing at the cell surface and crenation of the nuclear outline, leading to controlled fragmentation of both nucleus and cytoplasm which split up into particles of various sizes. Usually, the cell becomes a cluster of round, smooth, membrane-bounded "apoptotic bodies", some containing variably-sized, spherical, nuclear fragments of condensed chromatin. These bodies are phagocytosed by neighbouring viable tumour cells or macrophages (Wyllie *et al.*, 1980).

In phase 3 apoptosis, the residual nuclear and cytoplasmic structures undergo progressive degradation. Apoptotic nuclear masses lose their smooth, rounded appearance but are still recognisable as apoptotic as they consist of condensed chromatin forming unusual shapes with irregular outlines. In tissues these changes usually occur within the phagosome of the ingesting cell. Eventually membranes

disappear, organelles become unrecognisable and the appearance is that of a residual lysosomal body. This is the appearance of the majority of apoptotic bodies seen by light microscopy and sometimes the smooth outline of the surrounding phagosome, but earlier phases can also be recognised by their rounded contours and deeply hyperchromatic, fragmented nuclei. Apoptotic cells remain recognisable within tissues for 2 to 9 hours, a timecourse which coincides with that of complete degradation of other large biological structures within the phagosomes of macrophages. This relatively short period ensures that high rates of apoptosis produce only small increases in the proportion of apoptotic cells observed in tissue sections.

**Control of apoptosis in tumours**

Apoptosis is a genetically controlled process that can be regulated internally by various oncogenes and tumour suppressor genes, and also by external signals including cytokines, cellular ligands (e.g. *fas*), matrix attachment, chemotherapeutic drugs, and irradiation (Bellamy *et al.*, 1995). Expression of c-*Myc*, wild-type *p53*, and *APC* enhance susceptibility to apoptosis, whereas *Bcl-2*, retinoblastoma gene product (*Rb*) and Ha-*ras*, protect against or suppress apoptosis (Hockenbery *et al.*, 1990; Evan *et al.*, 1992; Clarke *et al.*, 1992 & 1993; Arends *et al.*, 1993 & 1994; Morin *et al.*, 1996). Cellular sensitivity or resistance to apoptosis in response to one type of stimulus is often associated with similar sensitivity or resistance to a variety of other agents (Wyllie, 1987; Bertrand *et al.*, 1991). It is postulated that this is because some cell types are "primed" for apoptosis and that different oncogenes and tumour suppressor genes stimulate or suppress the "priming events" for apoptosis by modulating the expression of a number of effector proteins in apoptosis, for example ICE-like proteases, endonucleases or transglutaminases (Wyllie, 1980; Arends *et al.*, 1990; Arends & Wyllie, 1991) Thus, whether a cell undergoes apoptosis in response to an external stimulus, such as injury due to mild or moderate ischaemia/hypoxia, or treatment with cytotoxic drugs or irradiation, depends on to what extent it is primed and hence susceptible to the triggering of apoptosis. For example, in transplanted tumours expressing wild-type *p53*, regions of hypoxia mapped to zones that were enriched for apoptosis, whereas in *p53*-deficient tumours hypoxic regions contained

little apoptosis (Graeber *et al.*, 1996). Hypoxia can induce p53 expression apparently by a different pathway than DNA-damaging agents (Graeber *et al.*, 1994). Hypoxia induces apoptosis in malignant cells and this appears to be largely *p53* mediated, such that loss of the *p53* gene or overexpression of *Bcl-2*, substantially reduces hypoxia-induced cell death (Graeber *et al.*, 1996). Hypoxia is a stress that is commonly found in growing solid tumours of diverse origin above 1-2mm in size. The ability of cells to survive hypoxia therefore represents a powerful and widely prevalent selection pressure, suggesting an explanation for why *p53* is one of the most commonly mutated genes in human cancer.

## MURINE MODELS OF COLORECTAL CANCER

Individuals inheriting the same mutation predisposing to cancer may show very different outcomes, ranging from early onset of aggressive cancer to disease free survival. Experimental mouse models can provide a powerful tool to identify factors in the environment and genetic background that account for such modifications. Furthermore, mouse models can provide *in vivo* experimental systems and also the opportunity to test chemotherapeutic drugs prior to clinical use. The murine models of human neoplasia used in this study are outlined below.

### *Min* mouse

The *Min* (Multiple intestinal neoplasia) mouse was generated by random germline mutagenesis with N-ethyl-nitrosourea and is heterozygous for a nonsense mutation at codon 850 of *APC* (Moser *et al.*, 1990; Su *et al.*, 1992). This strain closely models the human FAP cancer syndrome, with mice developing numerous adenomas in the small intestine and colon, some of which progress to become locally invasive adenocarcinomas. The exact number of adenomas which develop is strongly influenced by the genetic background of the strain and a second locus termed Modifier of *Min*-1 (*Mom*-1) (Dietrich *et al.*, 1993). On a sensitive (*Mom*-1 negative) C57BL/6J genetic background, in excess of 50 tumours develop per animal leading to an average life span of 120 days (Dove *et al.*, 1994). The gene encoding this strain difference has recently been identified as the *Pla2g2a* gene, which codes for secretory

phospholipase A2 (MacPhee *et al.*, 1995). This enzyme is involved in synthesising prostaglandins, hormone-like fatty acids that are believed to regulate colon cell proliferation (Prescott & White, 1996). Thus, mice resistant to colon cancer (*Mom-1* positive) carry functional *Pla2g2a*, while susceptible (*Mom-1* negative) mice carry a stop mutation in the *Pla2g2a* gene (Cormier *et al.*, 1997).

The *Min* mouse varies from human FAP in two important ways. First, the adenomas in the *Min* mouse are most prominent in the small intestine while in the human it is the colon that is the site of most lesions. The differential expression of the oncogene *Bcl-2* between the small intestine and the colon of mice, and its control over apoptosis, may account for this difference (Merritt *et al.*, 1995). Second, the mechanism of loss of the remaining wild-type allele is different between mice and humans. In the mouse, in 100% of adenomas examined, the entire chromosome 18 is lost (Luongo *et al.*, 1994). In humans loss of the remaining allele can only be detected in 71% of adenomas and occurs by intragenic inactivating mutations or interstitial deletions (Ichii *et al.*, 1992; Nagase & Nakamura, 1993). The reason for this difference is unknown, but one interpretation is that the mouse genome permits hemizygosity, because inbred strains have been bred to lack recessive lethal mutations.

*p53* gene targeted mice have been crossed to *Min* mice generating progeny that are *APC* $+/^{Min}$ *p53* -/- (Clarke *et al.*, 1995). Interestingly, given that 50% of colorectal carcinomas have a mutation in *p53* and the role of *p53* in maintaining genomic stability, no increase in the number or acceleration in the development of adenomas was observed in the intestines. However, there was a shift in phenotype with 83% of animals possessing abnormalities in the exocrine pancreas, with 22% displaying overt malignacy (Clarke *et al.*, 1995). Hence, *p53* and *APC* can co-operate in tumourigenesis although this synergism appears to be tissue specific.

### *p53*-deficient mice

Several strains of mice have been developed which bear constitutive inactivations of the *p53* gene (Donehower *et al.*, 1992; Clarke *et al.*, 1993; Lowe *et al.*, 1993a; Jacks *et al.*, 1994). Mice homozygous for these mutations are viable, but a significant proportion (23%) of female *p53* -/- mice die during embryogenesis from neural tube

defects including exencephaly and subsequent anencephaly (Sah *et al.*, 1995; Armstrong *et al.*, 1995). Surviving animals rapidly develop spontaneous tumours, predominantly thymic lymphomas with a smaller proportion succumbing to sarcomas, by the age of six months (Donehower *et al.*, 1992; Jacks *et al.*, 1994; Purdie *et al.*, 1994). *p53* +/- heterozygote mice develop both lymphomas and sarcomas in similar ratios although they exhibit a longer latency period before development of the tumours when compared to homozygote mice (Purdie *et al.*, 1994). In addition, the heterozygote mice develop a broader spectrum of tumours albeit at low levels including adenocarcinomas of the lung, pituitary and rarely colon. Indeed, the tumour spectrum of the *p53* +/- mice resembles to some extent that of Li-Fraumeni families suggesting that the *p53* +/- mouse is a useful model for the Li-Fraumeni syndrome (Li & Fraumeni, 1969; Purdie *et al.*, 1994). Recently, it has been reported that in the tumours arising in *p53* +/- mice approximately 50% retain an intact, functional, wild-type *p53* allele. Tumours which retain the remaining wild-type *p53* allele tend to arise later and display less chromosomal instability (L. Donehower, personal communication). Thus, a reduction in *p53* dosage alone may be sufficient for tumour development.

To examine the synergism between *MSH2* and *p53*, both of which are known to affect genomic stability and mutation rates, Cranston *et al.* (1997) interbred *MSH2* and *p53* null mice together to generate *MSH2* -/- *p53* -/- mice. Combined *MSH2* and *p53* ablation resulted in developmental arrest of all female embryos at 9.5 days (Cranston *et al.*, 1997). The exact cause of the female embryonic lethality remains unexplained, although embryos underwent "global catastrophic apoptosis". Viable male mice however succumbed rapidly to lymphomas, more rapidly than either *MSH2* -/- or *p53* -/- alone, demonstrating co-operativity between the two genes. Furthermore, in tumours from *MSH2* -/- *p53* -/- mice the frequency of microsatellite instability was not significantly different from *MSH2* -/- mice alone, demonstrating that *p53* status does not affect microsatellite instability. Hence, *MSH2* and *p53* can co-operate to accelerate tumourigenesis independently of each other by two separate mechanisms.

***MSH2*-deficient mice**

Mice with a homozygous deletion in the murine *MSH2* gene have been generated (de Wind *et al.*, 1995; Reitmair *et al.*, 1995). They have defective DNA mismatch repair and succumb to cancer. Homozygous *MSH2* -/- mice develop lymphomas beyond 2-3 months of age, which show microsatellite instability (de Wind *et al.*, 1995; Reitmair *et al.*, 1995 & 1996a). However, in 70% of mice surviving past 6 months of age, adenomas and carcinomas with microsatellite instability can be identified in the intestines providing a good model for the study of HNPCC (Reitmair *et al.*, 1996a). Furthermore up to 7% of these animals developed skin neoplasms analogous to those of the Muir-Torre syndrome (Reitmair *et al.*, 1996a). *MSH6* (*GTBP*) deficient mice have recently been generated and are similar to *MSH2* -/- mice developing both lymphomas and gastrointestinal tumours although they differ from *MSH2* -/- mice displaying an extended life span, an increase in B-cell derived lymphomas and an absence of microsatellite instability in the tumours that develop (Edelmann *et al.*, 1997).

By crossing *Min* mice to *MSH2* -/- mice progeny were generated that were heterozygous for *Min* and null for *MSH2* and therefore possessed absent DNA mismatch repair. In such progeny adenomas were both greater in number and developed more rapidly than in the *Min* controls, leading to reduced survival of the mice (Reitmair *et al.*, 1996b). Analysis of adenomas from these *APC* $+/^{Min}$ *MSH2* -/- mice showed that only a small fraction demonstrated loss of heterozygosity at the wild-type *APC* allele (Reitmair *et al.*, 1996b). It is presumed that *MSH2* deficiency confers a mutator phenotype upon the cell resulting in point mutation of the remaining allele and is thus responsible for the increased formation of tumours. Indeed, in $RER^{+}$ human colorectal tumours a substantial excess of mismatch type *APC* mutations can be identified (Huang *et al.*, 1996). Interestingly, defective mismatch repair and accelerated tumourigenesis has been documented in the clinical setting with rapid transition from adenoma to carcinoma being observed in HNPCC patients undergoing routine colonoscopies (Vasen *et al.*, 1995).

Although great strides into the evolution of colorectal cancer and its genetic control have been made through the study of tumours and mouse models of colorectal cancer,

a relative lack of knowledge exists in our understanding of the initial stages of carcinogenesis within normal intestinal crypt cells. For example, knowledge of the factors regulating apoptosis within crypt cells remain elementary, as does the contribution of apoptosis to the development of initiated stem cells. In addition, the available data on the contribution of *MSH2* to the *in vivo* mutation rate of intestinal cells is subject to a number of confounding factors. Furthermore, no data exists on the co-operation of the two established forms of genomic instability within cells which drive tumourigenesis. It is the these very early steps in colorectal tumourigenesis, and the role of *MSH2*, *p53* and apoptosis that are the subject of this thesis.

# AIM

# AIM

The aim of this study was to investigate the role of the murine *MSH2* gene in tumourigenesis. Specific areas of focus included apoptosis, *in vivo* mutation frequency, and interaction with other tumour suppressor genes including *p53* and *APC*.

Specific questions included:

1. Is *MSH2* involved in regulating apoptosis *in vivo* following genotoxic damage?

2. If correct, is this form of apoptosis dependent upon *p53*?

3. What is the role of $O^6$-Alkylguanine-DNA-alkyltransferase (AGT) in modulating *MSH2*-dependent apoptosis?

4. How does the *MSH2* status affect *in vivo* mutation rate?

5. Are the consequences of *MSH2* deficiency altered in environments mutant for *p53* and *APC*, and indeed is there any direct interaction between these genes?

Each of these questions is addressed separately in Parts I to V.

# Part I

# MSH2 and Apoptosis

## *MSH2* and Apoptosis

### Introduction

*MSH2* has been primarily characterised by its ability to recognise mismatches as a heterodimer with the *GTBP* (*MSH6*) protein (Drummond *et al.*, 1995; Kolodner, 1995) and as a direct consequence of failure of this process, microsatellite instability and mutation rates are increased in *MSH2* -/- cells (de Wind *et al.*, 1995; Reitmair *et al.*, 1997). However, the consequences of *MSH2* deficiency are complex, with *MSH2* -/- cells also showing hyper-recombination, failure to undergo $G_2$ arrest following DNA damage, and increased survival following exposure to methylating agents *in vitro* (de Wind *et al.*, 1995; Hawn *et al.*, 1995). Methylating agents are a diverse group of compounds which share the potential to transfer alkyl groups ($-CH_3$) to biologically important macromolecules, especially DNA. Alkylation of cellular DNA by the compound N-methyl-N'-nitro-N-nitrososguanidine (MNNG) or two therapeutic alkylating compounds Dacarbazine and Temozolomide occurs at a number of sites within DNA, the most prevalent of which is the $O^6$ position of guanine (Swann, 1990). It is thought that $O^6$-methylguanine is responsible for both the antineoplastic and carcinogenic properties of these compounds (Karran & Bignami, 1992). DNA replication of $O^6$-methylguanine base pairs results in the formation of $O^6$-methylguanine:thymine mispairs. Futile attempts to correct this mismatch base pairing by the DNA mismatch repair pathway results in the repeated generation of single strand DNA breaks (Branch *et al.*, 1993; Karran & Bignami, 1994). It is these DNA strand breaks that are postulated to mediate cell death, perhaps through *p53* (Nelson & Kastan, 1994; Rafferty *et al.*, 1996). Cell lines or tumours defective in components of the mismatch repair pathway would be predicted to be resistant to the cytotoxic effects of alkylating agents. Results from several different tumour cell lines deficient in mismatch repair are consistent with this hypothesis (Koi *et al.*, 1994; Branch *et al.*, 1995; Liu *et al.*, 1996b; Aebi *et al.*, 1997).

The antitumour agent *cis*-diamminedichloroplatinum (Cisplatin) is used in the treatment of several types of tumour and introduces cytotoxic DNA damage predominantly in the form of 1,2 diguanyl intrastrand crosslinks (Eastman, 1983).

*MSH2* is thought to be important in mediating the cellular cytotoxicity of Cisplatin for three reasons. First, the Cisplatin 1,2 intrastrand adducts can be directly recognised by the *MSH2/GTBP* complex (Duckett *et al.*, 1996; Yamada *et al.*, 1997). Second, cell lines deficient in either *MSH2* or *MLH1* are tolerant to the cytotoxic effects of Cisplatin *in vitro* (Anthoney *et al.*, 1996; Drummond *et al.*, 1996; Aebi *et al.*, 1996). Finally, *in vivo MSH2* -/- xenografts in nude mice are significantly less responsive to Cisplatin than *MSH2* +/+ tumours (Fink *et al.*, 1997).

Hence, there is considerable evidence to suggest that *MSH2* status of a cell may affect its survival following the introduction of DNA damage normally recognised by *MSH2*. Therefore, the hypothesis was formulated that *MSH2* is involved in the regulation of apoptosis. At present no direct evidence exists for a role of *MSH2* in regulating apoptosis *in vitro* or *in vivo*, since previous studies have focused only on cell survival or clonogenicity. To test this hypothesis that *MSH2* regulates apoptosis, wild-type mice and mice bearing a targeted null mutation of *MSH2* were exposed to MNNG, Temozolomide, Dacarbazine and Cisplatin. The nature and prevalence of apoptosis within their small intestines was studied.

**Results**

*Can methylating agents and Cisplatin induce apoptosis in the small intestine of MSH2 +/+ and MSH2 -/- mice?*

Cohorts of mice, either *MSH2* +/+ or *MSH2* -/-, were injected with the DNA damaging agents MNNG, Temozolomide, Dacarbazine, and Cisplatin. Mice were killed and their intestines removed and fixed at various time points post-injection. Haematoxylin and eosin (H&E) sections were prepared and the prevalence of apoptotic bodies in 50 half crypts was counted using the Highly Optimized Microscope Environment (HOME; see Materials and Methods). In both *MSH2* +/+ and *MSH2* -/- mice all four compounds induced small intestinal crypt cell apoptosis at levels significantly higher than baseline rates (Figure 1.1). The number of apoptotic bodies observed in individual crypts varied and ranged from zero up to a maximum of approximately twenty-five. Apoptotic bodies were particularly prevalent in the lower half of the crypt with a marked lack of, or near-total absence of, apoptotic cells in the

## Figure 1.1

**(A)** H&E stained section of untreated wild-type (*MSH2* +/+) murine small intestine. No apoptotic bodies are visible. (X250)

**(B)** H&E stained section of small intestine from a *MSH2* +/+ mouse injected i.p. with 100mg/kg Temozolomide 6 hours previously. Arrows mark apoptotic bodies visible within the crypt. Note that the apoptotic bodies occur mainly in the lower region of the crypt. (X250)

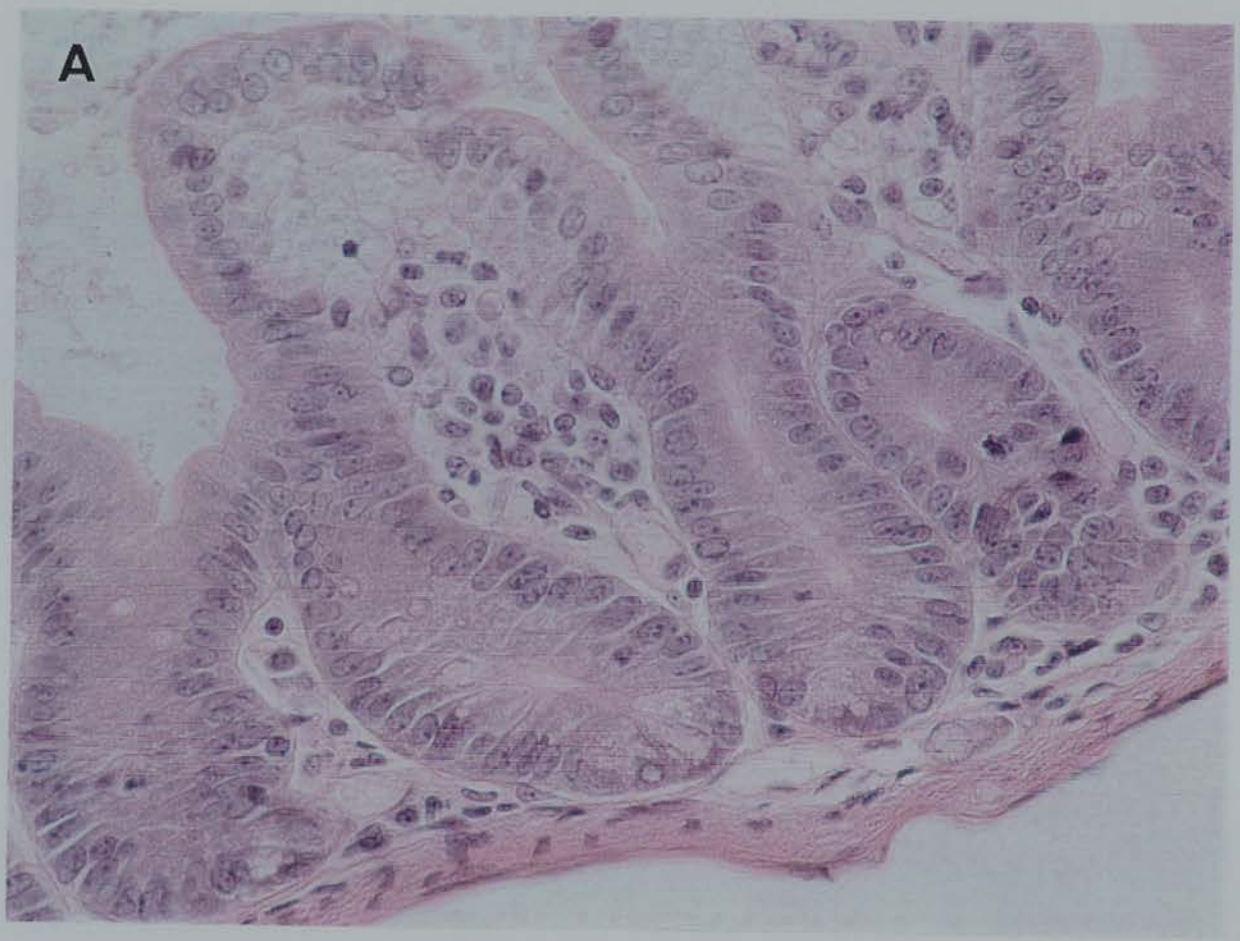
A

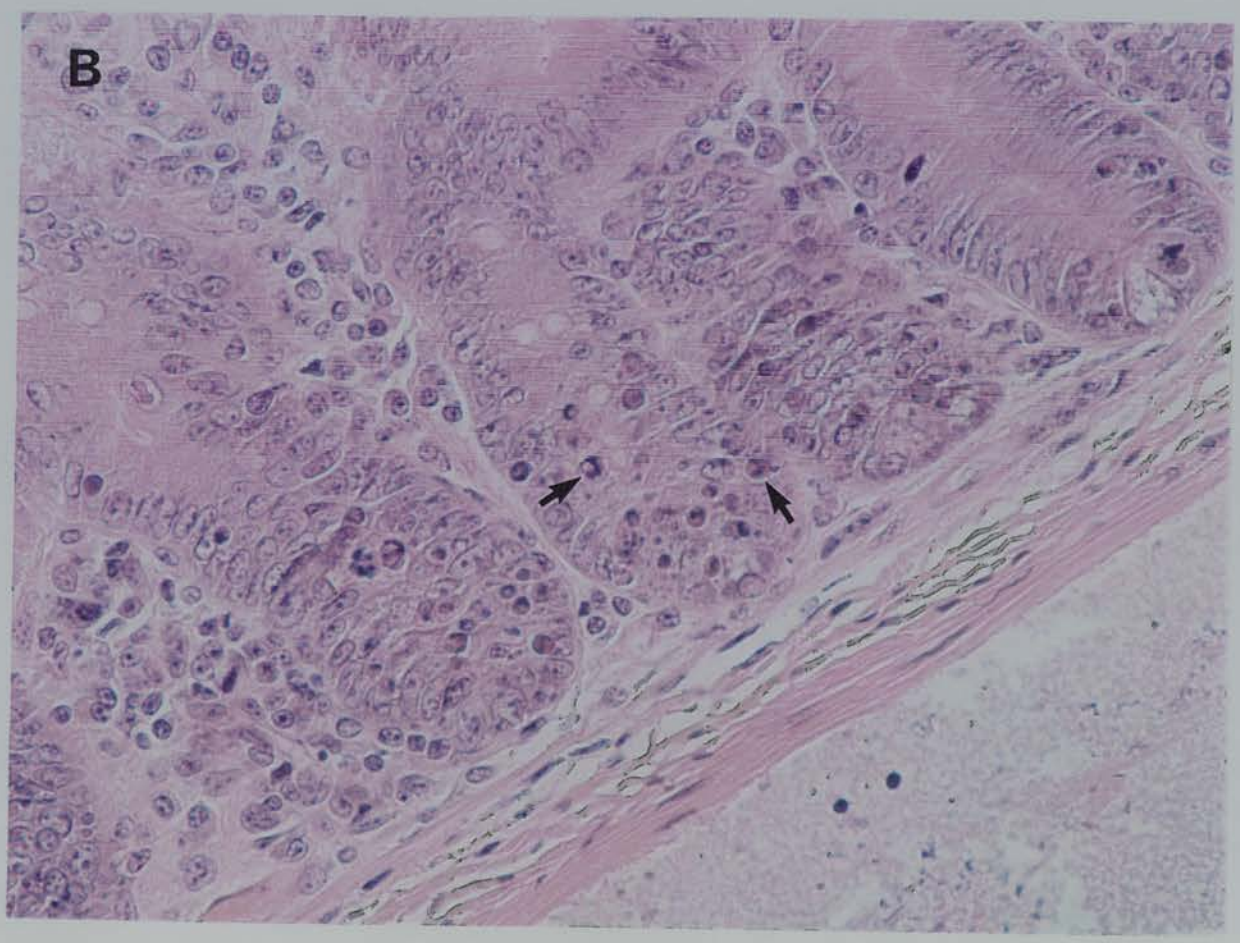
B

upper half of the crypt. The morphology of the apoptotic bodies induced by the different compounds was identical. In addition, the morphology of apoptosis observed in *MSH2* -/- mice was indistinguishable from that observed in *MSH2* +/+ mice.

*Which population of cells undergo apoptosis following exposure to methylating agents and Cisplatin?*

In order to characterise which population of cells within the crypt underwent apoptosis, cumulative counts of one hundred apoptotic bodies were performed in *MSH2* +/+ and *MSH2* -/- mice treated with MNNG, Temozolomide, Dacarbazine, and Cisplatin. Each apoptosis was assigned a crypt position from 1 to 22 as previously described by Potten (1990). The peak incidence of apoptotic bodies at six hours post-injection occurred at positions four, five, and six within the crypt with all four reagents (Figure 1.2 A-D). Positions four, five, and six are thought to represent the stem cell region of the small intestinal crypt (Potten, 1990). *MSH2* +/+ cells and *MSH2* -/- cells showed closely similar patterns in the distribution of apoptotic bodies within the crypts irrespective of the drug used. No apoptotic bodies were recorded above position 18 in the crypt for any drug at six hours.

*Does MSH2 status alter the level or the kinetics of apoptosis recorded in the small intestine following treatment with methylating agents and Cisplatin?*

Cohorts of *MSH2* +/+ and *MSH2* -/- mice were injected with MNNG, Temozolomide, Dacarbazine and Cisplatin at time zero. The prevalence of apoptotic bodies at 0, 3, 6, 12, 24, 48, and 72 hours post-injection was recorded (Figure 1.3 A-D). Peak prevalence of apoptotic bodies in both *MSH2* +/+ and *MSH2* -/- mice was observed at between 6 and 12 hours post-drug administration (except Dacarbazine which had a peak at 12 to 24 hours), with a mean of between five and eight apoptotic bodies per crypt recorded at this time point. The kinetics of apoptotic induction were similar for MNNG, Temozolomide, and Cisplatin with the apoptotic levels returning to near basal rates by 48 to 72 hours (Figure 1.3 A, B, D). Dacarbazine displayed different kinetics from the other compounds with a prolonged peak of apoptosis from 12 to 24 hours (Figure 1.3 C). No difference in the basal levels of apoptosis was observed

## Figure 1.2 (A&B)

Cumulative counts of one hundred apoptotic bodies were performed in *MSH2* +/+ and *MSH2* -/- animals. Each apoptosis was assigned a crypt position from 1 to 22. Apoptosis was scored 6 hours after exposure to **(A)** 50mg/kg MNNG and **(B)** 100mg/kg Temozolomide. Solid line, *MSH2* +/+; dotted line *MSH2* -/-.

A MNNG

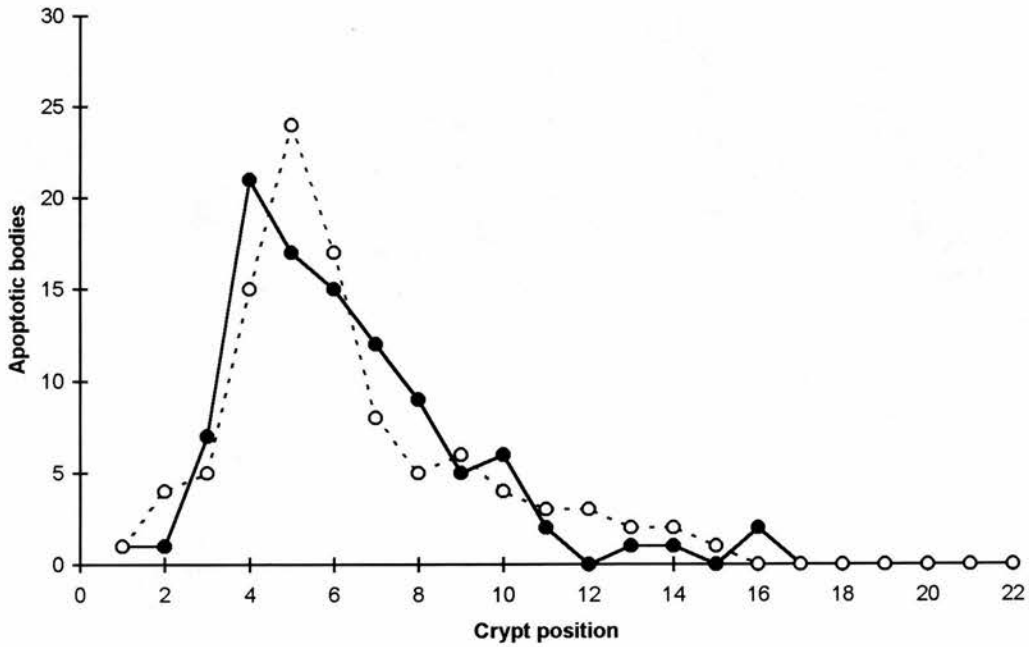


B Temozolomide

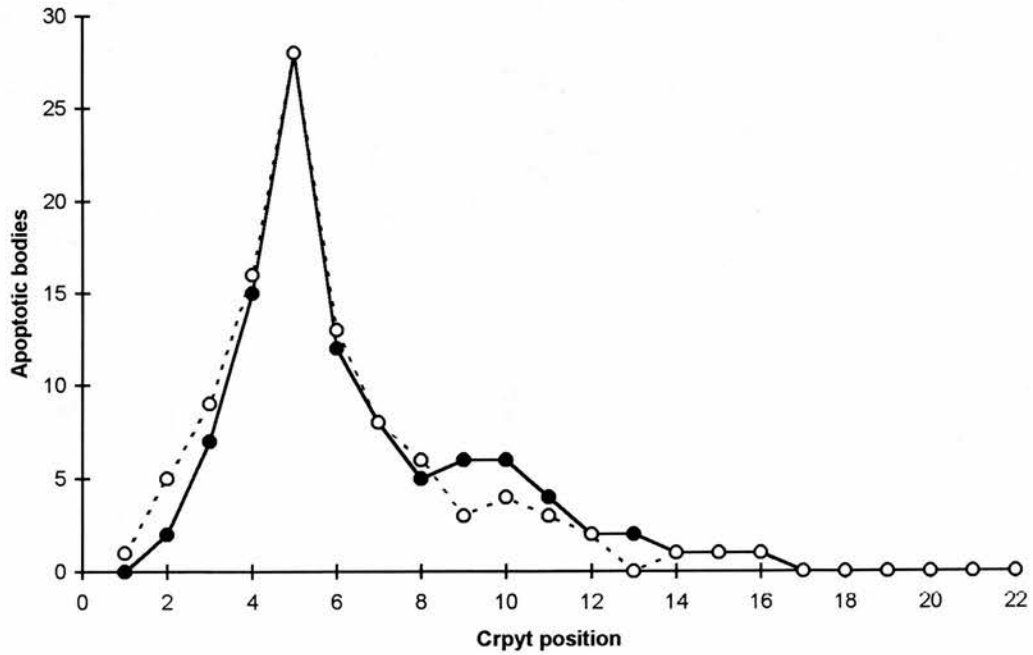

## Figure 1.2 (C&D)

Cumulative counts of one hundred apoptotic bodies were performed in *MSH2* +/+ and *MSH2* -/- animals. Each apoptosis was assigned a crypt position from 1 to 22. Apoptosis was scored 6 hours after exposure to **(C)** 150mg/kg Dacarbazine and **(D)** 10mg/kg Cisplatin. Solid line, *MSH2* +/+; dotted line *MSH2* -/-.

C Dacarbazine

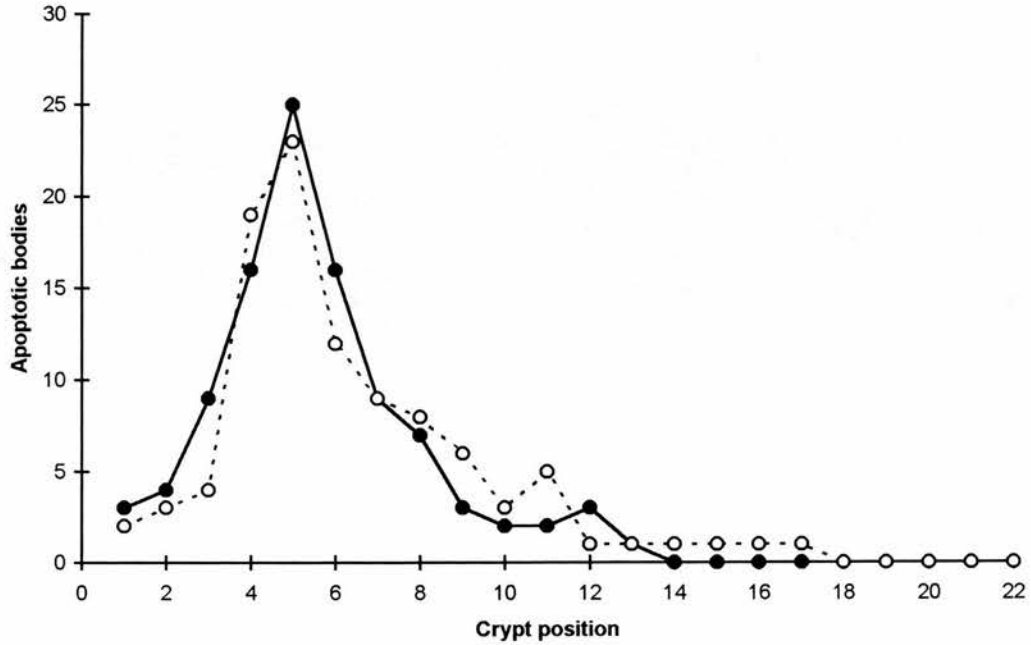


D Cisplatin

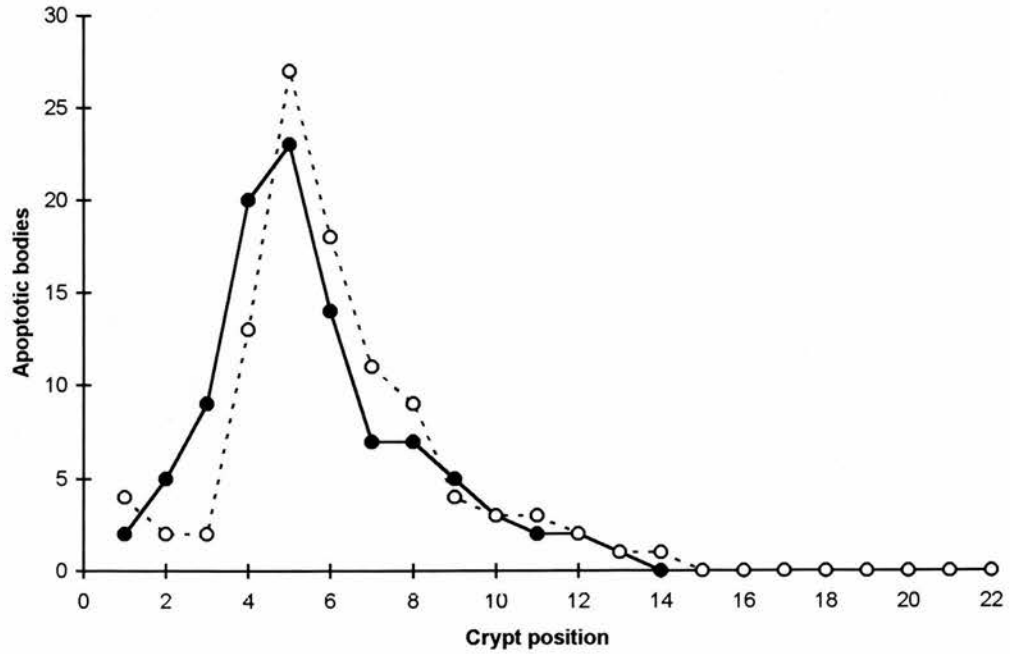

## Figure 1.3 (A&B)

Cohorts of *MSH2* +/+ or MSH2 -/- animals were given i.p. injections of **(A)** 50mg/kg MNNG and **(B)** 100mg/kg Temozolomide at time zero. The data show the means of the prevalence of apoptotic bodies per 50 half crypts at various time points after drug administration. Each point represents data from a minimum of 3 mice. Closed circle symbols, *MSH2* +/+; open circle symbols, *MSH2* -/-. Error bars represent standard error of the mean (sem).

A MNNG

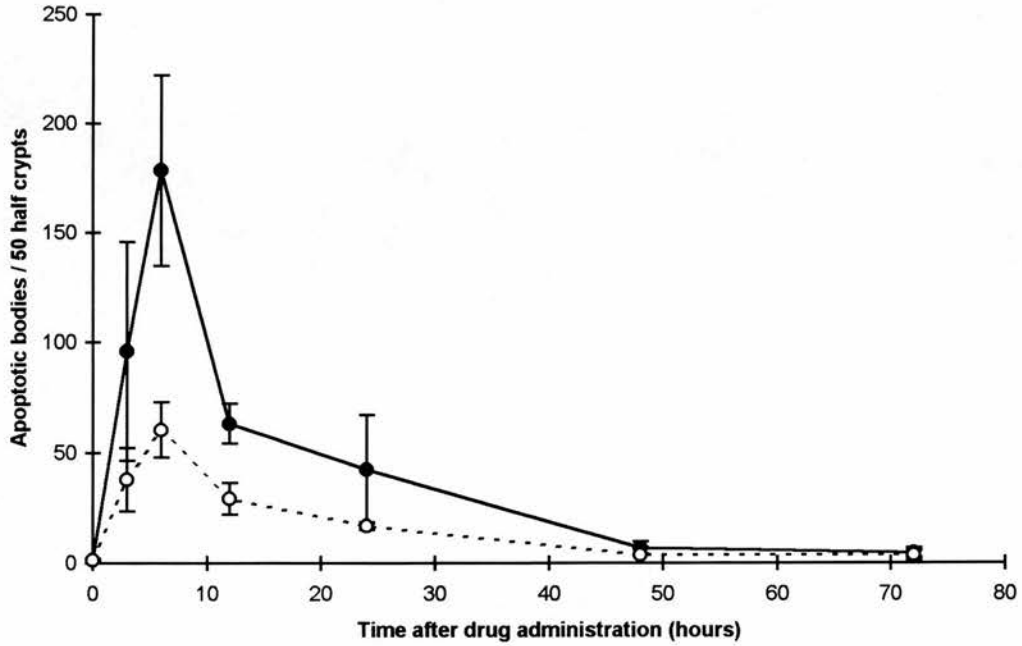


B Temozolomide

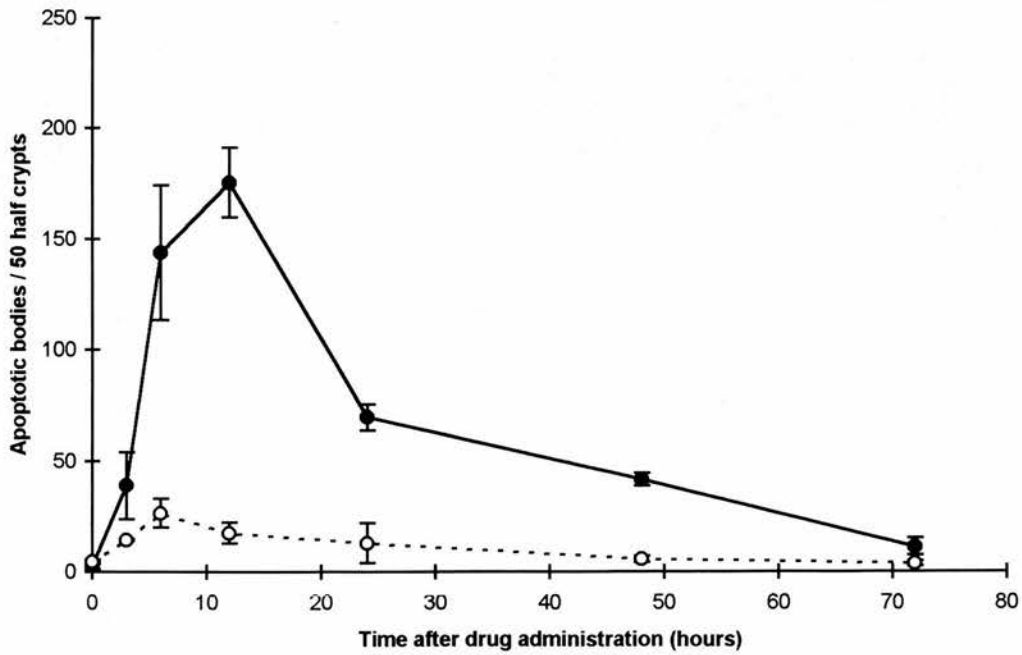

## Figure 1.3 (C&D)

Cohorts of *MSH2* +/+ or *MSH2* -/- animals were given i.p. injections of **(C)** 150mg/kg Dacarbazine and **(D)** 10mg/kg Cisplatin at time zero. The data show the means of the prevalence of apoptotic bodies per 50 half crypts at various time points after drug administration. Each point represents data from a minimum of 3 mice. Closed circle symbols, *MSH2* +/+; open circle symbols, *MSH2* -/-. Error bars represent sem.

C Dacarbazine

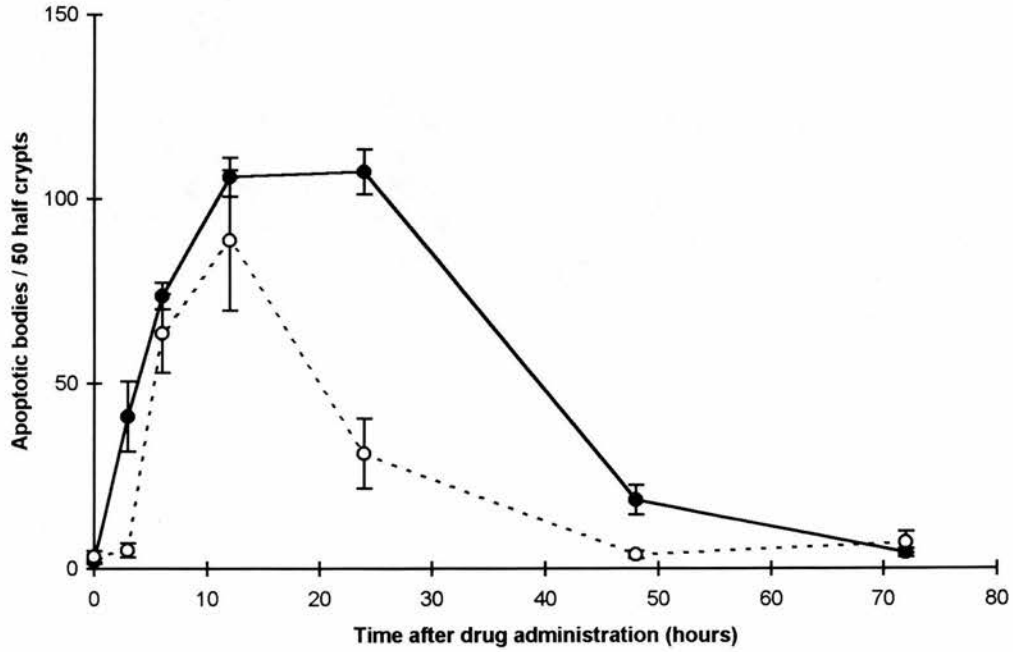


D Cisplatin

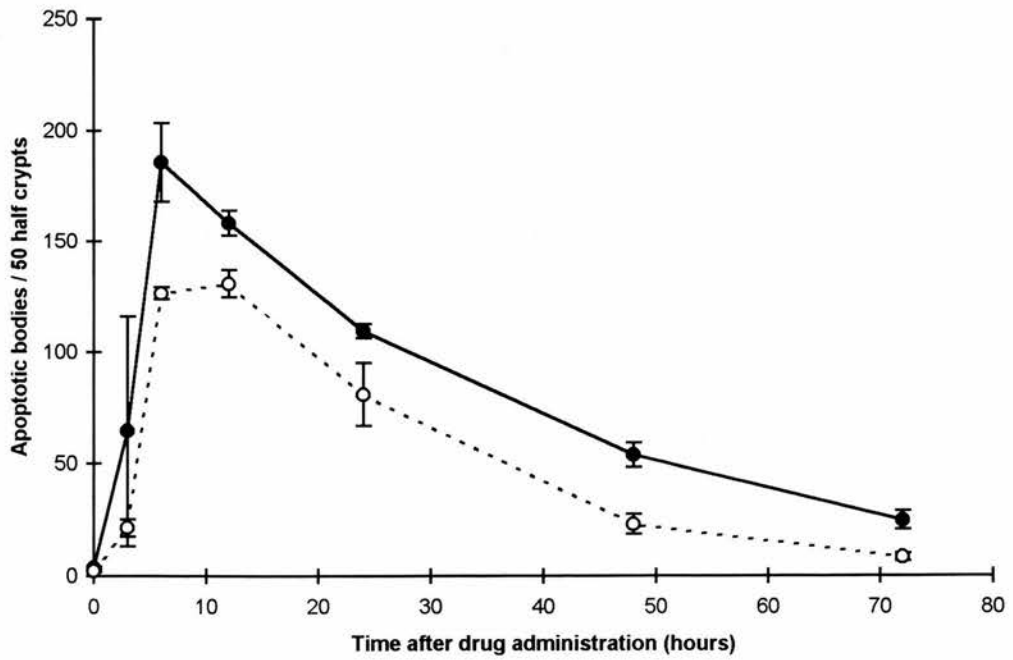

between untreated *MSH2* +/+ and *MSH2* -/- mice. However, following reagent administration *MSH2* -/- mice displayed markedly lower levels of apoptosis compared to wild-type (*MSH2* +/+) controls, with an *MSH2*-dependent decrease in apoptosis observed only after 12 hours in the case of Dacarbazine. In addition, the ratio of the levels of apoptosis observed in the presence and absence of *MSH2* varied with drug type, with the greatest reduction in apoptosis in the absence of *MSH2* being observed with Temozolomide and the least for Cisplatin. At peak prevalence of apoptosis *MSH2*-deficiency conferred a 9.9, 3.0, and 1.5-fold reduction in apoptosis following Temozolomide, MNNG, and Cisplatin respectively ($p<0.05$ for all drugs, Mann-Whitney U). Notwithstanding the lower levels of apoptosis, the kinetics of induction of apoptosis in *MSH2* -/- cells were closely similar to those in *MSH2* +/+ cells.

*Does a dose-response relationship exist between the dose of Temozolomide administered and the level of intestinal apoptosis recorded? Does MSH2 status affect this relationship?*

Cohorts of mice either *MSH2* +/+, *MSH2* +/-, or *MSH2* -/- were injected with a range of doses of Temozolomide from 25mg/kg to 500mg/kg. The prevalence of apoptotic bodies in the small intestine was recorded. Temozolomide induced apoptosis in wild-type, heterozygote, and homozygote *MSH2* mice above basal levels at all doses. This was performed initially as one large experiment and suggested that a dose response relationship may exist. However, pooled data from other relevant Temozolomide experiments demonstrated that no dose response relationship existed in wild-type and heterozygote mice between increasing doses of Temozolomide and the prevalence of apoptotic bodies recorded (Figure 1.4). The inclusion of such additional data highlights the inter-experimental error inherent to the calculation of the prevalence of apoptosis. The possible reasons for such error is addressed in the Materials and Methods section. However, an approximately linear relationship still existed in homozygote *MSH2*-/- mice. Homozygote mice *MSH2*-/- also displayed significantly lower levels of apoptosis than *MSH2* +/+ or *MSH2* +/- mice for any given dose ($p<0.05$, anova).

## Figure 1.4

Cohorts of *MSH2* +/+, *MSH2* +/-, *MSH2* -/- mice injected i.p. at time zero with a range of doses of Temozolomide (25mg/kg to 500mg/kg). Mice were sacrificed six hours post-injection and intestinal apoptosis scored. Closed circle symbols, *MSH2* +/+; closed triangle symbols *MSH2* +/-; open circle symbols, *MSH2* -/-. Each point represents data from a single mouse.

[Additional relevant data was included from Figures 1.3B, 1.5, and 3.3C]

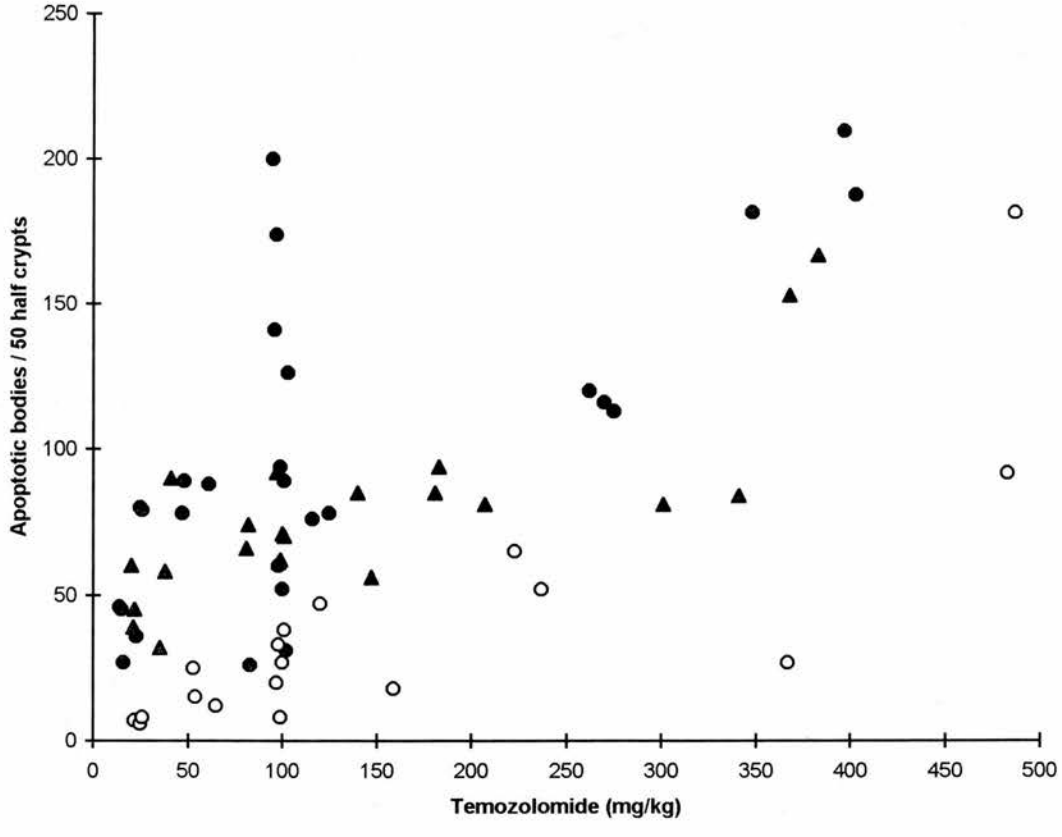
Apoptotic bodies / 50 half crypts
250
200
150
100
50
0
0
50
100
150
200
250
300
350
400
450
500
Temozolomide (mg/kg)

*Is a single copy of MSH2 able to couple DNA damage of mismatch type to apoptosis efficiently?*

The prevalence of apoptosis in *MSH2* +/+, *MSH2* +/- (which only have one functional copy of *MSH2*) and *MSH2* -/- mice was scored at 0, 3, 6, 12, 24, 48, and 72 hours after injection with 100mg/kg Temozolomide (Figure 1.5). Temozolomide induced high levels of apoptosis in both *MSH2* +/+ and *MSH2* +/- mice with peak levels occurring between 6 and 24 hours. By 72 hours the levels of apoptosis had returned to near basal rates. The kinetics of apoptosis induction were similar in *MSH2* +/+ and *MSH2* +/- mice, with no delay or reduction in absolute level being observed in heterozygotes compared to wild-types ($p>0.2$, Mann-Whitney U). *MSH2* -/- homozygote mice displayed similar kinetics to wild-type and heterozygote mice although the levels of apoptosis were markedly reduced at all time points between 6 and 48 hours post-injection when compared to wild-type or heterozygote mice ($p< 0.001$, Mann-Whitney U).

*Does the reduction in the level of apoptosis observed in MSH2 -/- mice following methylating agents result from MSH2 acting as a non-specific sensor of DNA damage or as a sensor of specific categories of DNA damage such as methylation?*

Cohorts of *MSH2* +/+ and *MSH2* -/- mice were exposed to 4 Gray of γ-irradiation, a dose shown to be effective in inducing apoptosis in small intestinal epithelium in previous experiments (Clarke *et al.*, 1994). γ-irradiation induces DNA strand breaks which are not known to be recognised by *MSH2*. The prevalence of apoptotic bodies in the small intestine was determined at 0, 4, 8, 24, 36, 48 and 60 hours post-irradiation (Figure 1.6). *MSH2* +/+ or *MSH2* -/- mice behaved identically in their apoptotic response with a rapid induction of apoptosis observed at four hours. This was followed by a decrease in the levels at eight hours with a second smaller peak of apoptosis being observed at 24 hours. Apoptotic frequencies returned to basal levels by 60 hours. No significant ($p>0.4$, Mann-Whitney U) difference in the prevalence of apoptosis between *MSH2* +/+ or *MSH2* -/- mice was observed at any of the time points recorded.

## Figure 1.5

Cohorts of *MSH2* +/+, *MSH2* +/-, *MSH2* -/- mice injected i.p. at time zero with 100mg/kg Temozolomide. A minimum of three mice were sacrificed at each time point and intestinal apoptosis scored. Closed circle symbols, *MSH2* +/+; closed triangle symbols *MSH2* +/-; open circle symbols, *MSH2* -/-. Error bars represent sem.

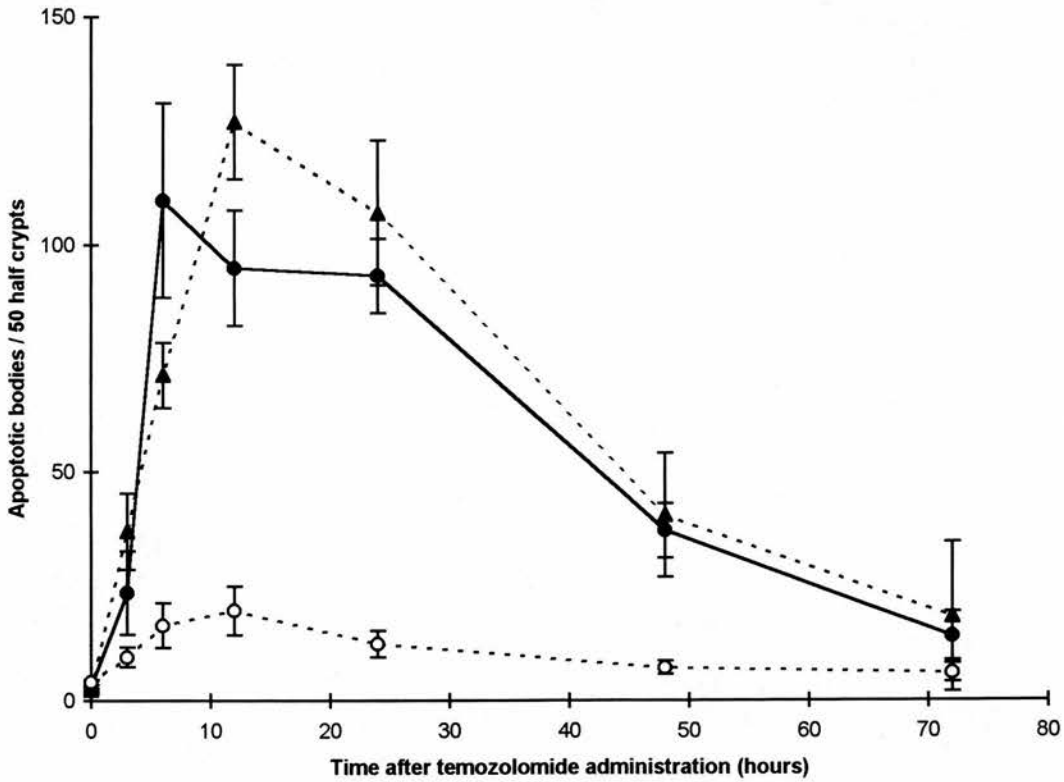
150
100
50
0
Apoptotic bodies / 50 half crypts
0
10
20
30
40
50
60
70
80
Time after temozolomide administration (hours)

## Figure 1.6

Cohorts of *MSH2* +/+ and *MSH2* -/- mice were exposed to 4 Gray of ionising γ-irradiation at time zero. Mice were killed at the indicated time points and intestinal apoptosis scored. Each point represents data from a minimum of three mice. Closed circle symbols, *MSH2* +/+; open circle symbols, *MSH2* -/-. Error bars represent sem.

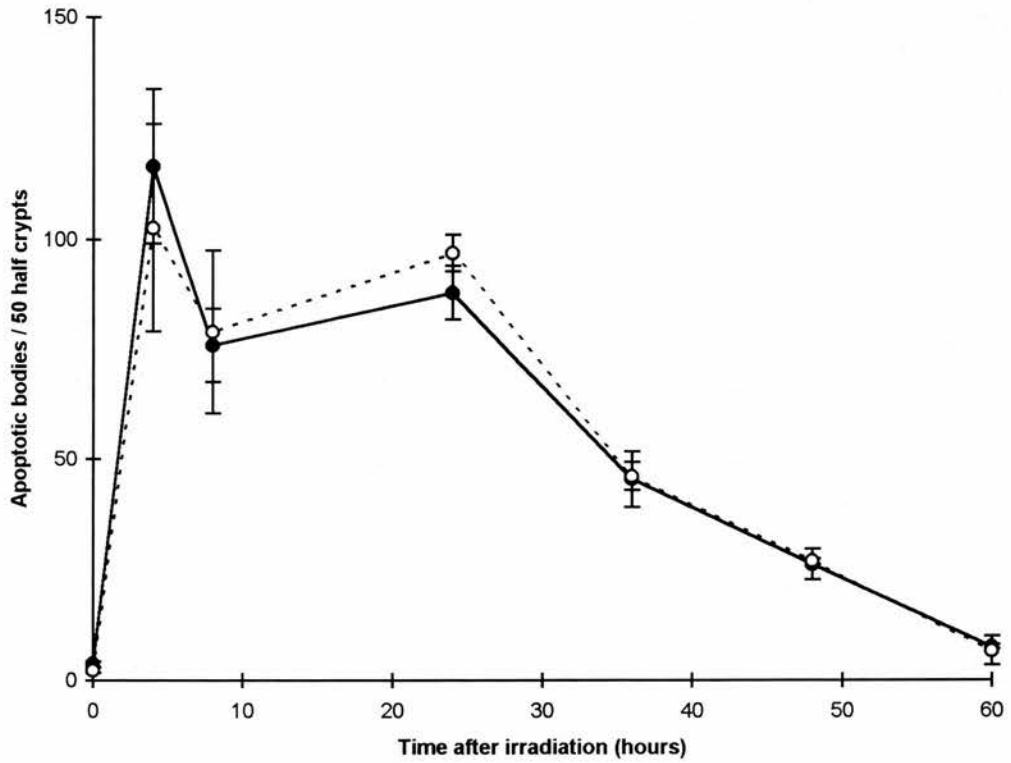
150
100
50
0
Apoptotic bodies / 50 half crypts
0
10
20
30
40
50
60
Time after irradiation (hours)

**Discussion**

To test directly if *MSH2* has a significant role in the induction of apoptosis *in vivo* *MSH2* +/+ and *MSH2* -/- mice were exposed to the methylating agents MNNG, Temozolomide, and Dacarbazine, and also to the cross-linking agent Cisplatin. All these compounds are known to induce DNA damage which is specifically recognised by *MSH2* (Karran & Bignami, 1992; Liu *et al.*, 1996b; Yamada *et al.*, 1997). The prevalence of apoptotic bodies within the small intestine was scored by microscopy. The murine small intestine was used as an *in vivo* model for the study of apoptosis for three principal reasons. First, the known intestinal expression of *MSH2* (J. Bubb, personal communication; Leach *et al.*, 1996). Second, the demonstrated role of *MSH2* in the prevention of intestinal neoplasia. Third, because apoptosis within the murine small intestine has been well characterised previously (Potten, 1990; Clarke *et al.*, 1994 & 1997). If *MSH2* is involved in the induction of apoptosis after DNA damage induced by these agents, then lack of *MSH2* is hypothesised to abolish any coupling between such DNA damage and apoptosis.

In both *MSH2* +/+ and *MSH2* -/- mice, all methylating agents and Cisplatin induced levels of apoptosis significantly higher than background rates alone. This novel finding was anticipated in view of previous work by Potten *et al.* (1992 & 1997) demonstrating that following a variety of DNA damaging agents, crypt cell apoptosis ensues. Apoptosis occurred at peak levels within the stem cell compartment of the crypt in both *MSH2* +/+ and *MSH2* -/- mice following exposure to methylating agents with the mode lying between positions 4 and 6 (Potten, 1990). This pattern of apoptosis was similar to that seen in the small intestine following N-nitroso-N-methylurea (NMU) and γ-irradiation, with stem cells in the crypt being the most susceptible (Potten *et al.*, 1992 & 1997; Clarke *et al.*, 1994). Cisplatin-induced apoptosis also occured predominantly within the stem cell region of the crypt - again indicating the specific sensitivity of cells at the stem cell position to apoptosis. *MSH2* -/- cells also underwent apoptosis peaking at positions 4 to 6, with *MSH2* status failing to alter the distribution of apoptosis within the crypt. Hence, both *MSH2*-dependent and *MSH2*-independent apoptosis occurred predominantly in the stem cell compartment.

The peak prevalence of apoptosis induced by methylating agents occurred in stem cells, at positions 4 to 6, but not at positions 8 to 10 which is the main site of DNA replication determined by bromodeoxyuridine (BrdU) incorporation (Potten, 1990; Clarke *et al.*, 1994). The current hypothesis on the mechanism of action of methylating agents is that following methylation of guanine bases, $O^6$-methylguanine must first undergo DNA synthesis with generation of an $O^6$-methylguanine:thymine mispair, fixing the mutation into the genome. Thus, one possibility is that a high prevalence of apoptosis in positions 8 to 10 of the crypt might have been expected. However, this was not found to be the case and the data suggest that methylating agents induce DNA damage capable of rapidly inducing apoptosis, without the need for DNA synthesis.

In *MSH2* +/+ animals, all of the drugs used induced measurable levels of intestinal apoptosis and in all cases the peak induction of apoptosis was seen between 8 and 24 hours. In comparison to the pattern observed in the *MSH2* +/+ animals, the apoptotic response of *MSH2* -/- mice was significantly diminished for all four drugs. Thus, *MSH2* must play a significant role in murine small intestinal apoptosis induced by DNA damage of mismatch type. The *MSH2* dependency was greatest for Temozolomide and least for Cisplatin, and only visible after 12 hours with Dacarbazine. Why should the degree of dependency on *MSH2* status vary with drug type? A simple explanation is that Temozolomide-induced lesions may be specifically recognised predominantly or almost entirely by *MSH2* and the mismatch repair pathway. By comparison, Cisplatin-induced cross-links which although recognised by *MSH2*, may be removed by alternative DNA repair pathways such as the nucleotide excision repair pathway (Duckett *et al.*, 1996; Moggs *et al.*, 1996). The difference in the kinetics of apoptosis induced by Temozolomide and Dacarbazine is surprising in view of the fact that both drugs methylate DNA through the same intermediate 5-(3-methyl-triazine-1-yl)imidazole-4-carboxamide (MITC) (Stevens *et al.*, 1987; Denny *et al.*, 1994). However, the method of generation of MITC differs between the two drugs with Temozolomide reacting spontaneously with water to give MITC, while Dacarbazine requires oxidative N-demethylation by cytochrome P450 enzymes (Figure 3.6). This difference in metabolism alone may account for the delay in the

kinetics of apoptosis in wild-type mice induced by Dacarbazine compared to Temozolomide. Other non-specific factors that may account for the differences between drugs include solubility, variations in the metabolic products formed during breakdown of the compounds, and possible differences in specificity of the alkyl group transfer may exist (e.g. to proteins and other DNA targets including thymine to give $O^4$-methylthymine) (Pegg & Byers, 1992). The reason why Dacarbazine differs in its *MSH2*-dependency from Temozolomide is unknown. However, with all four drugs tested, absence of *MSH2* compromised the ability of cells to enter apoptosis. It remains possible that the cohort of damaged cells protected from apoptosis by absence of *MSH2* may be removed by death outwith the time span analysed here, or that these cells may be prevented from propagating by some other mechanism, such as permanent cell cycle arrest. Nonetheless, the phenomenon of delayed apoptosis which has been observed in *p53* -/- mice following γ-irradiation (Clarke *et al.*, 1997; Merritt *et al.*, 1997) and seen here following Temozolomide (see Part II of this thesis) was not observed in *MSH2* -/- mice. Thus, the most direct conclusion is that a significant number of cells escape death by virtue of *MSH2* deficiency and are therefore potential founders of clones bearing unrepaired mutations.

Evidence for a dose response was obtained from one experiment, however, when all relevant data from other experiments were included this relationship was not confirmed. This highlights the difficulties with the reproducibility of *in vivo* apoptotic data between experiments and the inter-experimental variation that exists. Possible mechanisms to account for such variations are addressed in the Materials and Methods as is the methodology used to try to minimise this error. Data from Figure 1.4 does not therefore provide evidence for a relationship between increasing doses of Temozolomide and the prevalence of apoptosis recorded. Two possible explanations exist. First, at the doses of Temozolomide used the level of DNA damage induced is above the critical level required to induce apoptosis in susceptible cells. Thus, increasing the dose of Temozolmide will increase the level of cellular DNA damage but not apoptosis. Alternatively, at doses beyond approximately 100mg/kg Temozolomide, it is possible that the maximal prevalence of crypt cell apoptosis has been attained and hence the lack of dose response seen may reflect a limitation in the

apoptotic assay. It remains possible that such a dose response occurs but this has been masked by the inter-experimental error. Why should a dose response appear to exist only for the homozygote *MSH2* -/- mice? It is possible that the lower levels of apoptosis observed allowed a dose response to be recorded as maximal crypt cell apoptosis had not yet been reached. However, it is also possible that the *MSH2* - independent apoptosis responds proportionately to increasing doses of Temozolomide. At present no clear explanation exists for the lack of dose response observed in wild-type and heterozygotes, but not in homozygote mice.

Is a single copy of *MSH2* (as exists in the intestinal cells of HNPCC patients) capable of linking DNA damage to apoptosis? The apoptotic response of heterozygote *MSH2* +/- mice following Temozolomide treatment was closely similar to their wild-type *MSH2* +/+ counter parts. No evidence of a time delay in the onset of apoptosis was apparent in the heterozygote mice. These results demonstrate that a single functional allele of *MSH2* is capable of the effective induction of apoptosis even at high levels of DNA damage, unlike *p53* where a single allele compromises the efficiency of coupling DNA damage to apoptosis (Clarke *et al.*, 1994).

Apoptosis of lower crypt cells can be initiated by exposure to γ-irradiation (Clarke *et al.*, 1994; Merritt *et al.*, 1994 & 1997). γ-irradiation is thought to induce DNA strand breaks which are coupled to apoptosis by *p53*-dependent pathways in the immediate apoptotic response and to *p53*-independent pathways in the delayed apoptotic response. To exclude the possibility that *MSH2* was acting as a non-specific DNA damage sensor or was involved as a effector protein in the apoptotic cascade within small intestinal cells, *MSH2* +/+ and *MSH2* -/- mice were irradiated. If either possibility were true, absence of *MSH2* would be expected to compromise the induction of apoptosis in response to irradiation. However, apoptosis induced by γ-irradiation was quantitatively identical in *MSH2* +/+ and *MSH2* -/- animals, demonstrating that *MSH2* acts neither as a sensor of generalised DNA damage nor as an essential general effector protein of apoptosis in intestinal cells. Rather, the apoptosis-inducing function of *MSH2* appears to be specific for DNA methylation and to a lesser extent Cisplatin DNA cross-linking, with both types of lesion known to involve activation of the mismatch repair pathway. Hence, the signal for apoptosis in

lower crypt cells injured by methylating agents and Cisplatin arises subsequent to and is specified by recruitment of *MSH2*. The precise nature of this signal is unknown but presumably arises within the complex of *MSH2*-dependent repair proteins and DNA. The significance of the these findings to carcinogenesis is that cells with absent *MSH2* not only have a reduced capacity for DNA repair but also a compromised ability to enter apoptosis following methylating type DNA damage. Are cells of the intestine exposed to compounds capable of methylation? The relationship between saturated fat in the diet and colon cancer is well established (Bresalier & Kim, 1993). Indeed, there is a positive correlation between high levels of faecal bile acids (which are derived from fatty acids) and colorectal cancer incidence (Reddy & Wynder, 1973). Bile acid conjugates of glycoholic and taurocholic acid can undergo N-nitrosation form N-nitrosamides, very similar compounds to MNNG (Shuker *et al.*, 1981). Furthermore, N-nitroso bile acid conjugates are genotoxtic inducing the same spectrum of mutations that MNNG produces (Puju *et al.*, 1982). Therefore, cells of the small and large intestine are constantly subjected to nitrosated bile acid conjuates capable of inducing DNA damage of mismatch type. This has two consequences. First, any cell with compromised *MSH2* function would be predicted to accumulate point mutations at a greater rate than normal and also by virtue of *MSH2* deficiency have a greatly reduced probability of entering into apoptosis, thus predisposing itself to be a founder cell of an ensuing malignancy. Second, constant selection pressure from carcinogenic bile acids may encourage the emergence of methylation tolerant clones of cells. Such cells would be deficient in mismatch repair, possess the "mutator phenotype" with an unstable genome conferring a distinct growth advantage on that particular cell. However, absence of *MSH2* would only be relevant to methylating DNA damage and not other compounds which can induce alternative forms of DNA damage, since cells lacking *MSH2* exposed to γ-irradiation did not compromise their ability to induce apoptosis. In addition, cells with only one copy of *MSH2* are able to induce apoptosis effectively. HNPCC patients are therefore likely to possess intestinal cells which are not compromised in their ability to undergo apoptosis in response to methylating DNA damage at least initially. However, cells of HNPCC patients which lose the remaining copy of *MSH2* by somatic mutation, may also lose their ability to couple

DNA damage to apoptosis. Such cells are at high risk of being the founder cell of a colorectal cancer.

Can the finding that untransformed intestinal cells which lack *MSH2* show a reduced apoptotic potential be extrapolated to tumour cells themselves? This can only be answered by further *in vivo* studies of tumour cell apoptosis, tumour growth, and responsiveness to chemotherapy in *MSH2* +/+ and *MSH2* -/- cancers. Such studies may highlight the importance of *MSH2* in the later stages of carcinogenesis and responsiveness to chemotherapy.

# Part II

# Role of *p53* in *MSH2*-dependent Apoptosis

## Role of *p53* in *MSH2*-dependent Apoptosis

### Introduction

Wild-type *p53* is a critical regulator of apoptosis in a variety of cell types with loss of or mutation in *p53* compromising the ability of such cells to enter apoptosis (Lowe *et al.*, 1993b; Lyons & Clarke, 1997). There are a number of reasons why *p53* may be involved in *MSH2*-dependent apoptosis in the small intestine following exposure to methylating agents. First, *p53* is known to be a key protein in the apoptotic response of murine small intestinal crypt cells following DNA damage (Clarke *et al.*, 1994; Merritt *et al.*, 1997; Potten *et al.*, 1997). For example, following exposure to ionising irradiation, there is an increase in *p53* nuclear immunoreactivity which occurs most strongly in the stem cell zone. When *p53* immunoreactivity and apoptosis are recorded on a positional basis within the intestinal crypt, they overlay each other precisely (Merritt *et al.*, 1994). Second, small intestinal crypt cells which lack *p53* fail to undergo apoptosis in response to γ-irradiation, with *p53* being essential for the immediate (4 to 6 hour) wave of apoptosis (Clarke *et al.*, 1994; Merritt *et al.*, 1994). Third, *p53* is a critical regulator of the cell cycle and apoptosis in response to a variety of DNA damaging agents, including methylating agents (Zhan *et al.*, 1993; Lowe *et al.*, 1993b; Levine, 1997). Lastly, in addition to the role of *p53* in controlling cell cycle and apoptosis there is evidence that *p53* itself can act as a sensor of DNA damage in the form of insertion/deletion mismatches (Lee *et al.*, 1995). This raises the possibility that *p53* may also be involved in direct recognition of the mismatched bases that arise from the methylation of guanine residues. Thus, for all the above reasons the *MSH2*-dependent apoptotic response of small intestinal crypt cells to methylating agents may require *p53*.

To address the potential role of *p53* in *MSH2*-dependent apoptosis, *p53* null mice were exposed to methylating agents and Cisplatin. Furthermore, the timecourse of apoptosis in *p53* null mice and mice doubly null for both *MSH2* and *p53* (*MSH2* -/- *p53* -/-) following exposure to Temozolomide was recorded. Hence, the role of *p53* and any interaction with *MSH2*, in the apoptotic response of murine small intestine to methylating DNA damage was evaluated.

**Results**

*Is p53 required for the immediate wave of intestinal apoptosis seen following exposure to methylating agents and Cisplatin ?*

Cohorts of *p53* +/+ and *p53* -/- mice (Clarke *et al.*, 1993) were injected with 50mg/kg MNNG, 100mg/kg Temozolomide, 150mg/kg Dacarbazine, or 10mg/kg Cisplatin. Apoptosis was scored in the crypts of the small intestine six hours after drug administration (Figure 2.1). In *p53* +/+ mice high levels of apoptosis were evident (see Part I of this thesis). However, for all reagents tested, absence of *p53* resulted in significantly lower levels of apoptosis ($p<0.05$, Mann-Whitney U) and were similar to the background levels of spontaneous apoptosis that occur in small intestinal crypts.

*Does the phenomenon of delayed p53-independent apoptosis seen following γ-irradiation also occur following Temozolomide administration? If so, does MSH2 status affect it?*

Cohorts of *p53* -/- mice and mice null for both *MSH2* and *p53* (*MSH2* -/- *p53* -/-) were treated with 100mg/kg Temozolomide at time zero. Apoptosis was scored at intervals up to 120 hours post-injection (Figure 2.2). In the small intestines of *p53* null mice no measurable apoptosis was recorded up to 12 hours. From 24 to 96 hours levels of apoptosis were elevated and peaked at 72 hours. At no time did the prevalence of apoptosis reach values associated with wild-type mice. By 120 hours post-drug administration apoptosis had returned to basal levels. Double mutant (*MSH2* -/- *p53* -/-) mice displayed only baseline levels of apoptosis up to 96 hours after exposure to Temozolomide. Absence of *MSH2* effectively abrogated the *p53*-independent apoptotic response of the murine small intestine to Temozolomide.

*Does the p53-independent apoptosis induced by Temozolomide treatment alter the morphology or crypt position of the observed apoptosis?*

The morphology of the apoptotic bodies in *p53* -/- mice occurring 48 to 72 hours after injection of 100mg/kg Temozolomide differed from those seen in wild-type mice, and occurred mainly in the upper half of the crypt (Figure 2.3). They were approximately twice the volume and appeared to possess many condensed chromatin

## Figure 2.1

Bar chart showing the mean prevalence of apoptotic bodies in *p53* +/+ and *p53* -/- mice six hours after i.p. injections of 50mg/kg MNNG, 100mg/kg Temozolomide, 150mg/kg Dacarbazine, or 10mg/kg Cisplatin. Wild-type data reproduced from Figure 1.3. Each bar represents the data from three mice. Closed bars, *p53* +/+; open bars *p53* -/-. Error bars represent standard error of the mean .

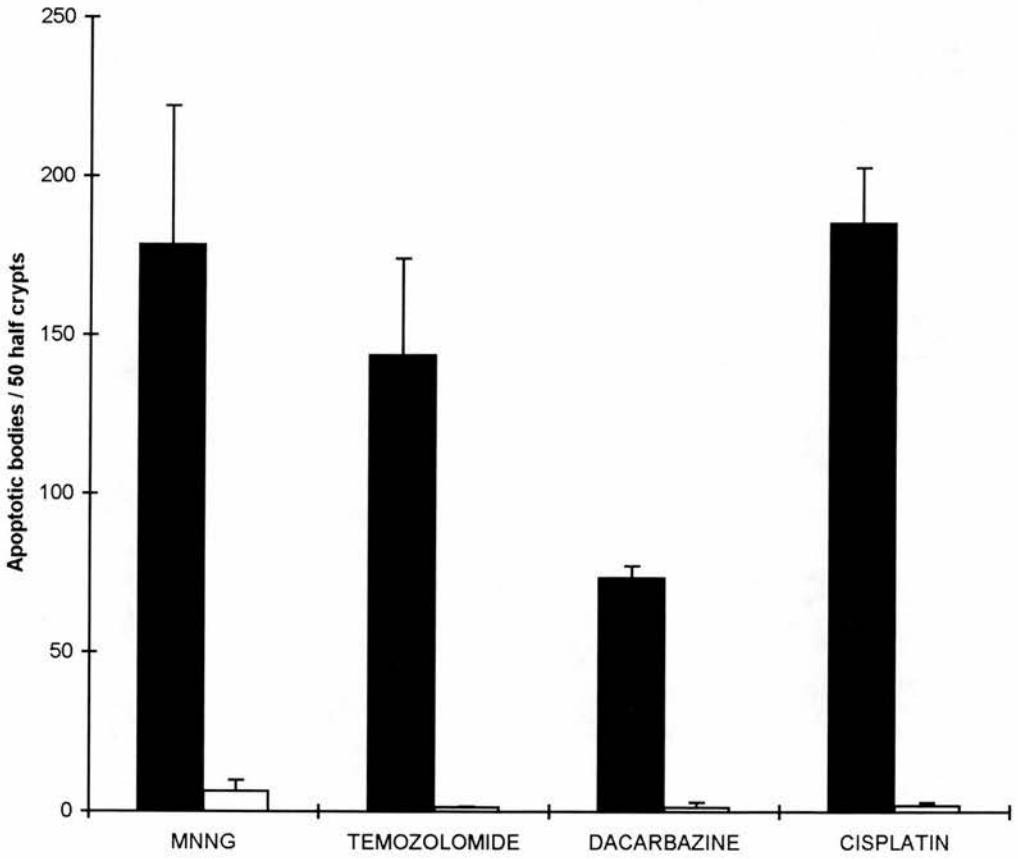
250
200
150
100
50
0
Apoptotic bodies / 50 half crypts
MNNG
TEMOZOLOMIDE
DACARBAZINE
CISPLATIN

## Figure 2.2

Timecourse of the levels of apoptosis in *p53* +/+ and *p53* -/- mice, and also mice doubly mutant for both *MSH2* and *p53* following i.p. injection of 100mg/kg Temozolomide at time zero. Each point represents data from a minimum of three mice. *MSH2* wild-type data is reproduced from Figure 1.3B. Closed circle symbols, *MSH2* +/+ *p53* +/+; open circle symbols, *MSH2* +/+ *p53* -/-; closed triangular symbols, *MSH2* -/- *p53* -/-.

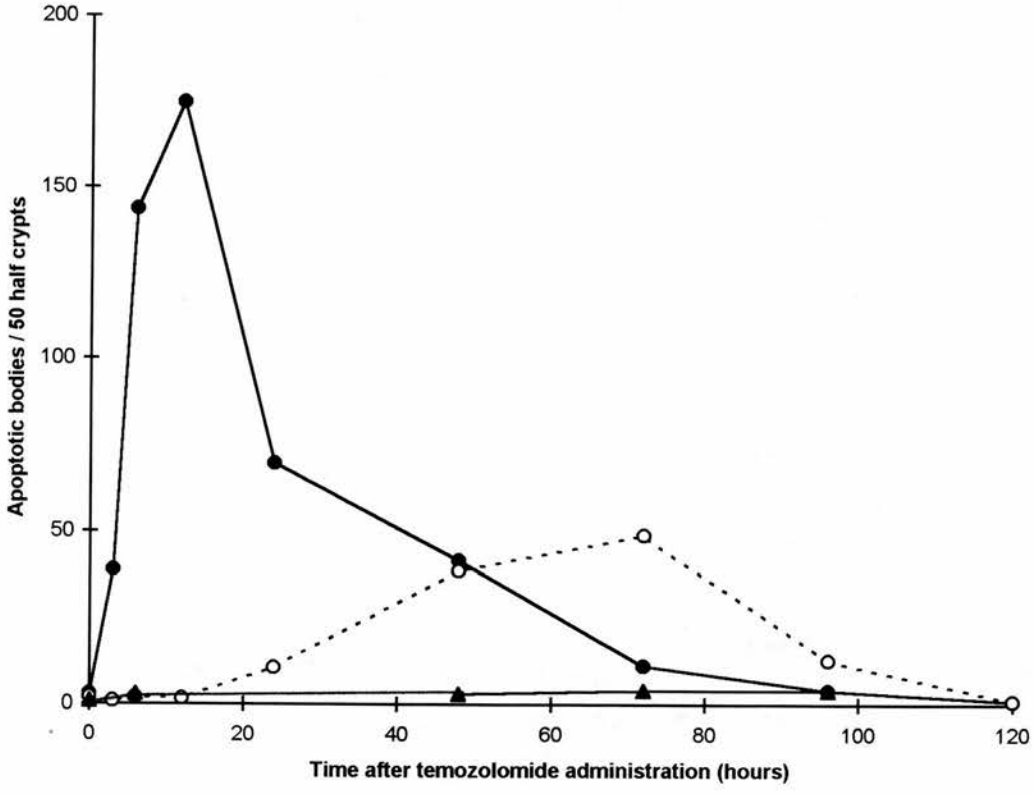
200
150
100
50
0
Apoptotic bodies / 50 half crypts
0
20
40
60
80
100
120
Time after temozolomide administration (hours)

## Figure 2.3

H&E stained section of small intestine from a *p53* -/- mouse treated with 100mg/kg Temozolomide 48 hours previously. Note the size and distribution of the apoptotic bodies (arrowed) within the crypt compared to those in Figure 1.1. (X250)

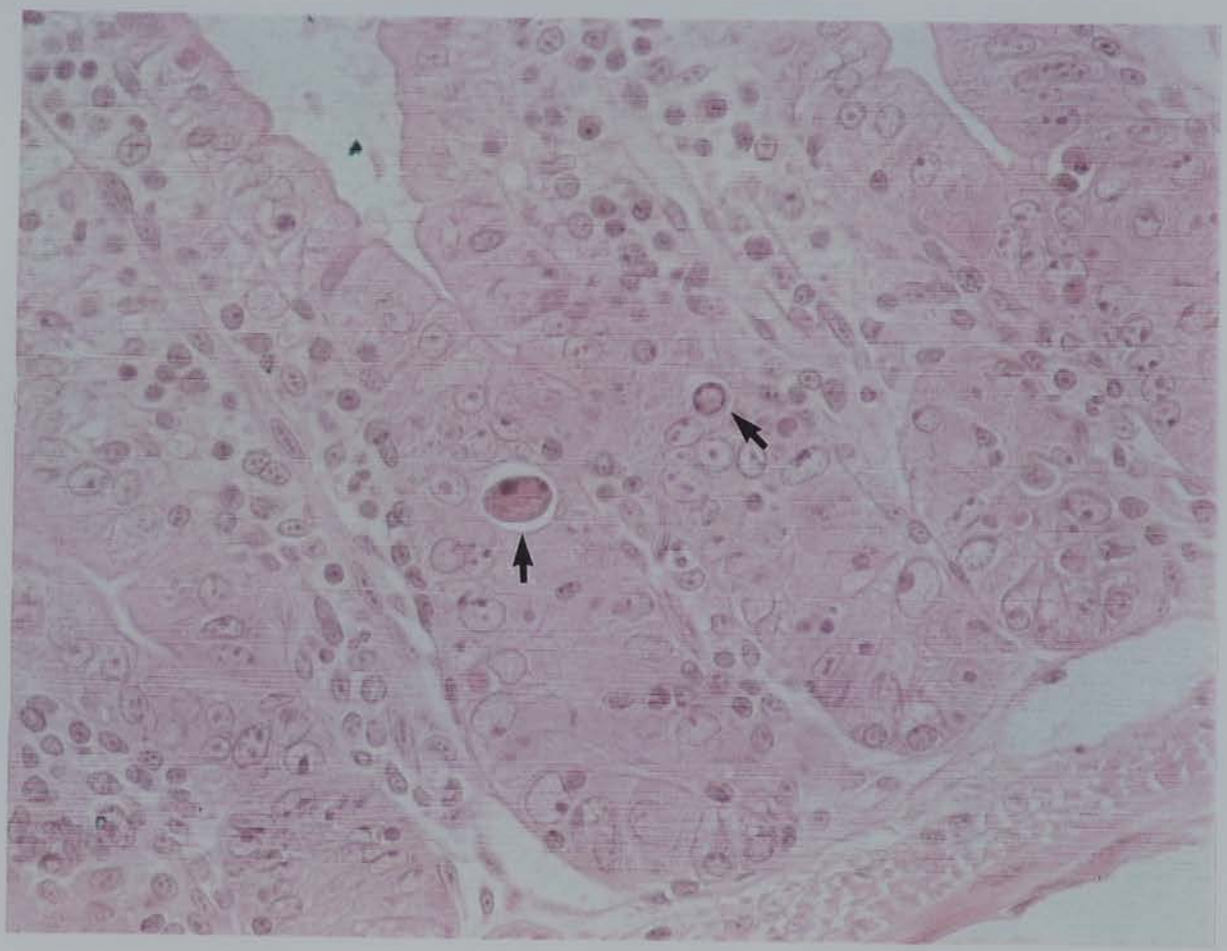

masses. To confirm that this delayed *p53*-independent apoptosis occurred at higher crypt positions cumulative counts of one hundred apoptotic bodies were performed in *p53* -/- mice 48 hours after treatment with 100mg/kg Temozolomide. Each apoptosis was assigned a crypt position and the frequency of apoptosis at each crypt position recorded (Figure 2.4). Peak prevalence of apoptotic bodies occurred at positions 13 and 14 which represent the proliferating compartment of the crypt. This differs from *p53*-dependent apoptosis which has a peak prevalence at positions 4 to 6, six hours post-injection when the prevalence of apoptotic bodies is maximal.

## Figure 2.4

Cumulative counts of one hundred apoptotic bodies in *p53* +/+ and *p53* -/- mice. Each apoptosis was assigned a crypt position from 1 to 22. Apoptosis was scored 6 hours after exposure to 100mg/kg Temozolomide in *p53* +/+ mice and 48 hours in *p53* -/- mice. Solid line, *p53* +/+; dotted line *p53* -/-.

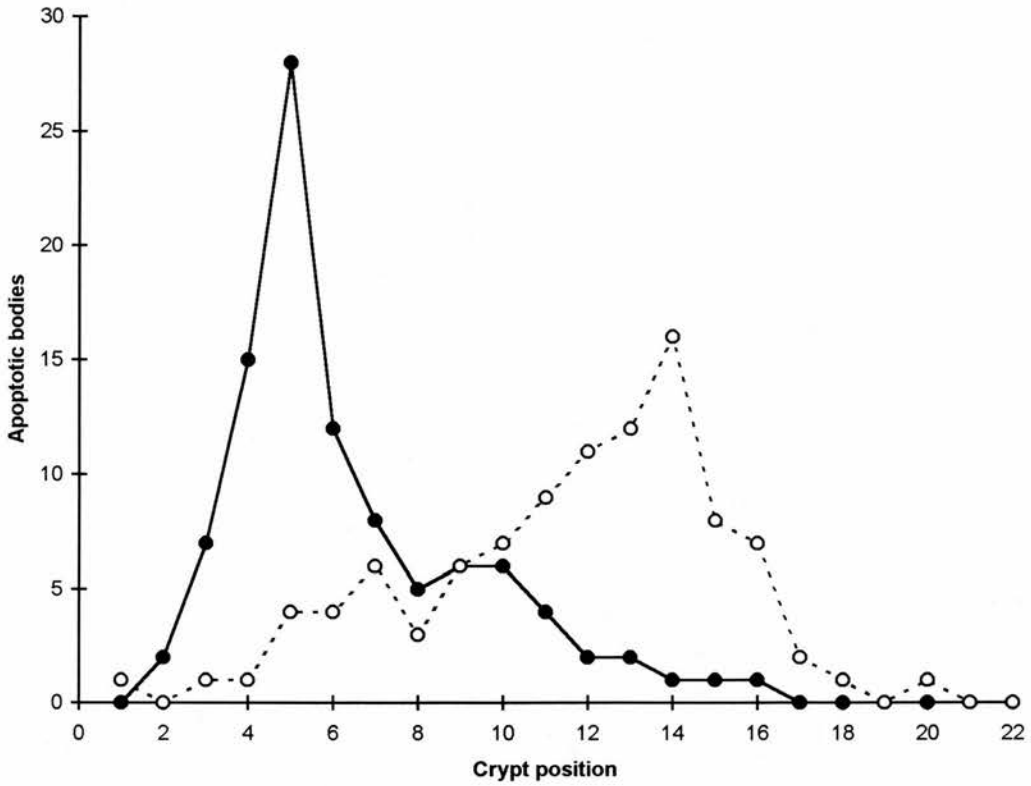
30
25
20
15
10
5
0
Apoptotic bodies
0
2
4
6
8
10
12
14
16
18
20
22
Crypt position

## Discussion

From the results presented here *p53* is required for small intestinal crypt cells to engage apoptosis following methylating agent or Cisplatin mediated DNA damage 6 hours post-drug administration. A similar critical dependence upon *p53* to couple DNA damage to apoptosis is also observed 4 hours after γ-irradiation (Clarke *et al.*, 1994 ; Merritt *et al.*, 1994). Thus, in lower crypt cells *p53* is essential to the successful generation of an early apoptotic signal following both mismatch-type and irradiation-type DNA damage resulting in the immediate wave of apoptosis seen in the first 4 to 6 hours.

The phenomenon of delayed *p53*-independent apoptosis, seen after γ-irradiation (Clarke *et al.*, 1997; Merritt *et al.*, 1997), was observed from 24 to 96 hours following Temozolomide administration to *p53* -/- mice. Furthermore, *MSH2* -/- *p53* -/- mice failed to show either the early wave or this delayed *p53*-independent wave of apoptosis ($p<0.05$ at 72 hours; Mann-Whitney U). These data clearly show that, in response to methylating agent damage, *MSH2* is required for the bulk of both the immediate and delayed apoptotic responses of lower crypt cells. Moreover, although the signal for apoptosis is processed through *p53* where this is available, a death signal is generated in the absence of *p53* albeit at a reduced level. The reduction in the number of apoptotic bodies observed in delayed *p53*-independent apoptosis suggests that *p53*-independent mechanisms are less efficient at coupling DNA damage to apoptosis. How might *p53* interact with *MSH2*? Although it is not known, one possible explanation is that *p53* links the DNA strand breaks generated by the futile attempts of the MMR system on the $O^6$-methylguanine:thymine mispairs to an apoptotic cascade (Nelson & Kastan, 1994; Rafferty *et al.*, 1996).

The morphology of the delayed apoptosis following Temozolmide was very similar to that observed by Merritt *et al.* (1994) following γ-irradiation. Such apoptosis is thought to result from aberrant mitosis, and is strongly reminiscent of vincristine induced apoptosis within the small intestine (Harmon *et al.*, 1992). Thus, it is possible that in the absence of *p53*, a cell bearing DNA damage of mismatch type escapes *p53*-induced $G_1$ arrest and proceeds through S-phase unhindered. However, during

mitosis, damaged DNA is recognised by *p53*-independent pathways and apoptosis initiated from the $G_2$/M phases of the cell cycle accounting for the alteration in apoptotic phenotype. The increased nuclear and cellular volume may therefore relate to the doubled DNA content of the cell following its passage through S phase.

The crypt position with the highest frequency of apoptotic bodies in *p53* null mice was more luminal than in wild-type mice. This may simply result from a combination of on-going crypt cell migration and a delay in the onset of apoptosis. Over a period of 42 hours the crypt position with the greatest frequency of apoptotic bodies shifted nine places towards the lumen (from position 5 to 14). Normally crypt cells migrate at 0.8 cell positions per hour (Kaur & Potten, 1986). However, following irradiation-induced DNA damage, this figure can fall to 23-30% of the normal rate (Potten, 1990). Given the similarities between Temozolomide and irradiation-induced apoptosis, it is distinctly possible that Temozolomide may also retard crypt cell migration. If this assumption can be made then, 42 hours at 0.8 positions per hour equates to a transit of 34 cell positions, when reduced to 26% would equal 9 positions. Thus, one plausible explanation for the alteration in crypt position is that stem cells which receive methylating DNA damage at positions 4 to 6 subsequently migrate slowly up the crypt with time, entering apoptosis in a delayed manner when they are in the more luminal regions of the crypt.

The implication of these findings to carcinogenesis is that *MSH2* and *p53* deficiency may predispose to malignancy not only by failing to repair DNA damage, but also by failing to engage apoptosis and delete cells (predominantly in the stem cell region of the crypt) which harbour DNA damage. If this pathway has real significance for the very early stages of carcinogenesis, it would be predicted that lesions in genes affecting this pathway, here shown to include both *MSH2* and *p53,* would arise early in the development of colorectal cancer. This is clearly not the case for the *p53* gene, where loss of function is primarily associated with late events such as the adenoma-carcinoma transition. The existence of delayed *p53*-independent apoptosis in itself, suggests that *p53* may not be a critical factor in the early stages of malignancy. Furthermore, the idea that the *p53*-dependent apoptotic response of intestinal cells may have limited relevance is supported by experiments analysing the intestinal

mutation frequency in *p53* null mice, where a *p53*-dependent increase was only observed following exposure to very high levels of DNA damage (Clarke *et al.*, 1997). However, *MSH2* may play a more significant role in the initial stages of carcinogenesis for three reasons. First, loss of DNA mismatch repair may occur early in colorectal neoplasia (Huang *et al.*, 1996). Second, no evidence of delayed *MSH2*-independent apoptosis was observed in *MSH2* -/- mice. Thus, in contrast to *p53*, no alternative pathway appears to exist in the absence of *MSH2* to delete cells with alkylation damage. Third, absence of *MSH2* significantly increases the mutation rate in intestinal stem cells, unlike *p53* (see Part IV of this thesis). Therefore, the consequences of failed apoptosis by virtue of *MSH2* deficiency may actually be more significant than those mediated through *p53* deficiency.

# Part III

# Role of $O^6$-Alkylguanine-DNA-alkyltransferase in *MSH2*-dependent Apoptosis

## Role of $O^6$-Alkylguanine-DNA-alkyltransferase in *MSH2*-dependent Apoptosis

### Introduction

The DNA repair protein $O^6$-alkylguanine-DNA-alkyltransferase (AGT) functions by recognising and removing specific alkyl lesions from DNA (Pegg & Byers, 1992). Substrates include $O^6$-methylguanine which is believed to be the major pre-mutagenic lesion induced by methylating agents. AGT mediated repair occurs via the transfer of the alkyl group to a cysteine residue in the AGT protein, a process which is stoichiometric and autoinactivating (Pegg, 1990). AGT therefore confers protection against the mutagenic effects of methylating agents, many of which are of clinical importance as anti-tumour agents such as Temozolomide (von Hofe & Kennedy, 1992; Dumenco *et al.*, 1993; Liu *et al.*, 1996b). Failure of AGT to repair $O^6$-methylguanine results in $O^6$-methylguanine:thymine mispairs following DNA replication and it is postulated that these mediate cell death *via* mismatch repair (Karran & Bignami, 1994). In addition, AGT activity is known to be up-regulated in a *p53*-dependent manner in response to DNA strand breaks following ionising irradiation (Rafferty *et al.*, 1996). Furthermore, AGT protein can be inactivated by exposure to Cisplatin (Wang & Setlow, 1989), although there are no reports of AGT-mediated removal of 1,2 diguanyl Cisplatin adducts. Hence, AGT activity may therefore modulate the levels of observed *MSH2*-dependent apoptosis by effectively removing methylation damage and so suppressing cell death such that the extent of *MSH2*-dependency is underestimated.

To assess the potential role of AGT in *MSH2*-dependent apoptosis following methylating agents and Cisplatin, functional AGT activity was depleted by administering the compound $O^6$-Benzylguanine to mice (Dolan *et al.*, 1990). Benzylguanine is a competitive and irreversible inhibitor of AGT which acts by binding to the $-CH_3$ cysteine acceptor site of AGT forming *S*-Benzylcysteine (Pegg *et al.*, 1993). Benzylguanine bound AGT is inactive and is subsequently degraded. Cellular AGT activity can be restored only by *de novo* protein synthesis (Pegg & Byers, 1992) and its depletion by Benzylguanine has been proposed as a useful

adjuvant to methylating and chloroethylating treatment of tumours in the clinic (Wedge & Newlands, 1996). Using Benzylguanine to deplete AGT activity *in vivo*, would allow the study of *MSH2*-dependent apoptosis in wild-type and *MSH2* null mice following treatment with methylating agents and Cisplatin. Any bias resulting from variations in AGT activity would therefore be removed. First, the possibility that *MSH2* status may alter cellular AGT activity levels was investigated.

**Results**

*Does MSH2 status influence the level of resting AGT activity in vivo?*

To investigate the possibility that absence of *MSH2* led to increased or decreased AGT levels six to nine male untreated *MSH2* +/+ mice and six male untreated *MSH2* -/- mice were sacrificed and their tissues removed for the measurement of AGT activity. Tissues studied included liver, kidney, small intestine, lung, brain, spleen, testes, colon, bone marrow, and thymus (Figure 3.1). Resting AGT activity was not significantly different in *MSH2* +/+ and *MSH2* -/- mice for the majority of tissues ($p>0.06$, Mann-Whitney U). However, *MSH2* -/- mice displayed significantly lower AGT activity in both their liver and lungs ($p<0.05$, Mann-Whitney U).

*Can Benzylguanine deplete AGT activity in murine tissues in vivo?*

Wild-type *MSH2* +/+ mice were injected with 60mg/kg Benzylguanine at time zero. Samples of tissue from liver, colon, and small intestine were assayed at several time points after injection for AGT activity (Figure 3.2). Within one hour of Benzylguanine delivery AGT activity fell to almost undetectable levels in all three tissues. AGT was depleted for up to 12 hours in all tissues examined, but after 12 hours functional AGT activity started to return. Levels of AGT activity similar to those prior to Benzylguanine delivery returned in all tissues examined by 72 hours. Benzylguanine therefore created an AGT deficient environment *in vivo* between 1 and 12 hours post-drug administration.

## Figure 3.1

AGT activity levels (fmoles/mg) in a range of untreated tissues from *MSH2* +/+ and *MSH2* -/- mice. Each bar represents data from six mice. Closed boxes, *MSH2* +/+; open boxes, *MSH2* -/-. Error bars represent standard error of the mean (sem).

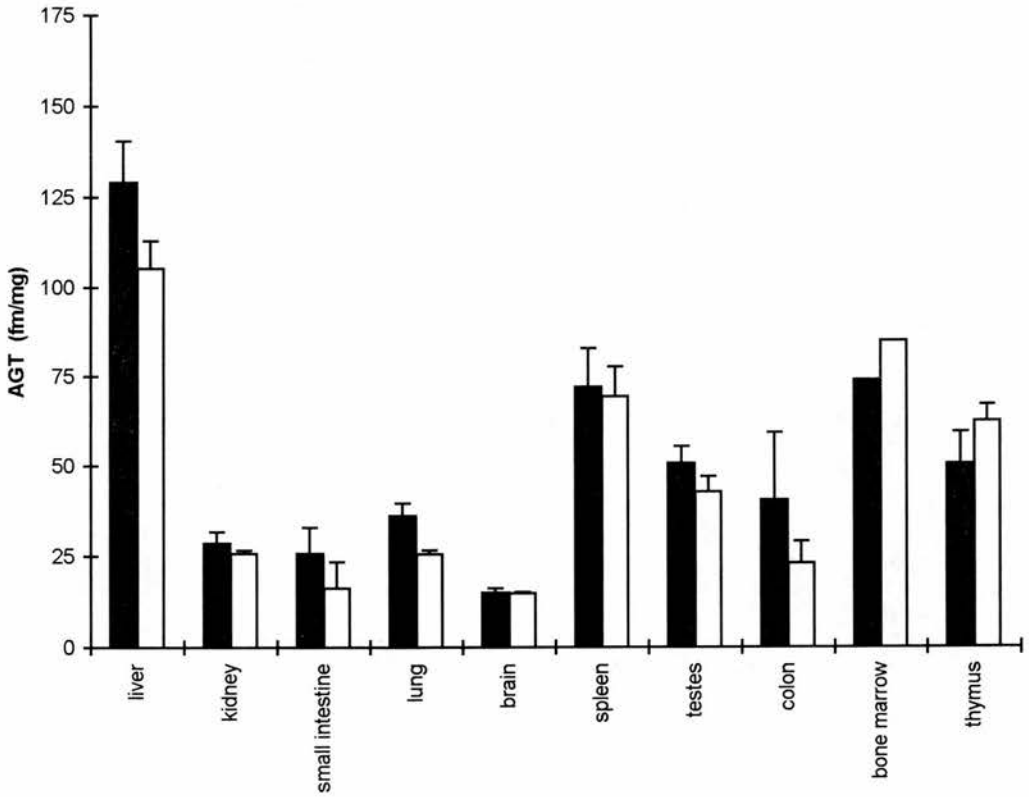
AGT (fm/mg)
175
150
125
100
75
50
25
0
liver
kidney
small intestine
lung
brain
spleen
testes
colon
bone marrow
thymus

## Figure 3.2

Timecourse of the average AGT activity levels (fmoles/mg) in the liver, colon and small intestine of *MSH2* +/+ mice injected i.p. with 60mg/kg Benzylguanine at time zero. Each point represents data from a minimum of three mice. Closed circle symbols, liver; open square symbols, colon; open circle symbols, small intestine. Error bars represent sem.

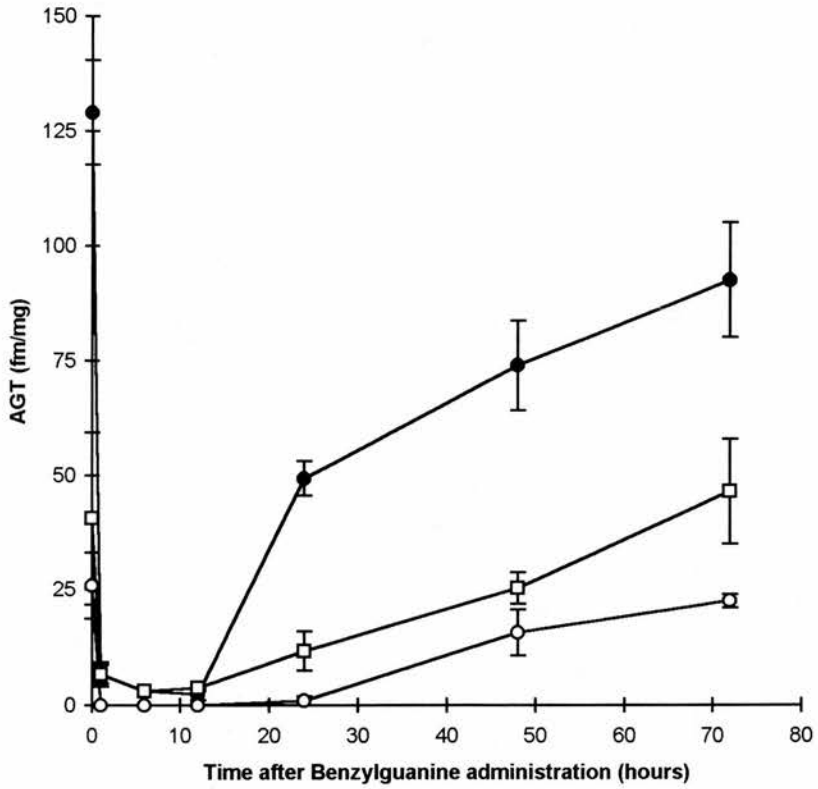
150
125
100
75
50
25
0
AGT (fm/mg)
0
10
20
30
40
50
60
70
80
Time after Benzylguanine administration (hours)

*Does the administration of Benzylguanine induce apoptosis within the murine small intestine?*

Addition of Benzylguanine, by inhibiting AGT, may increase endogenous alkylating DNA damage and thus induce apoptosis. To exclude this possibility cohorts of *MSH2* +/+ and *MSH2* -/- mice were injected with 60mg/kg Benzylguanine at time zero. Apoptosis was scored at 0, 3, 6, 12, 24, 48, and 72 hours after injection (Figure 3.3 A). Neither wild-type nor *MSH2* null mice displayed levels of apoptosis above baseline rates at any point up to 72 hours after Benzylguanine injection.

*Does AGT depletion by Benzylguanine alter the prevalence of apoptosis recorded in wild-type small intestine following exposure to methylating agents, Cisplatin or γ-irradiation?*

To investigate the possibility that endogenous AGT activity was modifying the observed crypt cell apoptosis, or the extent of DNA damage received by cells at a given dose, wild-type mice were pre-treated with Benzylguanine (60mg/kg). One hour later 100mg/kg Temozolomide, or 50mg/kg MNNG, or 10 mg/kg Cisplatin, or 4 Gray of γ-irradiation were administered. Apoptosis was scored in the small intestine six hours later (Figure 3.3 B). No significant differences in the prevalence of apoptosis were observed between Benzylguanine and non-Benzylguanine treated animals ($p>0.4$ in all cases, Mann-Whitney U).

*Is there a difference in the prevalence of apoptosis following low dose Temozolomide in the presence and absence of Benzylguanine?*

To exclude the possibility that the doses of methylating agents used in Figure 3.3 B were inactivating AGT by depleting cellular pools of active AGT, and therefore rendering Benzylguanine treatment irrelevant, very low doses of Temozolomide (range 0.5 to 16mg/kg) were administered to mice with and without Benzylguanine cover. Six hours later apoptosis was scored (Figure 3.3 C). The rationale behind this approach was that at low doses of Temozolomide not all functional AGT activity would be abolished by the methylating agent, and thus if AGT could actually alter the level of apoptosis, a difference between Benzylguanine and non-Benzylguanine

## Figure 3.3

**A** Graph showing the prevalence of apoptotic bodies in the small intestine of *MSH2* +/+ and *MSH2* -/- mice at various time points following 60mg/kg Benzylguanine i.p. Each point represents data from a minimum of three mice. Closed circle symbols, *MSH2* +/+; open circle symbols, *MSH2* -/-.

**B** Bar chart showing the prevalence of apoptosis in the murine small intestine 6 hours after reagent administration and 7 hours after i.p Benzylguanine (60mg/kg). Cohorts of *MSH2* +/+ mice were treated with 100mg/kg Temozolomide, or 50mg/kg MNNG, or 10mg/kg Cisplatin, or exposed to 4 Gray γ-irradiation in the presence and absence of Benzylguanine. Each bar represents data from six mice. Closed boxes, *MSH2* +/+ Benzylguanine-untreated; open boxes, *MSH2* +/+ Benzylguanine-treated. Error bars represent sem.

**C** Line graph showing the prevalence of apoptosis 6 hours after 100mg/kg Temozolomide administration and 7 hours after i.p Benzylguanine (60mg/kg). Cohorts of *MSH2* +/+ mice were dosed with i.p. Temozolomide (range 0.5-16mg/kg) in the presence and absence of Benzylguanine pretreatment. Each point represents data from three mice. Closed circle symbols, *MSH2* +/+ Benzylguanine-untreated; open circle symbols, *MSH2* +/+ Benzylguanine-treated. Error bars represent sem.

A

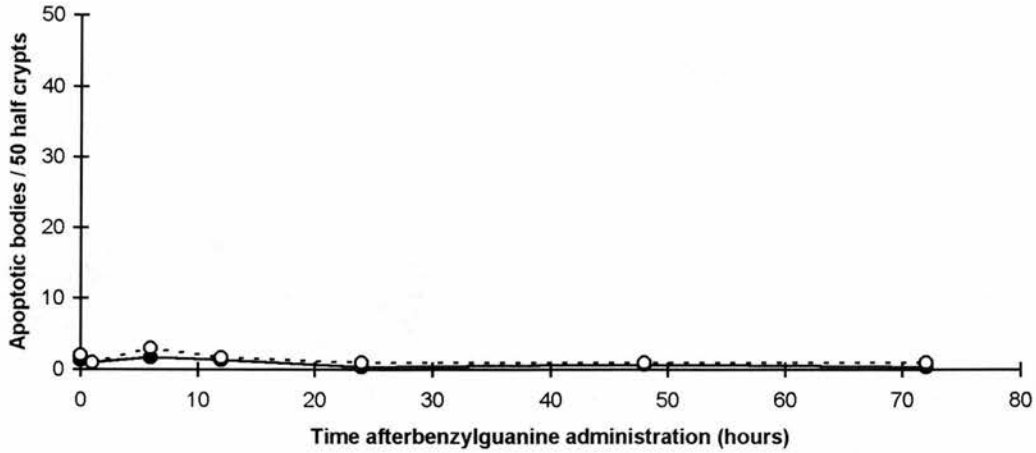
Apoptotic bodies / 50 half crypts
50
40
30
20
10
0
0
10
20
30
40
50
60
70
80
Time afterbenzylguanine administration (hours)

B

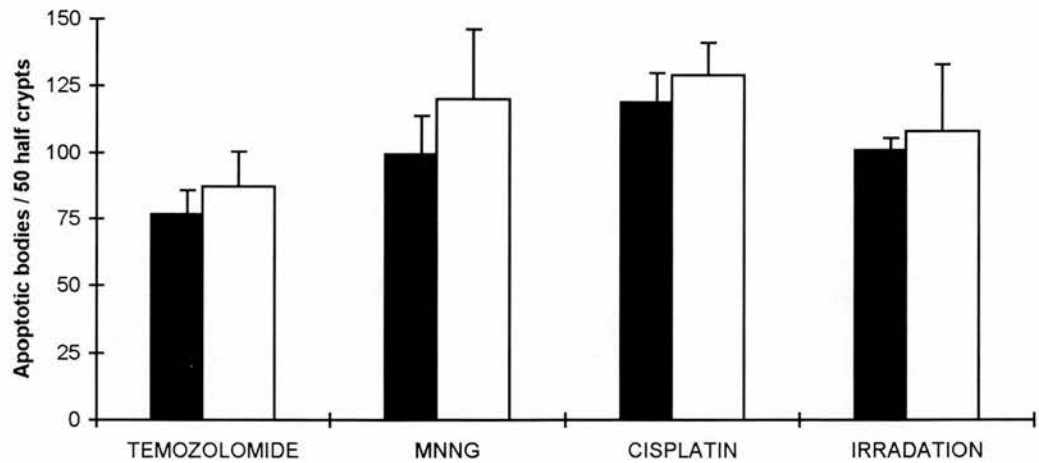
Apoptotic bodies / 50 half crypts
150
125
100
75
50
25
0
TEMOZOLOMIDE
MNNG
CISPLATIN
IRRADATION

C

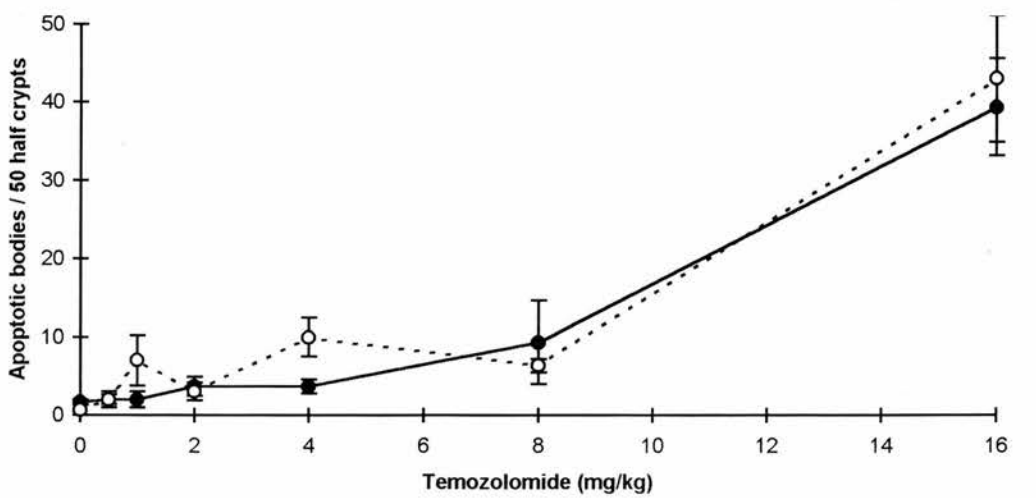
Apoptotic bodies / 50 half crypts
50
40
30
20
10
0
0
2
4
6
8
10
12
14
16
Temozolomide (mg/kg)

treated mice may become apparent. No significant differences in the prevalence of apoptosis were observed between Benzylguanine treated and non-Benzylguanine treated mice at any of the doses of Temozolomide used ($p>0.07$ for all doses, Mann-Whitney U).

*In the absence of AGT is the level of reduction in apoptosis seen in MSH2 -/- mice following methylating agent or Cisplatin treatment identical to that seen in the presence of AGT activity?*

To investigate whether AGT could modulate *MSH2*-dependent apoptosis cohorts of *MSH2* +/+ and *MSH2* -/- mice were injected with 60mg/kg Benzylguanine. One hour after the administration of Benzylguanine, mice were injected with 100mg/kg Temozolomide, or 50mg/kg MNNG, or 10mg/kg Cisplatin. Apoptosis was scored in the small intestine at 6 hours (Figure 3.4). For all reagents tested the level of reduction in the prevalence of apoptosis recorded in *MSH2* -/- mice in the absence of AGT was not significantly different from the level of reduction observed in the presence of AGT ($p>0.9$ for all three drugs, Mann-Whitney U). Thus, AGT does not modulate *MSH2*-dependent apoptosis in the murine small intestine following Temozolomide, MNNG or Cisplatin.

*Does AGT play any role in MSH2-dependent apoptosis in the small intestine? What is the role of AGT in Dacarbazine-induced apoptosis?*

In order to assess the potential role of AGT in Dacarbazine induced apoptosis a single dose of Benzylguanine (60mg/kg) was administered to wild-type mice at time zero. *MSH2* +/+ mice were subsequently injected with 150mg/kg Dacarbazine at 0, 1, 6, 12, 24, 48, or 72 hours after Benzylguanine delivery. Six hours after each Dacarbazine injection, levels of apoptosis were scored in the small intestine (Figure 3.5). Prior to Benzylguanine delivery, Dacarbazine induced high levels of apoptosis with a mean of over 60 apoptotic bodies per 50 half crypts. However, from 1 to 6 hours after Benzylguanine injection, Dacarbazine was unable to induce apoptosis above baseline rates. At 12 hours the apoptosis-inducing properties of Dacarbazine returned albeit at a diminished level. Twenty-four hours after Benzylguanine delivery Dacarbazine was

## Figure 3.4

One hour following 60mg/kg i.p. Benzylguanine (BeG), cohorts of *MSH2* +/+ and *MSH2* -/- mice were treated with Temozolomide (100mg/kg), or MNNG (50mg/kg), or Cisplatin (10mg/kg). Small intestines were harvested 6 hours following drug treatment and apoptosis scored. Data is presented showing the percentage reduction in observed apoptosis in the *MSH2* -/- mice (open bars) relative to that in *MSH2* +/+ mice (closed bars, standardised to 100%). Non-Benzylguanine treated controls are shown for comparison. Each bar represents data from 6 mice. Error bars represent sem.

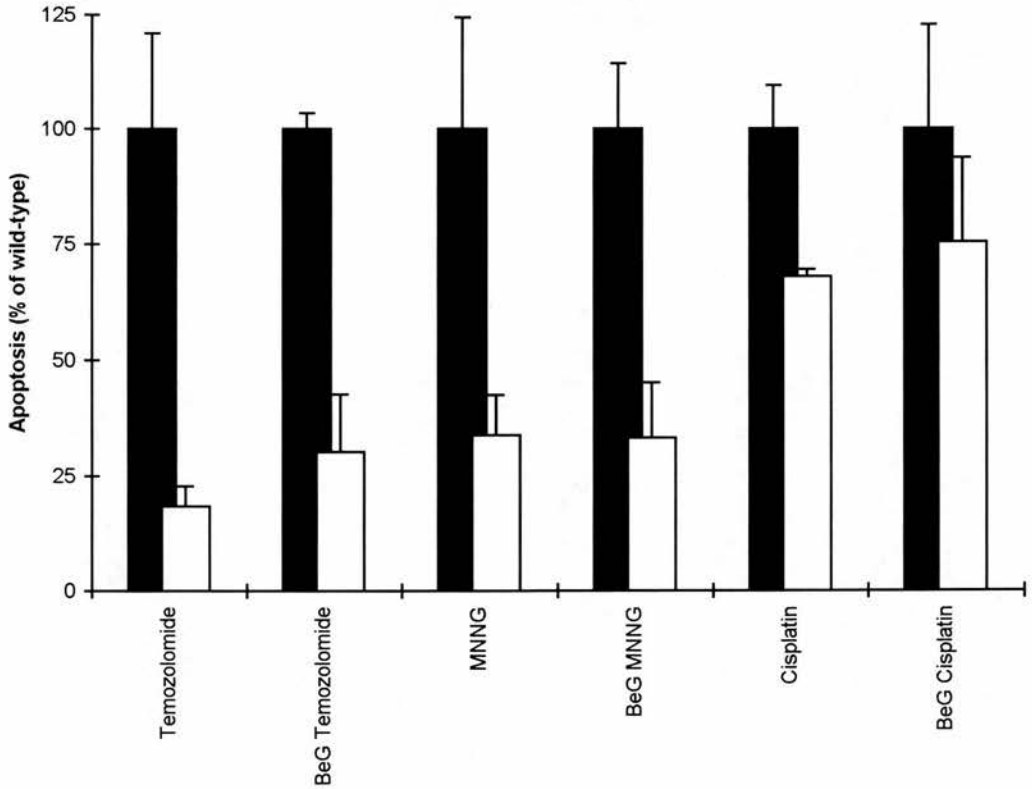
Apoptosis (% of wild-type)
125
100
75
50
25
0
Temozolomide
BeG Temozolomide
MNNG
BeG MNNG
Cisplatin
BeG Cisplatin

## Figure 3.5

Following a single dose of Benzylguanine (60mg/kg) at time zero, *MSH2* +/+ mice were injected with 150mg/kg Dacarbazine at 0, 1, 6, 12, 24, 48, or 72 hours after Benzylgunaine delivery. Six hours after each Dacarbazine injection levels of apoptosis were scored in the small intestine. Each point represents data from 3 mice. Error bars represent sem.

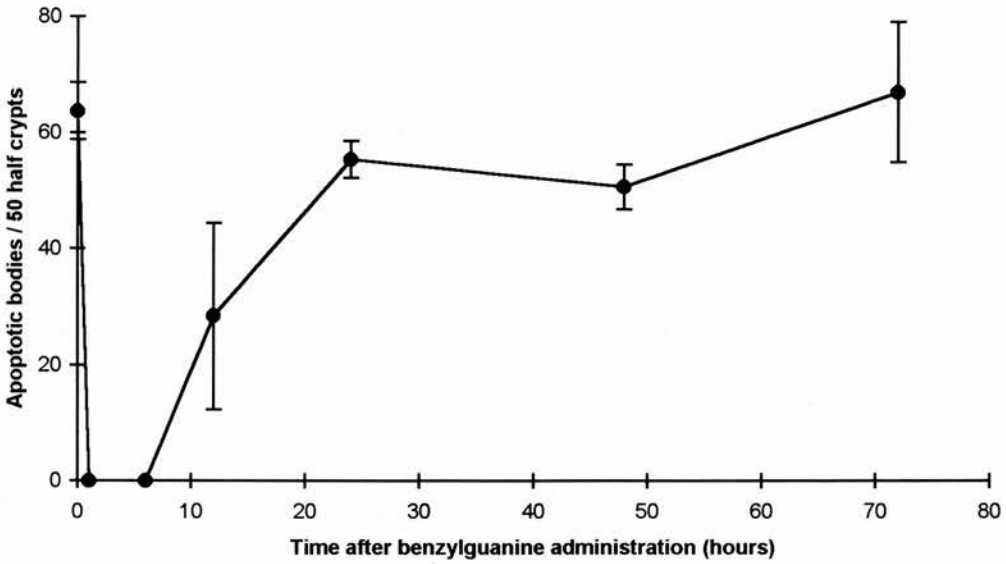
Apoptotic bodies / 50 half crypts
0
20
40
60
80
0
10
20
30
40
50
60
70
80
Time after benzylguanine administration (hours)

able to induce apoptosis with the same efficiency as before. Hence, Benzylguanine administration reversibly inhibited the apoptosis-inducing action of Dacarbazine.

**Discussion**

In the untransformed cells of the small intestine and colon *MSH2* status did not affect resting AGT levels. Loss of *MSH2* which occurs in a proportion of $RER^+$ sporadic tumours is therefore unlikely to alter cellular AGT levels *per se*. This may be of clinical relevance since tumour cells which display high levels of AGT activity render themselves resistant to methylating agents (Koc *et al.*, 1996; Preuss *et al.*, 1996). The lower levels of AGT observed in the liver and lungs of *MSH2* -/- mice suggest that *MSH2* may play a role in the regulation of AGT levels. However, this finding is perhaps of limited significance as such a role for *MSH2* would be predicted to lead to an increased tumour sensitivity in these tissues, which has not been observed in *MSH2* null mice.

Effective depletion of AGT activity was confirmed in tissue from the liver, colon and small intestine with no detectable AGT activity occurring between 1 and 12 hours after Benzylguanine administration. This confirms previous studies by (Liu *et al.*, 1996c) showing that Benzylguanine is active *in vivo*, and capable of depleting AGT activity in the liver which is known to possess the highest levels of AGT activity (Pegg & Byers, 1992). In addition, Benzylguanine successfully depleted AGT from both the colon and small intestine, creating a "window" of AGT depletion in which to study *MSH2*-dependent apoptosis without any confounding effects of AGT.

No induction of apoptosis was associated with Benzylguanine treatment alone in *MSH2* +/+ or *MSH2* -/- mice. This excluded the possibility that either Benzylguanine itself or depletion of AGT could induce apoptosis in the murine small intestine. In the absence of AGT activity Temozolomide, MNNG, Cisplatin, and γ-irradiation all induced apoptosis. The levels of apoptosis recorded were similar to the levels observed in the presence of AGT. Thus, in wild-type mice AGT depletion neither reduced nor augmented the prevalence of apoptosis in the intestine following a variety of DNA damaging agents. Three possible explanations exist for this surprising result. First, it is possible that AGT plays no role in *MSH2*-dependent and -independent apoptosis in the small intestine. This is unlikely since preincubation of colorectal cell lines with Benzylguanine is known to potentiate the cytotoxicity of Temozolomoide (Wedge *et al.*, 1996). A second explanation stems from the possibility that Temozolomide treatment ablates cellular AGT activity by depleting pools of unmethylated AGT, and

therefore masking a potential role for AGT in apoptosis (Pegg & Byers, 1992; Lacal *et al.*,1996). This explanation also seems unlikely given the levels of apoptosis were similar in both Benzylguanine treated and untreated mice following a range of low doses of Temozolomide. The most plausible explanation stems from the fact that the murine small intestine possesses very low resting levels of AGT, and thus the predicted increase in apoptosis following pre-treatment with Benzylguanine is too small to be detected. Hence, in the presence and absence of Benzylguanine, the number of methylated guanine residues is likely to be similar, and the number of cells possessing levels of damage which are processed into lethal intermediates through *MSH2,* also similar. This is the most satisfactory reason for the non-significant difference between Benzylguanine and non-Benzylguanine treated wild-type mice, although it is impossible to exclude the other possibilities discussed above.

Apoptosis scored in *MSH2* +/+ and *MSH2* -/- mice 6 hours following administration of Temozolomide, MNNG, and Cisplatin and 7 hours after Benzylguanine, was again observed to be dependent on *MSH2* status, with a significant reduction observed in *MSH2* -/- mice ($p<0.02$ with Temozolomide and MNNG, Mann-Whitney U). The degree of *MSH2* dependency was comparable to non-Benzylguanine treated mice demonstrating reproducibility in the absence of AGT. This result substantiates *in vitro* data which demonstrate that mismatch repair status, overrides AGT status in determining the apoptotic response of cells to Temozolomide (Liu *et al.*,1996b; Wedge *et al.,* 1996).

What role if any does AGT play in small intestinal apoptosis? It is clear from the results presented here that Benzylguanine administration blocks Dacarbazine-induced apoptosis. This must be occurring either because AGT activity is required by Dacarbazine to induce apoptosis, or because Benzylguanine is blocking the normal metabolism of Dacarbazine. Dacarbazine is known to undergo oxidative N-demethylation to its active compound 5-(3-methyltriazen-1-yl)imidazole-4-carboxamide (MITC) (Newell *et al.,* 1987; Dollery, 1991; D'Incalci, 1994). This metabolic pathway occurs in hepatocytes through the action of cytochrome P450 enzymes (Meer *et al.,* 1986; Mudipalli *et al.,* 1995). Two observations argue in favour of the possibility that Benzylguanine is blocking the normal metabolism of Dacarbazine. First, Temozolomide is able to induce apoptosis in the presence of AGT depletion. Thus, the inhibitory action of Benzylguanine cannot be arising subsequent to

## Figure 3.6

Diagram of the metabolism of Dacarbazine (DITC) and Temozolomide to the active compound 5-(3-methyltriazen-1-yl)imidazole-4-carboxamide (MITC). It is MITC which is capable of methylating the $O^6$ of guanine in DNA, creating $O^6$-methylguanine, the major pre-mutagenic lesion. DITC requires oxidative N-demethylation by cytochrome P450 enzymes to form MITC, unlike Temozolomide which reacts spontaneously with water to give MITC.

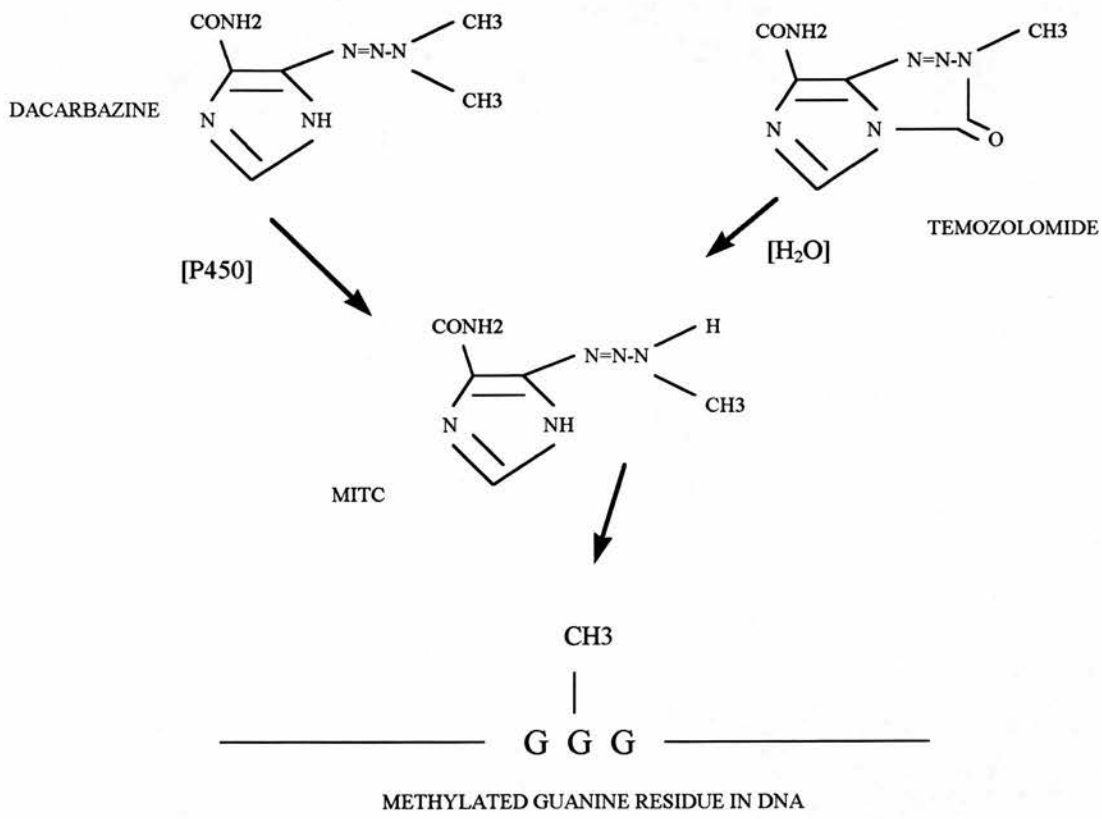
CONH2
N=N-N
CH3
CH3
DACARBAZINE
N
NH
CONH2
N=N-N
CH3
N
N
O
TEMOZOLOMIDE
[P450]
[H2O]
CONH2
N=N-N
H
CH3
N
NH
MITC
CH3
G G G
METHYLATED GUANINE RESIDUE IN DNA

the generation of MITC since it is also the active compound formed when Temozolomide undergoes spontaneous chemical transformation (Stevens *et al.*, 1987; Denny *et al.*, 1994) (Figure 3.6). Second, one of the major routes of metabolism of Benzylguanine in mice involves oxidation to form $O^6$-Benzyl-8-oxoguanine (Dolan *et al.*, 1994) which occurs exclusively through the cytochrome P450 system (Nebert & Weber, 1990). The possibility therefore arises that Benzylguanine metabolism may competitively deplete cytochrome P450 activity.

Benzylguanine used at high doses of 60mg/kg appears capable of inhibiting the demethylating ability of cytochrome P450 enzymes in the mouse liver. The consequences of this novel finding are likely to be significant in view of the pivotal role of P450 enzymes in the metabolism of drugs and carcinogens. Important drugs metabolised by P450 enzymes include antibiotics (e.g. erythromycin), immunosuppressants (e.g. cyclosporin), steroids (e.g. testosterone), cholesterol and ethanol (Funae & Imaoka, 1993; Guengerich, 1992). Moreover, carcinogens such as aflatoxin B1, 2-aminoanthracene, and the mammary carcinogen fluoranthene-2,3-diol are also known to be metabolised by hepatic P450 enzymes (Guengerich, 1992; Shimada, *et al.*, 1997).

There is increasing interest in the possible use of Benzylguanine clinically as an adjuvant to alkylating agent chemotherapy to overcome tumour resistance mediated by AGT and also to potentiate the cytotoxic effects of the chemotherapy (Wedge & Newlands, 1996; Kurpad *et al.*, 1997). For a number of reasons the potential clinical benefits of Benzylguanine may be overestimated. First, alkylating agents themselves are capable of inactivating AGT activity by depleting cellular pools (Pegg & Byers, 1992). Second, the addition of Benzylguanine to cells treated with MNNG or Temozolomide is known to increase mutation rates and chromosome aberrations within cells, although there is a proportional increase in apoptosis (Lukash *et al.*, 1991; Bean *et al.*, 1994; Chinnasamy *et al.*, 1997). Third, from the data presented in this thesis, it is clear that in the murine small intestine AGT depletion does not elevate *in vivo* apoptotic levels at six hours following methylating DNA damage. However, the possibility that a delayed elevation in apoptosis in the absence of AGT was not excluded. In addition, the data is this thesis indicate that Benzylguanine can alter the metabolism of drugs or carcinogens, exemplified here by Dacarbazine, and may therefore be a cause of unexpected adverse drug reactions if used clinically.

# Part IV

## *MSH2* and *in vivo* Mutation Frequency

## *MSH2* and *in vivo* Mutation Frequency

### Introduction

Deleterious genetic changes, known as mutations, are the basis of cancer (Bodmer *et al.*, 1994). Activating mutations in oncogenes or inactivating mutations in tumour suppressor genes can contribute to the deregulation of cell turnover and progression to a malignant state (Vogelstein & Kinzler, 1993). Mutations within cells can arise through infidelity in the cellular DNA synthesis machinery, or defects in DNA repair pathways or through environmental genotoxic insult (Kaufmann & Paules, 1996). The DNA mismatch repair pathway, of which *MSH2* is one component, combines a dual function being essential for repairing mismatches and small DNA loops that arise through errors in DNA replication and also for the cytotoxicity of mismatched methylated guanine residues arising from alkylating carcinogens (Karran & Bignami, 1994). Absence of *MSH2* within normal cells may therefore facilitate the acquisition of new mutations within key growth controlling genes, accelerating progression through the multi-step process of cancer formation (Karran, 1996). Indeed, *in vitro* studies demonstrating one hundred to six hundred-fold elevations in mutation rate at the hypoxanthine guanine phosphoribosyltransferase (*hprt*) locus in colorectal cell lines, deficient in mismatch repair, confirm the essential role of *MSH2* in maintaining DNA integrity (Bhattacharyya *et al.*, 1994 & 1995; Eshelman *et al.*, 1995; Branch *et al.*, 1995). Furthermore, studies of mutation rates in *MSH2* -/- mice reveal five to fifteen-fold elevations in the spontaneous mutation frequency (Andrew *et al.*, 1997).

The role of *MSH2* in maintaining genomic stability within small intestinal stem cells *in vivo* was investigated by determining the mutation frequency at the *Dlb-1* locus (Winton *et al.*, 1988). The contribution of *MSH2* in counteracting the mutagenic effects of Temozolomide, MNNG, and Cisplatin was examined. The *Dlb-1* assay detects genetic change (including point mutations and deletions) at a single polymorphic locus, *Dlb-1*, which determines a lectin binding site within mouse intestinal epithelium. Two forms of the *Dlb-1* allele exist. The *Dlb-1* a allele specifies binding of the lectin *Dolichos biflorus* agglutinin (DBA) to vascular epithelium while the *Dlb-1* b allele specifies binding to intestinal epithelium. Any inactivating mutation

in the *Dlb-1* b allele of *Dlb-1* heterozygote mice (*Dlb-1* a/b) renders that cell unable to bind the lectin. Following stem cell proliferation and clonal expansion, an entire clone of cells unable to bind the lectin is formed. Such clones are easily identified and quantitated by staining wholemount preparations of the small intestine with a peroxidase conjugate of DBA (Winton *et al.*, 1988). These mutant clones of cells migrating up the villus appear as white ribbons a brown-staining background (Figure 4.1). Therefore, mutation frequency may be expressed as the number of negative-staining ribbons per ten thousand villi counted. Interbreeding *MSH2* heterozygote *Dlb-1* a/a mice to *MSH2* heterozygote *Dlb-1* b/b mice generated cohorts of *MSH2* +/+, *MSH2* +/-, and *MSH2* -/- mice which were also heterozygous (a/b) at the *Dlb-1* locus. These mice were used to assess the mutation frequency of intestinal stem cells.

**Results**

*Is there an elevated spontaneous mutation frequency in small intestinal stem cells of MSH2-deficient mice?*

The number of negative-staining clones per 10 000 villi was counted in thirteen week old *Dlb-1* a/b mice, four of which were *MSH2* +/+, four *MSH2* +/-, and four *MSH2* -/- (Figure 4.2). Both untreated *MSH2* wild-type and heterozygote mice demonstrated low mutation frequencies (between 3 and 5 negative-staining ribbons per 10 000 villi) similar to the spontaneous mutation rates of small intestinal cells recorded in previous studies (Winton *et al.*, 1988; Clarke *et al.*, 1997). In contrast, *MSH2* null mice demonstrated spontaneous mutation rates 6-fold greater than either wild-type or heterozygote mice ($p<0.001$, Mann-Whitney U).

*What is the role of MSH2 in protecting against the mutagenic effects of different doses of Temozolomide, MNNG and Cisplatin?*

Ten week old cohorts of *MSH2* +/+, *MSH2* +/-, and *MSH2* -/- *Dlb-1* a/b mice were injected i.p. with 0, 25, 50, and 100mg/kg Temozolomide. Twenty-one days later the number of negative-staining ribbons per 10 000 small intestinal villi was counted (Figure 4.2). Low mutation frequencies were observed in both *MSH2* wild-type and heterozygote mice at all doses of Temozolomide which were not significantly different

## Figure 4.1

Small intestinal villus from a *Dlb-1* a/b *MSH2* -/- mouse stained with *Dolichos biflorus* agglutinin (DBA) peroxidase. A ribbon of unstained (i.e. DBA-negative) cells is arrowed. (X125)

## Figure 4.2

Mutation frequency in *Dlb-1* a/b heterozygote mice, which also segregated for *MSH2* status, following treatment with Temozolomide. Mice were injected i.p. with 0, 25, 50, and 100mg/kg of Temozolomide and the number of negative-staining ribbons per 10 000 villi counted 21 days later. Each bar represents data from a minimum of three mice and error bars correspond to the standard error of the mean. Wild-type, *Dlb-1* a/b *MSH2* +/+; Heterozygote, *Dlb-1* a/b *MSH2* +/-; Homozygote, *Dlb-1* a/b *MSH2* -/-

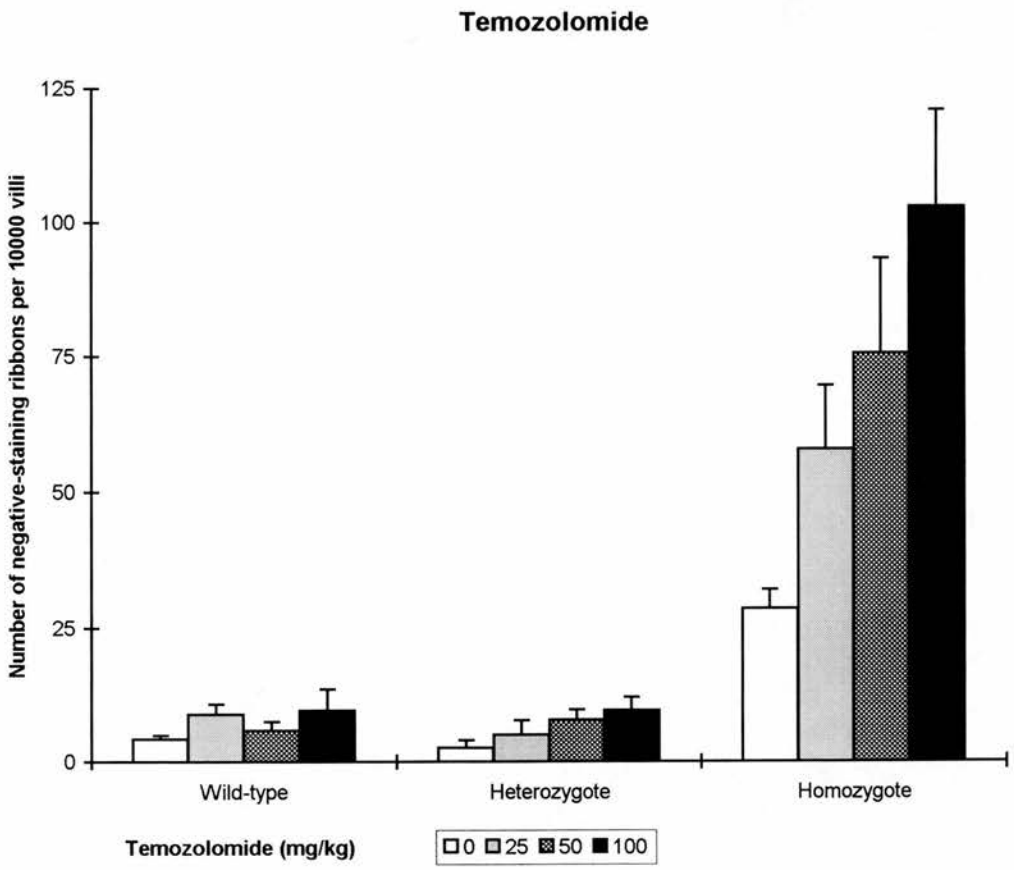
Temozolomide
Number of negative-staining ribbons per 10000 villi
125
100
75
50
25
0
Wild-type
Heterozygote
Homozygote
Temozolomide (mg/kg)
0 25 50 100

from untreated mice ($p>0.1$, Mann-Whitney U). In contrast, a significant *MSH2*-dependent difference in mutation frequency was observed at all doses of Temozolomide in *MSH2* null homozygotes ($p<0.02$ for all doses, Mann-Whitney U).

Similar cohorts of mice were injected i.p. with 0, 10, 25, and 50mg/kg MNNG and mutation frequency assessed 21 days later (Figure 4.3). At 10 mg/kg low mutation frequencies were observed in both *MSH2* wild-type and heterozygote mice. However, doses of 25 and 50 mg/kg MNNG induced mutations at a frequency of between 50 and 150 ribbons per 10 000 villi. Comparing *MSH2* +/- mice with *MSH2* +/+ mice no gene dosage effect was observed in the heterozygotes even at 50mg/kg. In *MSH2* null homozygotes all doses of MNNG induced high mutation frequencies with up to 400 negative-staining ribbons per 10 000 villi recorded at 50 mg/kg. At all doses of MNNG *MSH2*-deficient mice showed elevated mutation rates above those observed in wild-type and heterozygote controls. However, only 10 and 50 mg/kg of MNNG were statistically significant ($p<0.001$, Mann-Whitney U).

Finally, Cisplatin was injected i.p. at 0, 0.5, 1, and 5mg/kg to cohorts of *Dlb-1* a/b mice which segregated for *MSH2* status. The number of negative-staining ribbons was counted 21 days post-injection (Figure 4.4). In *MSH2* wild-type and heterozygote mice Cisplatin was weakly mutagenic, with increasing doses of reagent increasing the mutation frequency observed. Cisplatin was also mutagenic in *MSH2* null homozygote mice, although the absolute mutation frequency was low (up to 60 ribbons per 10 000 villi). At 5mg/kg Cisplatin a minor, but not statistically significant, degree of *MSH2* dependency was detected, which was not present at lower doses.

## Figure 4.3

Mutation frequency in *Dlb-1* a/b heterozygote mice, which also segregated for *MSH2* status, following treatment with MNNG. Mice were injected i.p. with 0, 10, 25, and 50mg/kg of MNNG and the number of negative-staining ribbons per 10 000 villi counted 21 days later. Each bar represents data from a minimum of three mice and error bars correspond to the standard error of the mean. Wild-type, *Dlb-1* a/b *MSH2* +/+; Heterozygote, *Dlb-1* a/b *MSH2* +/-; Homozygote, *Dlb-1* a/b *MSH2* -/-.

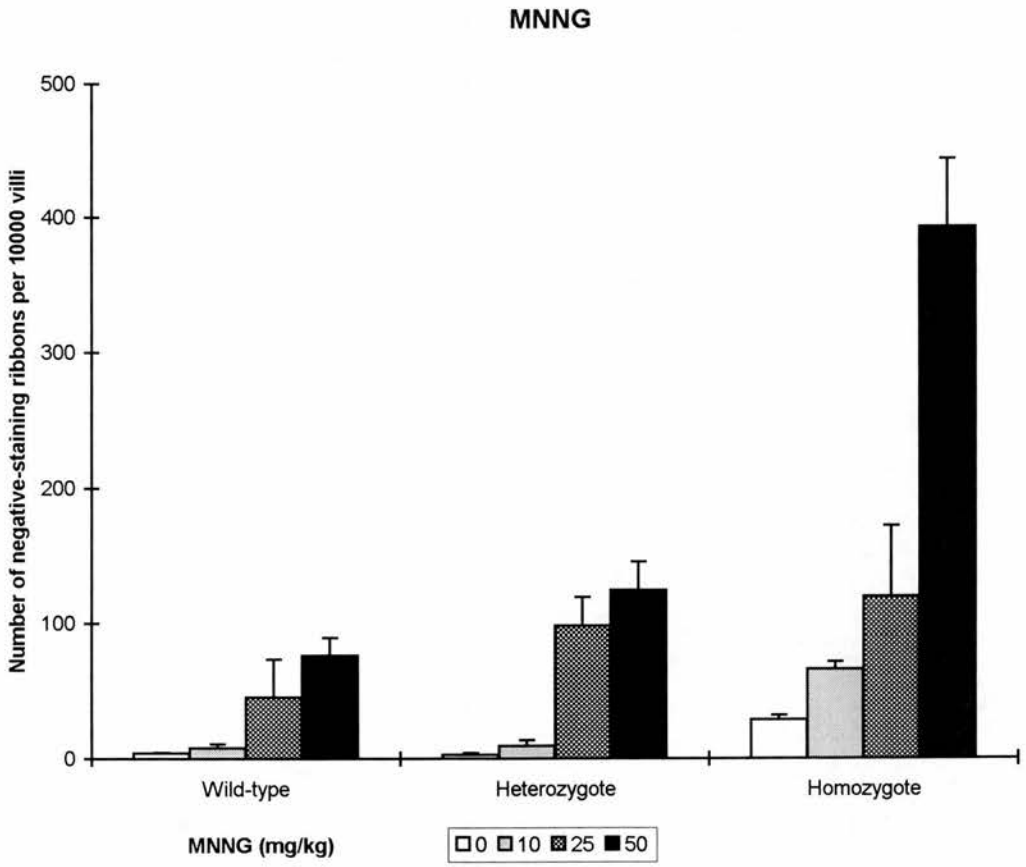
MNNG
Number of negative-staining ribbons per 10000 villi
500
400
300
200
100
0
Wild-type
Heterozygote
Homozygote
MNNG (mg/kg)
0 10 25 50

## Figure 4.4

Mutation frequency in *Dlb-1* a/b heterozygote mice, which also segregated for *MSH2* status, following treatment with Cisplatin. Mice were injected i.p. with 0, 0.5, 1, and 5mg/kg of Cisplatin and the number of negative-staining ribbons per 10 000 villi counted 21 days later. Each bar represents data from a minimum of three mice and error bars correspond to the standard error of the mean. Wild-type, *Dlb-1* a/b *MSH2* +/+; Heterozygote, *Dlb-1* a/b *MSH2* +/-; Homozygote, *Dlb-1* a/b *MSH2* -/-.

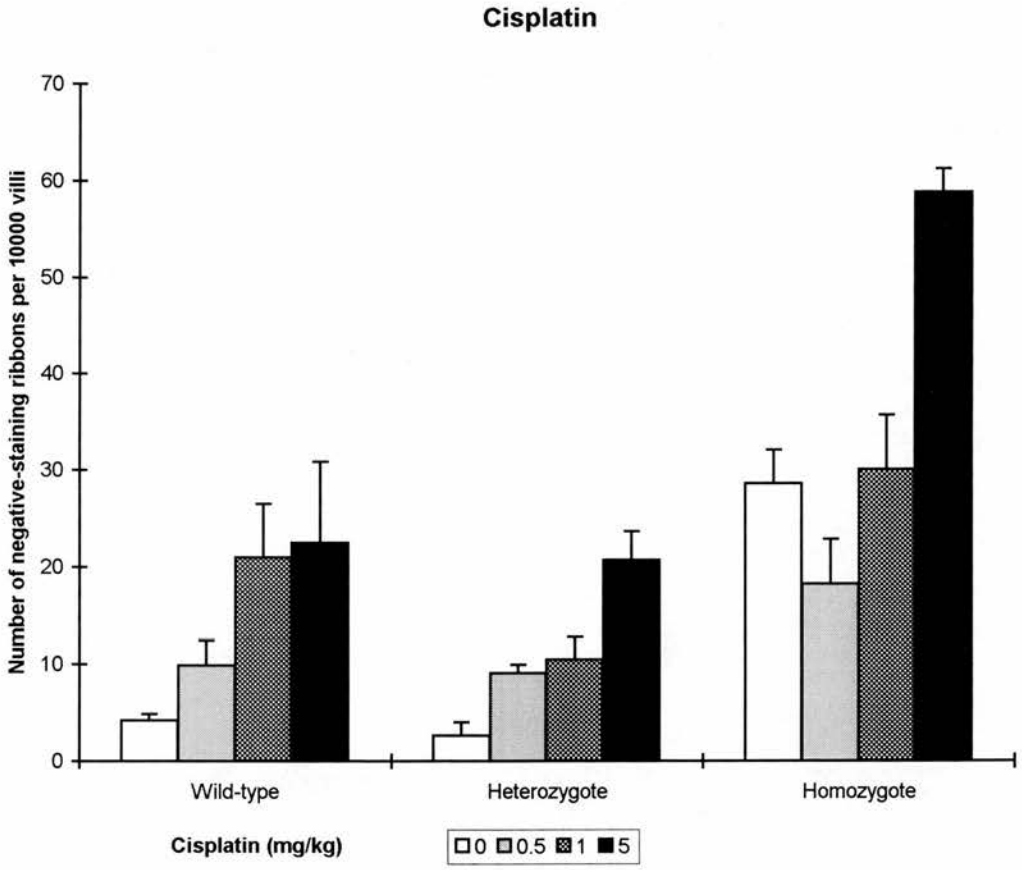
Cisplatin
Number of negative-staining ribbons per 10000 villi
70
60
50
40
30
20
10
0
Wild-type
Heterozygote
Homozygote
Cisplatin (mg/kg)
0 0.5 1 5

**Discussion**

To date only one study has documented the *in vivo* mutation rate in *MSH2*-deficient mice (Andrew *et al.*, 1997). Mice homozygous null for *MSH2* and containing a retrievable transgenic *lacI* reporter gene revealed 4.8, 11 and 15.2-fold elevations in spontaneous mutation frequencies in tissue from the brain, small intestine and thymus respectively, compared to wild-type controls (Andrew *et al.*, 1997). However, mutation rate studies using lamda shuttle vectors harbouring the *lacI* gene are subject to multiple confounding factors. First, the *lacI* gene is heavily methylated and is not expressed (Provost & Short, 1994). This is important since there is evidence to suggest that actively transcribed genes are preferentially repaired (Bohr, 1991). Second, insertions larger than 8kb are packaged ineffectively into phage particles because of the size constraint on genomic DNA that a phage particle can accommodate. Furthermore, large deletions may involve the reporting construct itself. Thus, chromosomal rearrangements, gene amplifications or large deletions or insertions may not be detected by this method of analysis (Nishino *et al.*, 1995). Third, the integration of the transgene may disrupt a cellular gene that is involved in DNA repair, DNA replication, or the metabolic processes that contribute to DNA damage (Gossen *et al.*, 1991). Lastly, *de novo* mutations may arise in *Escherichia coli* during analysis. Alternatively, *Escherichia coli* may repair lesions in the transgene that were present in the mouse DNA. The *Dlb-1* assay is not subject to these potential sources of error and therefore constitutes a more accurate and meaningful determination of the *in vivo* mutation frequency in *MSH2* -/- mice.

In both *MSH2* wild-type and heterozygote mice Temozolomide, at the doses used, was unable to increase the mutation frequency at the *Dlb-1* locus. In contrast, in an *MSH2* null environment the mutation frequency was elevated at all doses with *MSH2* deficiency resulting in a 13.8-fold increase at 100mg/kg Temozolomide compared to wild-type controls. These results confirm *MSH2* as a key defence mechanism against alkylating-type DNA damage. Variations in $O^6$-alkylguanine-DNA-alkyltransferse (AGT) activity are unlikely to modulate these observations since AGT levels in the murine small intestine are independent of *MSH2* status (see Part III of this thesis) and high doses of alkylating agent deplete functional AGT activity (Pegg & Byers, 1992).

MNNG proved to be a more potent mutagen than Temozolomide, generating over 400 negatively staining ribbons per 10 000 villi at the doses studied. However, in contrast to Temozolomide, MNNG was mutagenic in wild-type and heterozygote animals at doses of 25 and 50mg/kg. Thus, at these doses the combined protective mechanisms of *MSH2* and AGT were inadequate to prevent mutations. Notwithstanding such differences between MNNG and Temozolomide, the MNNG mutation data clearly demonstrate again that *MSH2* forms a critical defence mechanism against the mutagenic properties of alkylating agents. Indeed, at the highest dose of MNNG (50mg/kg), *MSH2* deficiency resulted in a 5.0-fold elevation in mutation frequency at the *Dlb-1* locus compared to *MSH2* +/+ mice.

Cisplatin was found to be weakly mutagenic in small intestinal cells with increasing doses of Cisplatin resulting in increased mutation frequencies in *MSH2* wild-type and heterozygote mice. However, in contrast to alkylating agents, *MSH2* deficiency led to an small increase in mutation frequency only at the highest dose of Cisplatin (5mg/kg). Moreover, the *MSH2* dependency of this response was less than that of either Temozolomide or MNNG, with only a 1.7-fold elevation in mutation frequency being observed at 5mg/kg Cisplatin. The most direct conclusions from these results are twofold. First, Cisplatin is weakly mutagenic in small intestinal cells. Second, *MSH2* plays little or no role in counteracting Cisplatin induced mutagenic DNA damage, except perhaps at high doses when *MSH2* deficiency may become significant. Given that *MSH2* is known to bind 1,2 diguanyl Cisplatin cross-links these findings are surprising. This may be explained by the observation that platinated DNA is not *per se* a good substrate for the *MSH2* repair complex, but on the other hand Cisplatin adducts occurring on mismatched base pairs bind *MSH2* effectively (Yamada *et al.*, 1997). Alternatively, it may be that within small intestinal cells 1,2 diguanyl adducts do not mediate the mutagenic effects of Cisplatin or that stem cells with Cisplatin-DNA lesions are effectively removed by apoptosis signalled by other pathways, and do not contribute to the mutation frequency.

The mutation data presented in this chapter correlates positively with the apoptotic response of small intestinal cells to the same reagents, although this should be interpreted with caution given that data is available for only three genotoxic agents.

However, a marked *MSH2* dependency exists for both the reduction in apoptosis and the increase in mutation frequency observed after treatment with Temozolomide. In contrast, the apoptotic and mutagenic effects of Cisplatin show little *MSH2* dependency with the responses following MNNG exposure being intermediate in nature (Figure 4.5). Taken together these findings provide supportive evidence for the hypothesis that apoptosis is involved in the deletion of crypt cells bearing DNA damage and preventing the propagation of mutant daughter cell clones. Furthermore, these data suggest that the specificity of *MSH2* for the DNA lesion may determine both the mutation frequency and the apoptotic response in *MSH2* null mice.

The significance of this mutation data to tumourigenesis is threefold. First, cells which lose *MSH2* function develop spontaneous mutation frequencies of approximately six-fold higher than normal cells. Second, intestinal cells that lack *MSH2,* such as those that may occur in the intestines of HNPCC patients, are particularly susceptible to the mutagenic effects of alkylating agents. Indeed, intestinal epithelia may be exposed to an alkylating agent rich environment in the form of bile acid conjugates which have undergone N-nitrosation, or components of the normal diet capable of DNA methylation (Shuker *et al.,* 1981; Hall *et al.,* 1991; Bingham *et al.,* 1996). Thus, loss of the DNA mismatch repair pathway in such an environment may result in mutation frequencies several fold higher than those due to MMR deficiency alone. Third, treatment of $RER^{+}$ tumours with methylating agents such as Temozolomide may actually increase the mutation frequency within the tumour cells themselves and consequently accelerate, rather than retard, tumour progression.

## Figure 4.5

A positive correlation (r=0.99) exists between the increase in mutation frequency at the *Dlb-1* locus due to *MSH2* deficiency and the reduction in apoptosis due to *MSH2* deficiency following treatment with Temozolomide, MNNG, and Cisplatin. The reduction in apoptosis resulting from *MSH2* deficiency was calculated from the ratio of the areas under the graphs of *MSH2* wild-type and *MSH2* null mice in Figures 1.3 A, B, and D. The contribution of *MSH2* deficiency to the mutation frequency was calculated by determining the ratio of the increase mutation frequency (taking into account background mutation rates) in *MSH2* null mice compared to wild-type mice at the highest dose of each drug used (Temozolomide 100mg/kg; MNNG 50mg/kg; Cisplatin 5mg/kg).

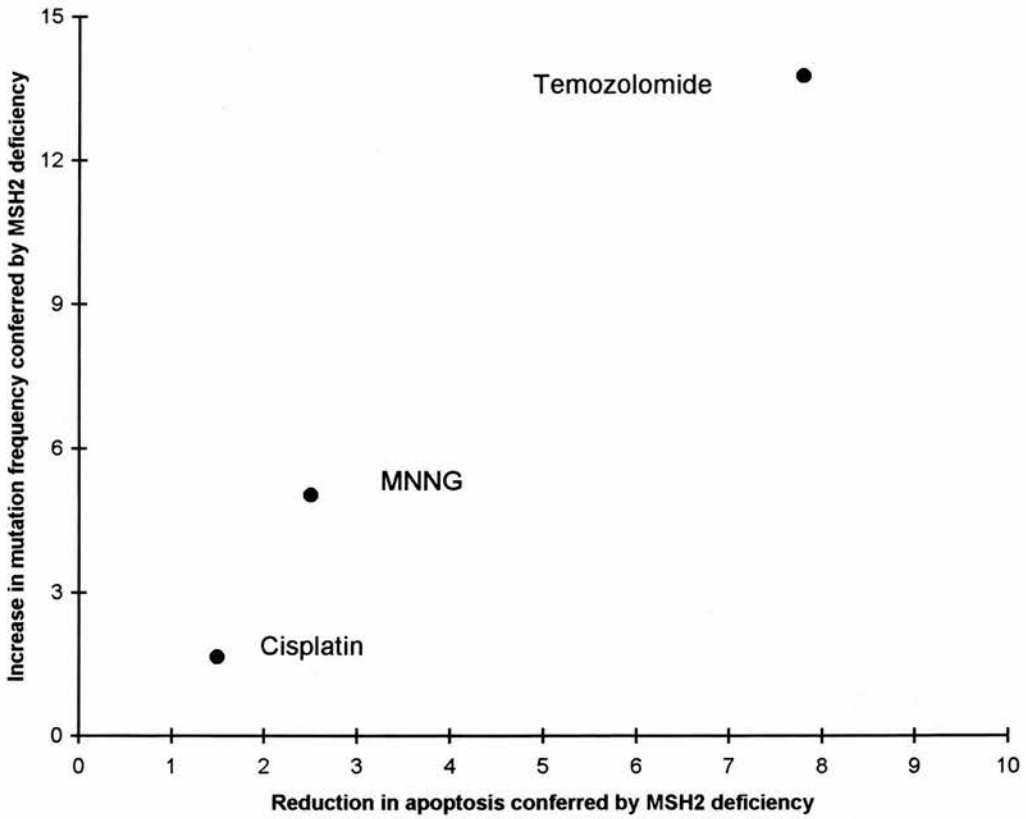
Increase in mutation frequency conferred by MSH2 deficiency
15
12
9
6
3
0
Temozolomide
MNNG
Cisplatin
0
1
2
3
4
5
6
7
8
9
10
Reduction in apoptosis conferred by MSH2 deficiency

# Part V

## *MSH2, p53* and Tumourigenesis

## *MSH2, p53* and Tumourigenesis

### Introduction

Cancer is the endpoint of an evolutionary-like process whereby normal cells are transformed into malignant cells by the cumulative acquisition of genetic changes which confer proliferative, invasive, and metastatic properties upon the cell (Vogelstein & Kinzler, 1993). This process can be rapidly accelerated by the loss of systems that safeguard genomic stability resulting in an increased rate of mutagenesis and chromosomal rearrangements (Hartwell, 1992; Kolodner, 1995).

Acquisition of genomic instability in colorectal cancers involves two separate pathways (Schlegel *et al.*, 1995; Cottu *et al.*, 1996; Lengauer *et al.*, 1997). First, in a small proportion of colorectal cancers, defects in components of the DNA mismatch repair pathway, for example *MSH2* deficiency, lead to microsatellite instability - an indication of a "mutator phenotype" at the nucleotide sequence level (Liu *et al.*, 1995). In addition, loss of *MSH2* has been shown to suppress homologous recombination between diverged DNA sequences and confer resistance to methylating agents (de Wind *et al.*, 1995). Furthermore, the mismatch repair system is essential for a functional $G_2$ cell cycle checkpoint (Hawn *et al.*, 1995). Thus, *MSH2* is a key component in the maintenance of cellular genomic stability. Second, in the majority of colorectal cancers no evidence of microsatellite instability can be identified. However, genomic instability in terms of major changes to chromosomes occurs leading to aneuploidy - abnormal chromosome number (Reichmann *et al.*, 1981). Defects in *p53* are thought to contribute to this gross form of instability for three reasons. First, in colorectal cancer alterations in *p53* precede and are correlated with the divergence of aneuploid sub-clones (Carder *et al.*, 1993). Second, normal non-permisssive cells become permissive for DNA amplification when *p53* is lost (Livingstone *et al.*, 1992; Yin *et al.*, 1992). Third, *p53* null cells display elevated mutation rates following $\gamma$-irradiation induced DNA strand breaks (Clarke *et al.*, 1997). In addition to an important role in maintaining chromosome stability, *p53* may also be involved in maintaining stability at the nucleotide level since the C-terminal domain of *p53* binds DNA mismatches (Lee *et al.*, 1995). Thus *p53*, like *MSH2*, plays a pivotal role in

maintaining DNA integrity and preventing malignancy. The controls governing which pathway of instability predominates in colorectal cancer are unknown. Furthermore, no data exists on the interaction between mismatch repair-mediated genomic instability and *p53*-mediated genomic instability.

To study the interactions of these two genes at the level of the organism, mice doubly null for *MSH2* and *p53* were generated. Since both *MSH2* null and *p53* null mice develop tumours spontaneously, any acceleration in tumourigenesis or shift in tumour phenotype observed in double null mice would provide evidence of a positive interaction between *MSH2* and *p53* deficiency. Furthermore, by examining tumours arising in double null mice the contribution of each type of genomic instability to tumourigenesis, either *MSH2*-mediated or *p53*-mediated, could be addressed. First, the effects of *MSH2* nullizygosity upon *p53* null-associated female embryonic lethality were investigated.

**Results**

*Are mutant MSH2 / p53 inter-crossed mice viable?*

The F1 progeny from mating *MSH2* -/- mice to *p53* -/- mice were all viable and developed normally. Crossing the F1 progeny (*MSH2* +/- *p53* +/-) together generated a large cohort of mice which segregated for both *MSH2* and *p53*, and produced mice with all genotypic combinations. Only mice with the following genotype were studied: *MSH2* -/- *p53* +/+, *MSH2* +/+ *p53* -/-, *MSH2* -/- *p53* +/-, *MSH2* +/- *p53* -/-, and *MSH2* -/- *p53* -/-. All of these groups of mice appeared phenotypically normal with no profound aberrant effects on early viability being observed. Both males and females in all five genotype groups were fertile beyond eight weeks of age.

*Does MSH2 status affect p53 null-associated female embryonic lethality?*

In cohorts of *MSH2* +/+, *MSH2* +/-, and *MSH2* -/- mice (on a wild-type *p53* background) the number of male and female mice was in accordance with the expected 1:1 Mendelian ratio (Table 5.1). However, in all *p53* -/- mice, irrespective of their *MSH2* status, a significant reduction (average 40%; $p<0.01$, Chi-squared test) in

**Table 5.1**

| | *p53* +/+ | *p53* -/- |
|---|---|---|
| *MSH2* +/+ | 262/254 (-2%) | 26/12 (-37%) |
| *MSH2* +/- | 118/94 (-11%) | 52/21 (-42%) |
| *MSH2* -/- | 166/177 (+3%) | 61/22 (-47%) |

the number of live-born female mice was observed (Table 5.1). Thus, *MSH2* status does not affect *p53*-associated female embryonic lethality.

*Can MSH2 and p53 deficiency co-operate to accelerate tumourigenesis in murine tissues?*

Cohorts of *MSH2 +/+ p53 +/+*, *MSH2 +/- p53 +/+*, *MSH2 -/- p53 +/+*, *MSH2 +/+ p53 -/-*, *MSH2 +/- p53 -/-*, *MSH2 -/- p53 +/-*, and *MSH2 -/- p53 -/-* mice were studied to investigate survival and tumourigenesis. Colonies were monitored for up to 240 days. Mice were killed when they appeared visibly ill and their age was calculated in days. Kaplan-Meier survival plots were generated for all genotypes of *MSH2 / p53* inter-crossed mice (Figure 5.1). Survival data for *MSH2 +/+ p53 +/-* mice was generated from historical controls (Purdie *et al.*, 1994). Wild-type mice, together with both *MSH2* and *p53* heterozygotes, were viable and healthy up to 240 days. However, all mutant *MSH2 / p53* inter-crossed mice succumbed earlier to tumours. The median age of survival for each colony was as follows: *MSH2 -/- p53 +/+* 142 days; *MSH2 +/+ p53 -/-* 121 days; *MSH2 +/- p53 -/-* 106 days; *MSH2 -/- p53 +/-* 99 days; *MSH2 -/- p53 -/-* 65 days. Thus, *MSH2 -/- p53 -/-* mice developed tumours and died significantly earlier than either *MSH2 -/-* or *p53 -/-* mice alone ($p< 0.0006$, log rank test), demonstrating co-operativity between the two genes. *MSH2* heterozygosity on a *p53* null background did not significantly alter survival from *p53* nullizygosity alone ($p>0.09$, log rank test). In contrast, *MSH2* nullizygosity in *p53* heterozygote mice resulted in a dramatic reduction in survival compared with *p53* heterozygote mice possessing intact *MSH2* ($p<0.00001$, log rank test). Thus, *MSH2* deficiency accelerated tumourigenesis in *p53* heterozygote mice, although *p53* deficiency did not accelerate tumourigenesis in *MSH2* heterozygote mice.

*What is the incidence and spectrum of tumours that develop in mutant MSH2 / p53 inter-crossed mice?*

Full autopsies were performed on mice which were identified as sick. All findings were recorded and any gross pathology, including tumours noted. H&E sections of the tissues taken at autopsy were examined by a histopathologist. No developmental

## Figure 5.1

Kaplan-Meier survival plots for different cohorts of mutant *MSH2* / *p53* inter-crossed mice. Age of animals is given in days. Survival of *p53* +/- mice was reproduced from historical data (Purdie *et al.*, 1994). All cohorts of mice are labelled accordingly. The red line represents data from *MSH2* -/- *p53* +/- mice whereas the blue line represents data from *MSH2* +/- *p53* -/- mice. Note that all *MSH2* -/- *p53* -/- mice died or were killed within the first 100 days of observation.

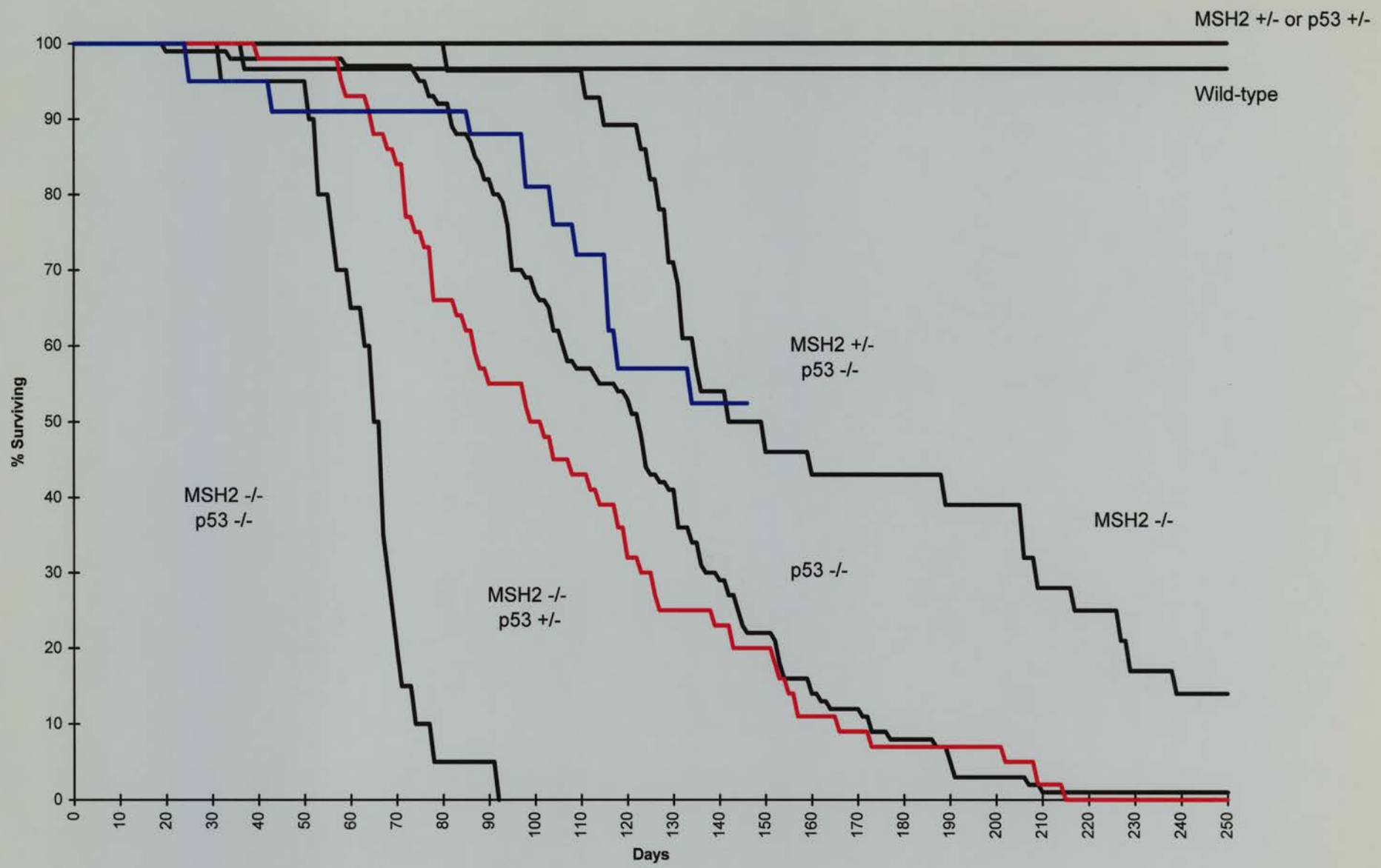
MSH2 +/- or p53 +/-
Wild-type
MSH2 +/-
p53 -/-
MSH2 -/-
p53 -/-
p53 -/-
MSH2 -/-
p53 +/-
MSH2 -/-
p53 -/-
% Surviving
Days
0
10
20
30
40
50
60
70
80
90
100
110
120
130
140
150
160
170
180
190
200
210
220
230
240
250

abnormalities were noted in any group of mice although a variety of tumours including thymic and extra-thymic lymphomas, leiomyosarcomas, and adenomas and adenocarcinomas from the small and large intestine were found (Figure 5.2 & 5.3). The incidence of the various tumours identified in mutant *MSH2 / p53* inter-crossed mice is summarised in Table 5.2. *MSH2* null mice all succumbed to lymphoma with approximately half of these being extra-thymic in origin. In addition, adenomas and adenocarcinomas were found in 15% and 25% of the animals' small and large intestines respectively. The majority (88%) of *p53* null mice died from lymphoma although a small proportion (12%) died from either leiomyosarcoma or osteosarcoma. No gastrointestinal tract lesions were identified in *p53* null mice. Ninety-five percent of *MSH2 -/- p53 +/-* mice died of lymphoma with equal proportions of thymic and extra-thymic origins being observed. 11% of these mice had identifiable gastrointestinal tract neoplasms. *MSH2 +/- p53 -/-* mice were similar to *p53 -/-* mice in that they developed lymphoma (67%) or sarcoma (33%). However, in contrast to *MSH2 +/+ p53 -/-* mice all of the lymphomas in *MSH2 +/- p53 -/-* were extra-thymic in origin and both sarcomas were located in the caecal wall. *MSH2 -/- p53 -/-* all succumbed to thymic lymphomas. No adenomas or adenocarcinomas were identified in their intestines.

*Does $APC^{Min}$ heterozygosity alter the nature and incidence of tumours arising in mice doubly null for MSH2 and p53?*

*Min* (*APC* $+/^{Min}$) mice were crossed to *MSH2 -/- p53 +/-* mice generating a colony of *APC* $+/^{Min}$ *MSH2 -/- p53 -/-* mice (Table 5.2). These mice developed thymic lymphoma at a similar age to *MSH2 -/- p53 -/-* mice ($p>0.2$, log rank test). However, 50% of these mice also developed acinar pancreatic adenomas and adenocarinomas analogous to those found in *APC* $+/^{Min}$ *p53 -/-* mice by Clarke *et al.* (1995). In addition, all of the *APC* $+/^{Min}$ *MSH2 -/- p53 -/-* mice developed adenomas and adenocarcinomas in both their small and large bowels. The adenomas and adenocarcinomas were similar to those found in *Min* mice alone (Moser *et al.*, 1990) or in *APC* $+/^{Min}$ *MSH2 -/-* mice (Reitmair *et al.*, 1996b). Thus, $APC^{Min}$ heterozygosity

## Figure 5.2

**(A)** H&E stained section of a thymic lymphoma arising in a *MSH2* -/- *p53* -/- mouse. Note the abundance of apoptotic bodies present (arrowed) and their contribution to the classical "starry sky" appearance often seen in lymphomas. (X250)

**(B)** H&E stained section of a leiomyosarcoma arising in the caecum of a *MSH2* +/- *p53* -/- mouse. An arrow depicts an island of normal colonic epithelium surrounded by tumour tissue. (X250)

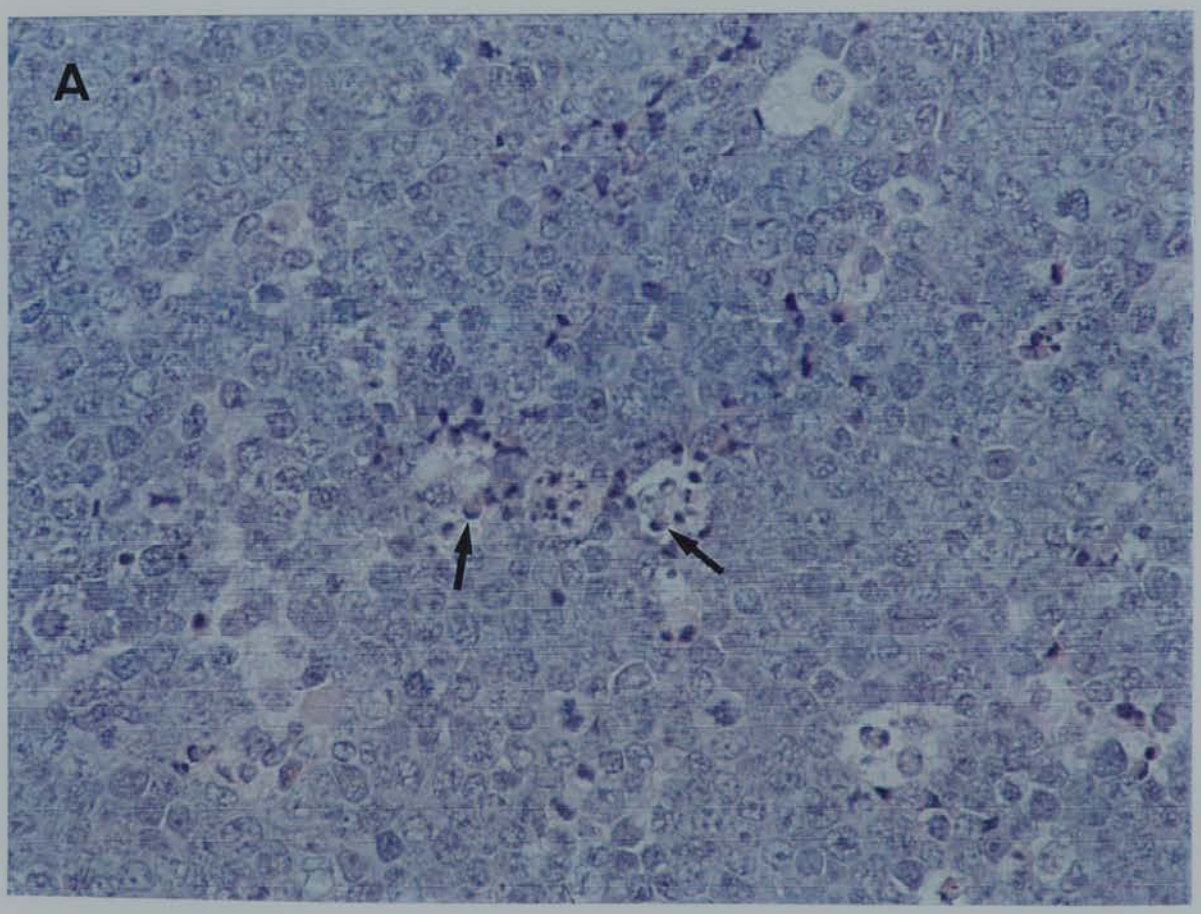
A

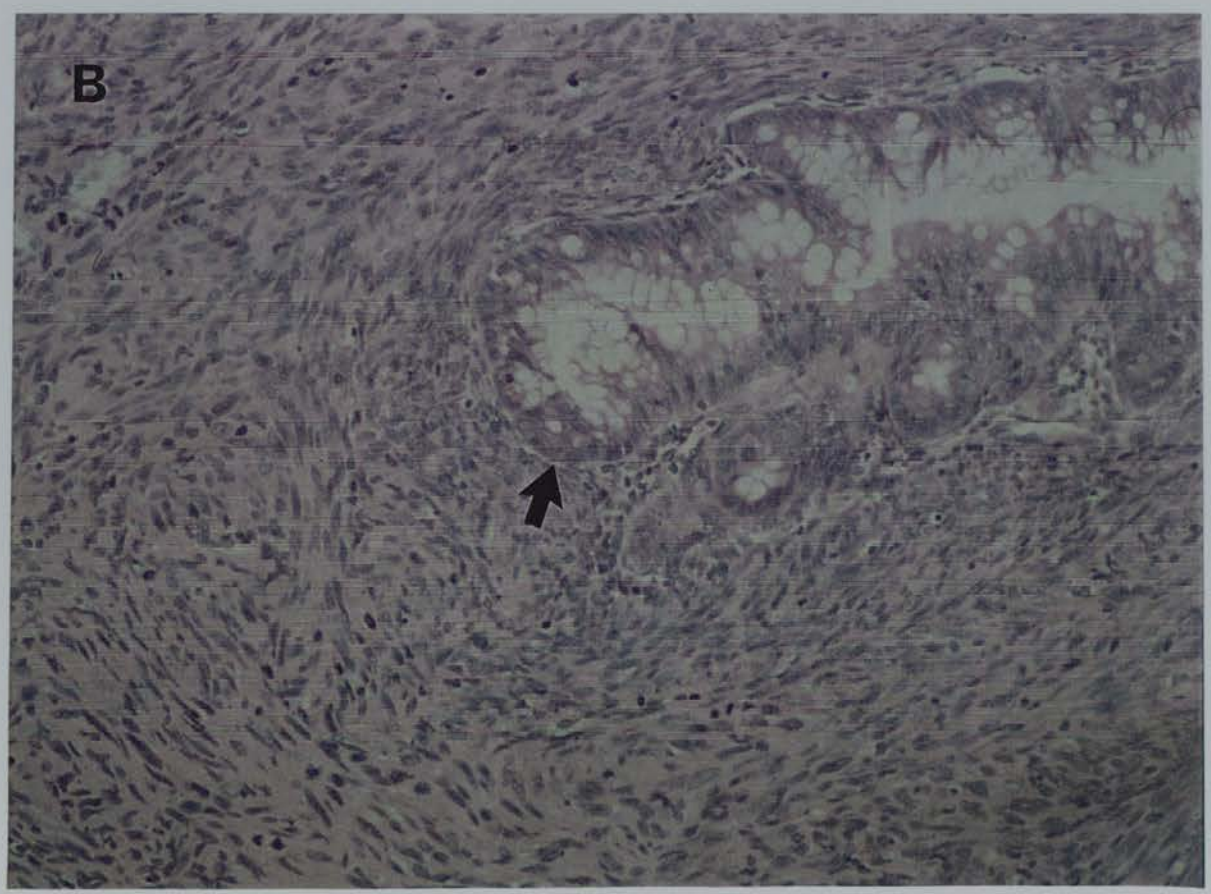
B

## Figure 5.3

**(A)** H&E stained section of mouse colon with an early benign adenoma. The genotype of the mouse was *APC* $+/^{Min}$ *MSH2* -/- *p53* -/-. Note the cellular hyperplasia, pleomorphism and hyperchromatism evident within the neoplastic glands. (X250)

**(B)** H&E stained section of a colonic adenocarcinoma removed from a 7 month old *MSH2* -/- mouse. The arrow depicts tumour cells which have invaded into the muscularis propria. (X250)

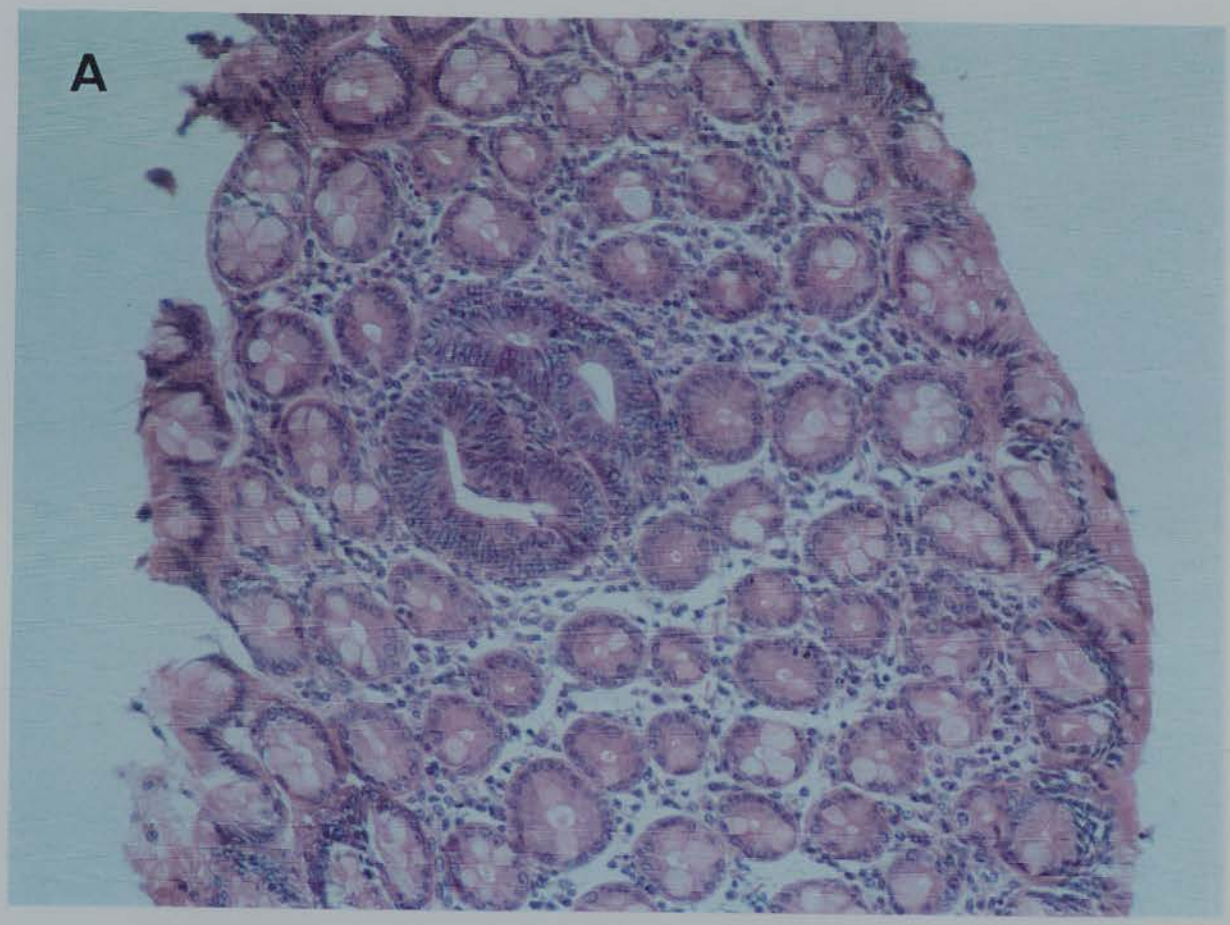
A

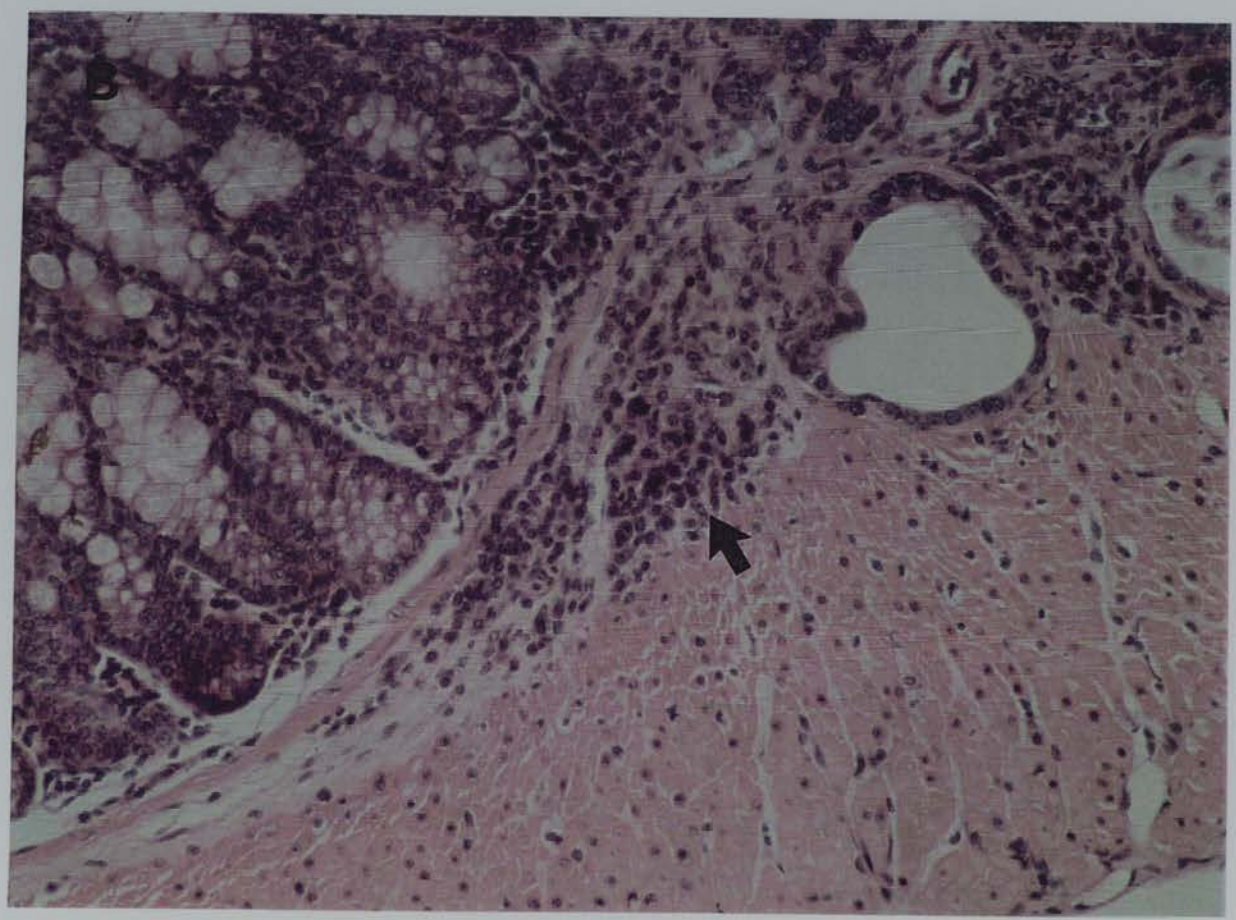
B

## Table 5.2

Autopsy results and median age of death in days of cohorts of mutant *MSH2 / p53* inter-crossed mice. Lymphomas were subdivided into those of thymic origin and those in which an extra-thymic site was primarily involved. Sarcomas encompassed both leiomyosarcomas and osteosarcomas while all pancreatic neoplasms identified were acinar in origin. Neoplasia in the small intestine and colon referred to the presence of both benign adenomas and malignant adenocarcinomas arising within epithelial cells. Number of autopsies from which the data was collected is shown in brackets.

## Table 5.2

| | Median Age of Death | Lymphoma | % Thymic Lymphoma | % Extra-thymic Lymphoma | Sarcoma | Pancreatic Neoplasia | Neoplasia -Small Intestine | Neoplasia -Colon |
|---|---|---|---|---|---|---|---|---|
| *MSH2* +/+ | N/A | Nil | Nil | Nil | Nil | Nil | Nil | Nil |
| *MSH2* +/- | N/A | Nil | Nil | Nil | Nil | Nil | Nil | Nil |
| *MSH2* -/- | 142 | 100% (n=23) | 57% | 43% | 0% | 0% | 15% (n=20) | 25% |
| *p53* -/- | 121 | 88% (n=57) | 84% | 16% | 12% | 0% | 0% (n=57) | 0% |
| *MSH2* -/- *p53* +/- | 99 | 95% (n=39) | 51% | 49% | 0% | 0% | 11% (n=28) | 11% |
| *MSH2* +/- *p53* -/- | 106 | 67% (n=6) | 0% | 100% | 33% | 0% | 0% (n=4) | 0% |
| *MSH2* -/- *p53* -/- | 65 | 100% (n=18) | 100% | 0% | 0% | 0% | 0% (n=15) | 0% |
| *APC* $+/^{Min}$ *MSH2* -/- *p53* -/- | 56 | 100% (n=5) | 100% | 0% | 0% | 50% (n=4) | 100% (n=4) | 100% (n=4) |

did not significantly alter the survival of *MSH2* -/- *p53* -/- mice but did alter the tumour spectrum substantially.

*What is the immunophenotype of the thymic lymphomas that arise within mutant MSH2 / p53 inter-crossed mice? Does genotype influence the immunophenotype of lymphomas?*

Thymic lymphomas from sick mice of genotypes *MSH2* -/- *p53* +/+, *MSH2* +/+ *p53* -/-, *MSH2* -/- *p53* +/-, and *MSH2* -/- *p53* -/- of known age were characterised by immunophenotyping studies. Antibodies specific to CD2, CD4, CD8, CD24, CD45, Thy-1, macrophages (F4-80), B cells (anti-mouse IgG) and the interleukin-2 receptor (IL-2R) were used to assess the cell surface markers present on lymphoma cells by flow cytometry. All of the tumours examined were of T-cell origin. B-cell and macrophage markers failed to stain tumour cells above background levels. Levels of IL-2R positivity were low with less than 10% of cells staining positive with no relationship to genotype being observed (data not shown). However, tumours from *MSH2* -/- *p53* -/- mice retained high levels of expression of CD2, CD4, CD8, CD24, CD45 and Thy-1 molecules (Figure 5.4 & 5.5). In contrast, tumours from *MSH2* -/- *p53* +/- mice, which succumbed at a later stage, displayed lower levels of all the cell surface molecules examined ($p<0.01$ for all markers, Mann-Whitney U). Single null mice (*MSH2* -/- or *p53* -/-) displayed variable patterns of expression of cell surface markers, with some tumours retaining molecules and others losing them. No consistent pattern of antibody staining could be assigned to tumours arising in *MSH2* null or *p53* null mice.

*What effect does MSH2 deficiency have on the remaining wild-type copy of p53 in tumours arising in MSH2 null p53 heterozygote mice?*

DNA from thymic lymphomas arising in *MSH2* -/- *p53* +/- mice was amplified by a *p53*-specific PCR reaction (Figure 5.6). No loss of heterozygosity (LOH) was observed in any of the nine thymic lymphomas examined, thus demonstrating that no gross chromosomal deletion of the remaining wild-type *p53* allele had occurred. In addition, total RNA was extracted from three of these tumours and reverse

## Figure 5.4

Immunophenotype of thymic lymphomas arising in mutant *MSH2 / p53* mice. Data presented as a scatter plot of the percentage of tumour cells staining positive for cluster of differentiation (CD) antigens CD2, CD4, and CD8 against the age of the mouse's death in days. Open circle symbols, *MSH2 -/- p53 +/+*; closed square symbols, *MSH2 -/- p53 +/-*; open triangular symbols, *MSH2 -/- p53 -/-*; crosses, *MSH2 +/+ p53 -/-*

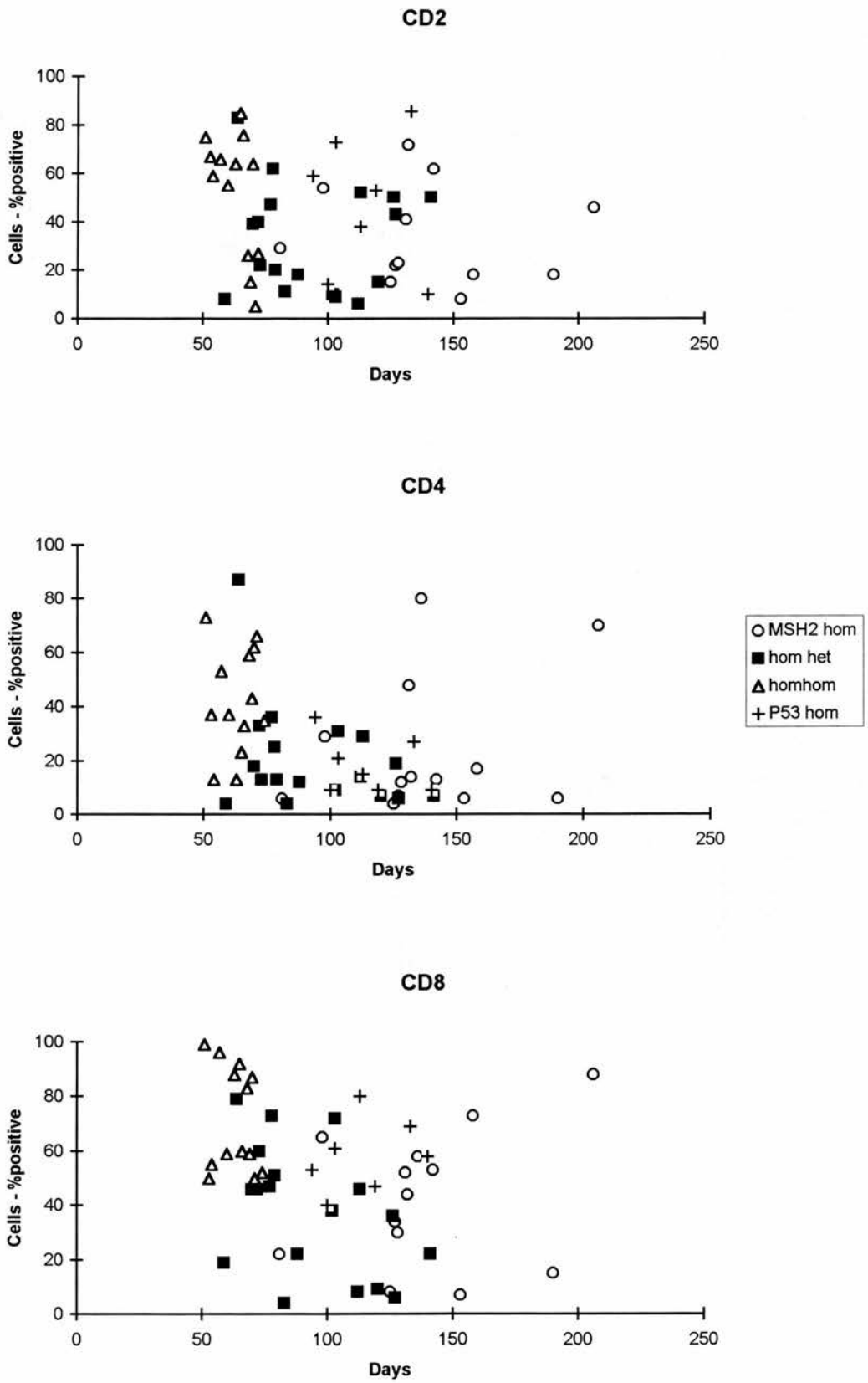
CD2
Cells - %positive
Days
CD4
Cells - %positive
Days
MSH2 hom
hom het
homhom
P53 hom
CD8
Cells - %positive
Days

## Figure 5.5

Immunophenotype of thymic lymphomas arising in mutant *MSH2 / p53* mice. Data presented as a scatter plot of the percentage of tumour cells staining positive for membrane antigens CD24, CD45, and Thy-1 against the age of the mouse's death in days. Open circle symbols, *MSH2 -/- p53 +/+*; closed square symbols, *MSH2 -/- p53 +/-*; open triangular symbols, *MSH2 -/- p53 -/-*; crosses, *MSH2 +/+ p53 -/-*

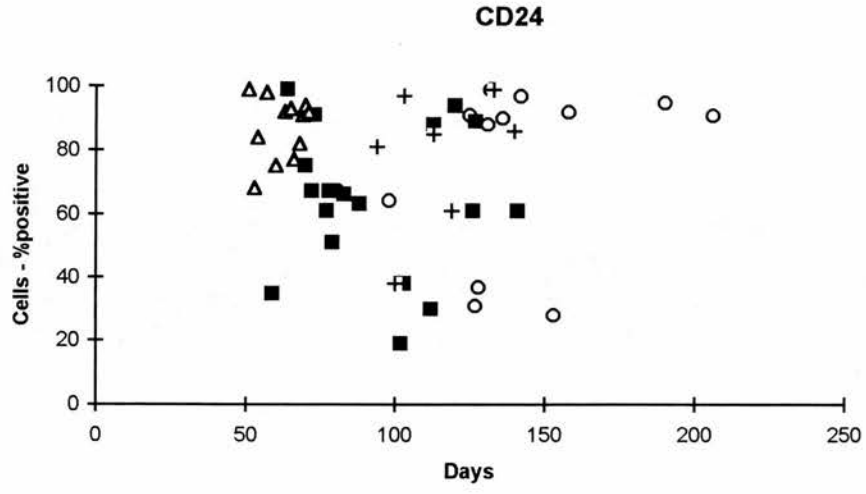
CD24
Cells - %positive
Days
0
20
40
60
80
100
0
50
100
150
200
250

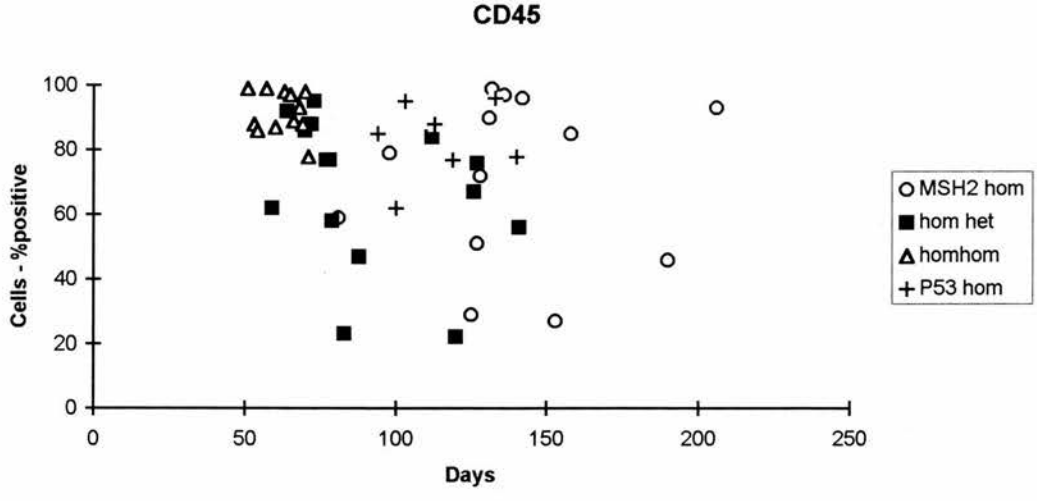
CD45
Cells - %positive
Days
MSH2 hom
hom het
homhom
P53 hom

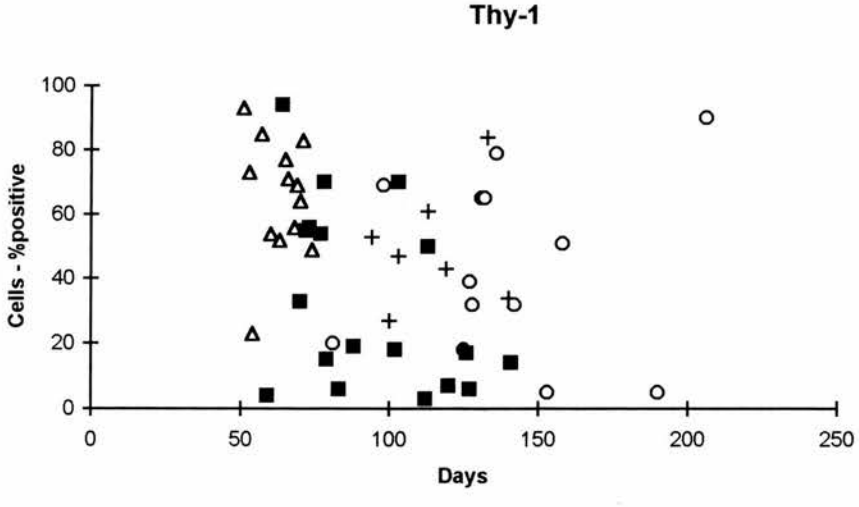
Thy-1
Cells - %positive
Days

## Figure 5.6

UV-transilluminated, ethidium bromide stained 2% TBE agarose gel showing retention of the wild-type *p53* allele in lymphomas from *MSH2* -/- *p53* +/- mice by specific PCR reaction. The arrow denotes the retained wild-type *p53* allele. **L** DNA ladder molecular weight marker; **C** PCR negative control with only the *p53* targeted event detected; **1-9** Tumour DNA from 9 separate thymic lymphomas arising in 9 different *MSH2* -/- *p53* +/- mice.

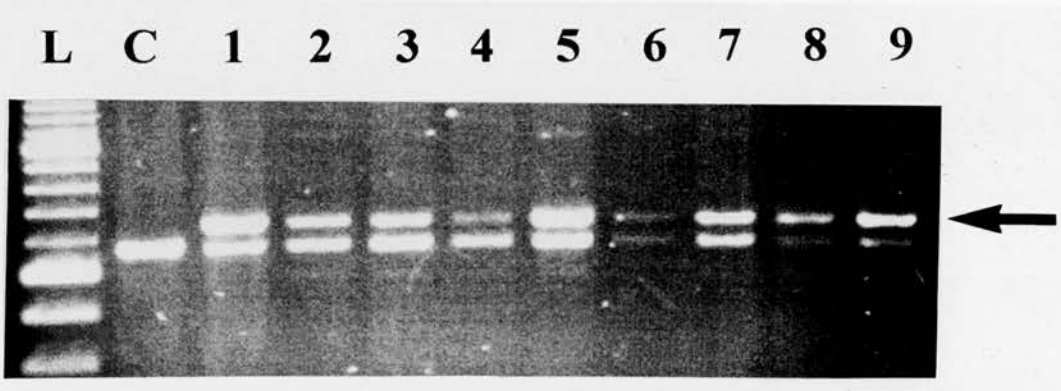
L C 1 2 3 4 5 6 7 8 9

transcribed into cDNA. Exons 5-9 of the wild-type *p53* allele were amplified by PCR and sequenced (Table 5.3). A single G→A transition was observed at codon 234 in one of the tumours and was predicted to give an amino acid change from methionine to isoleucine. In the remaining two tumours no mutation was identified in exons 5-9 of *p53*.

*How do mutant MSH2 and p53 interact in the development of aneuploidy in tumours?*

The DNA content of cells from thymic lymphomas arising in *MSH2 -/- p53 +/+*, *MSH2 +/+ p53 -/-*, *MSH2 -/- p53 +/-* and *MSH2 -/- p53 -/-* mice was analysed by flow cytometry. The DNA content of the tumours was classified as either diploid or as aneuploid if an additional $G_1$ or $G_2$ peak with a different DNA index was present (Figure 5.7). All lymphomas from *MSH2 -/- p53 +/+*, *MSH2 -/- p53 +/-* and *MSH2 -/- p53 -/-* mice displayed a diploid karyotype (Table 5.4). In contrast, 2 out of 7 (29%) of the lymphomas from *MSH2 +/+ p53 -/-* mice showed evidence of aneuploidy.

*What is the nature of the genomic instability, assessed by comparative genomic hybridisation (CGH), in tumours from MSH2 null, p53 null, MSH2 null p53 heterozygote, and doubly null mice?*

DNA from thymic lymphomas arising in *MSH2 -/- p53 +/+*, *MSH2 +/+ p53 -/-*, *MSH2 -/- p53 +/-* and *MSH2 -/- p53 -/-* mice was analysed by CGH. CGH was performed on a minimum of five metaphase spreads per tumour and an average green/red profile generated for each chromosome. A green / red ratio outside the limits of 1.125 or 0.875 was scored as an increase or decrease in DNA content for a single chromosome. *MSH2 -/- p53 +/+*, *MSH2 -/- p53 +/-* and *MSH2 -/- p53 -/-* tumours displayed stable genomes with few gains in the DNA content of individual chromosomes being identified (Table 5.5). In contrast, *MSH2 +/+ p53 -/-* tumours showed a considerable number of amplified regions of DNA within their chromosomes (Table 5.5). However, all the tumours examined, irrespective of genotype, showed few areas of gross chromosomal deletions.

## Table 5.3

Mutational analysis of exons 5-9 of the wild-type *p53* allele in thymic lymphomas arising in three different *MSH2* -/- *p53* +/- mice. An in frame G →A transition was identified at codon 234 which was predicted to give an amino acid change from methionine to isoleucine. No mutations were identified in the other two tumours. N/A - not applicable.

**Table 5.3**

| Tumour [*MSH2* -/- *p53* +/-] | Mutations in exons 5-9 wild-type *p53* allele | Predicted amino acid change |
|---|---|---|
| Thymic lymphoma 1 | G → A [codon 234] | Methionine → Isoleucine |
| Thymic lymphoma 2 | none detected | N/A |
| Thymic lymphoma 3 | none detected | N/A |

## Figure 5.7

Examples of diploid **(A)** and aneuploid **(B)** flow cytometric analyses of DNA content of murine thymic lymphomas. The arrow denotes an aneuploid $G_1$ peak arising in a tumour from a *p53* null mouse. The $G_2$ aneuploid peak is lost in the S phase of the cell cycle.

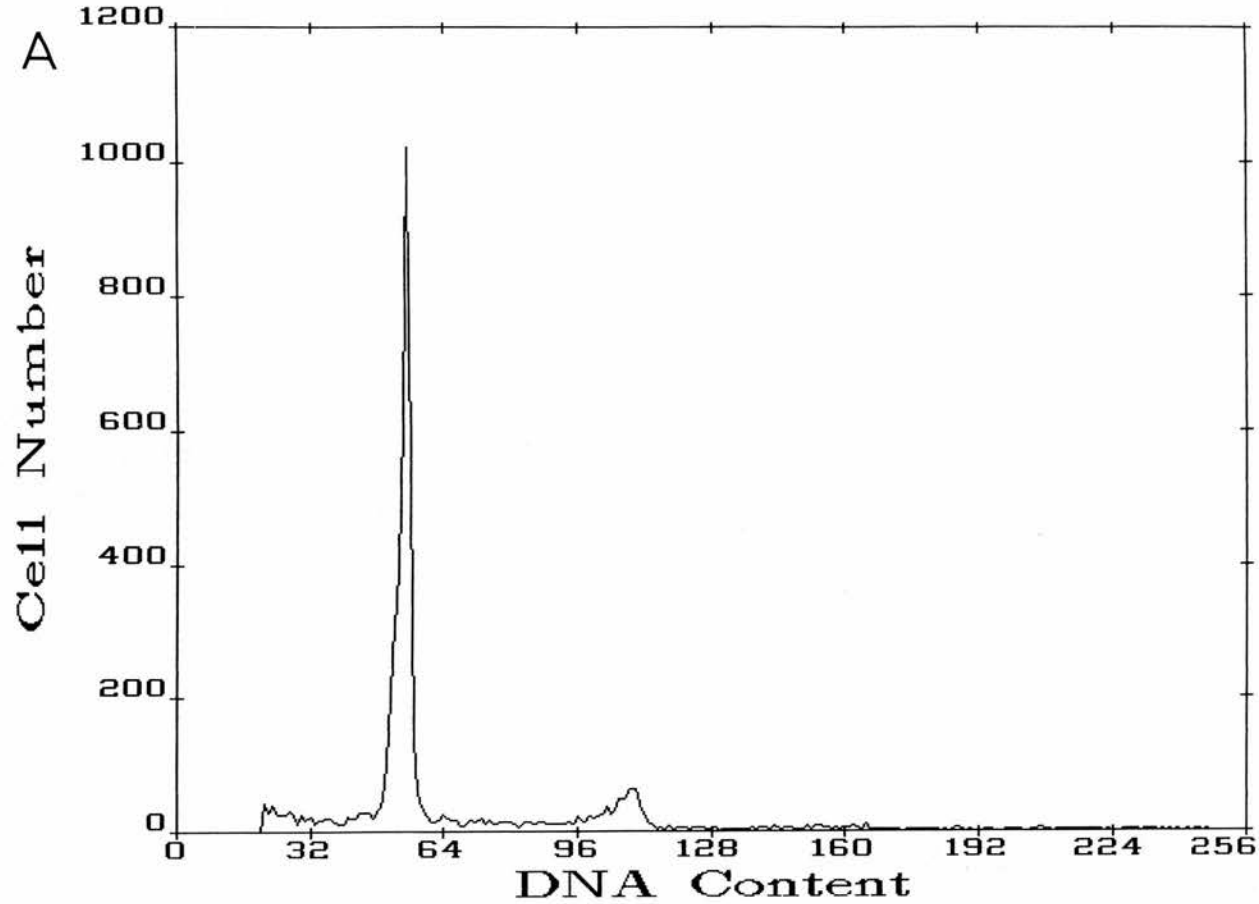
A
1200
1000
800
600
400
200
0
Cell Number
0
32
64
96
128
160
192
224
256
DNA Content

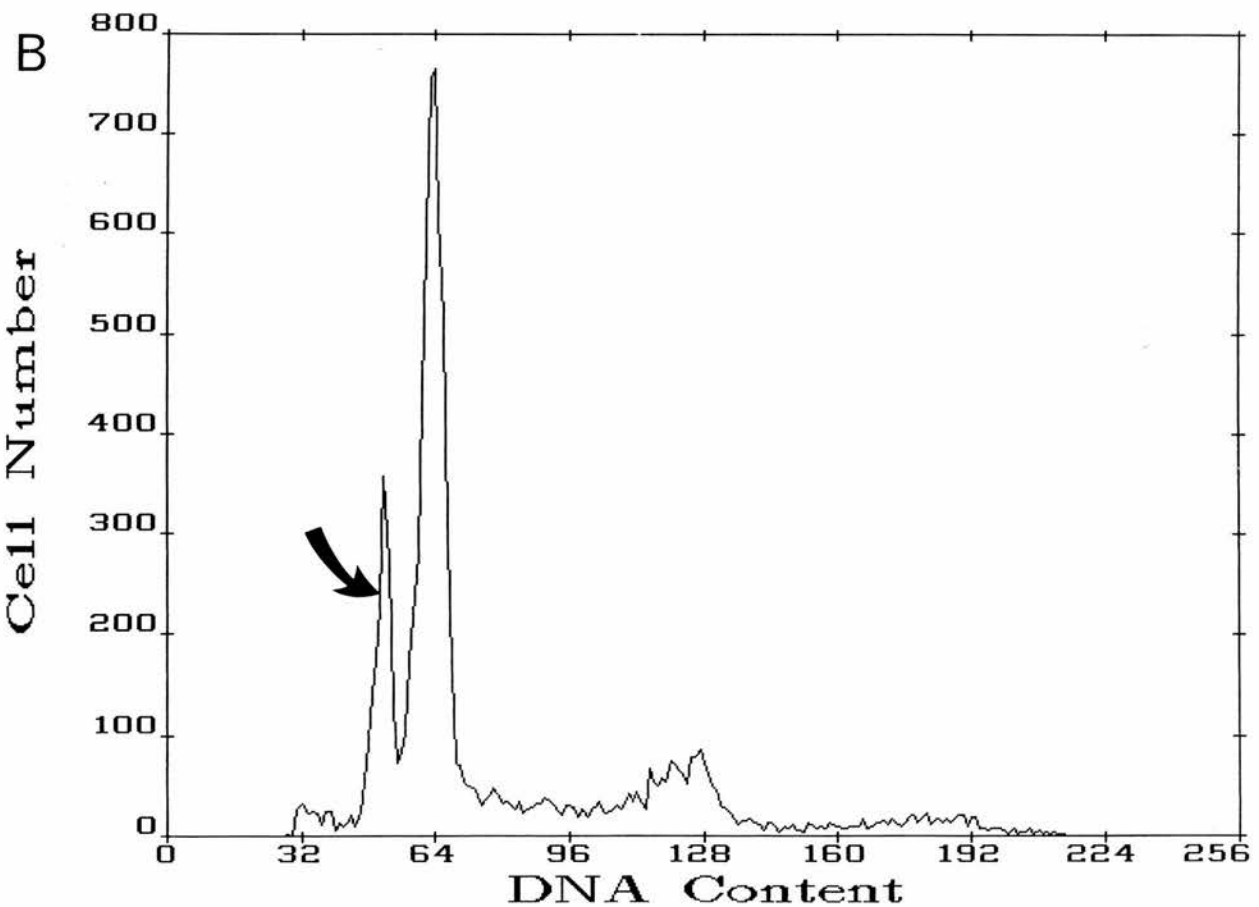
B
800
700
600
500
400
300
200
100
0
Cell Number
0
32
64
96
128
160
192
224
256
DNA Content

## Table 5.4

Flow cytometric analyses of thymic lymphomas from *MSH2 -/- p53 +/+*, *MSH2 +/+ p53 -/-*, *MSH2 -/- p53 +/-*, *MSH2 -/- p53 -/-* mice. Tumours were classified as either diploid or as aneuploid. Aneuploidy was identified by the presence of an additional $G_1$ or $G_2$ peak within the cellular DNA content.

**Table 5.4**

| Thymic Lymphoma | Total number of tumours | Diploid | Aneuploid |
|---|---|---|---|
| *MSH2 -/-* | 7 | 7 | 0 |
| *p53 -/-* | 7 | 5 | 2 |
| *MSH2 -/- p53 +/-* | 7 | 7 | 0 |
| *MSH2 -/- p53 -/-* | 7 | 7 | 0 |

## Table 5.5

Comparative genomic hybridisation (CGH) analyses of murine thymic lymphomas arising in mice of varying *MSH2* and *p53* genotypes. Regions of amplified DNA (**G** for gained) or areas of deleted DNA (**L** for loss) are shown for all of the 19 mouse autosomes. CGH was performed on a minimum of five metaphase spreads per tumour and an average green/red profile generated for each chromosome. An increased or decreased DNA content of a single chromosome corresponded to a green/red ratio outside of 1.125 or 0.875 respectively which was equivalent to gain or loss of one whole chromosome in 25% of diploid cells.

## Table 5.5

| TUMOUR | 1 | 2 | 3 | 4 | 5 | 6 | 7 | 8 | 9 | 10 | 11 | 12 | 13 | 14 | 15 | 16 | 17 | 18 | 19 |
|---|---|---|---|---|---|---|---|---|---|---|---|---|---|---|---|---|---|---|---|
| MSH2 -/- | | | | | | | | | | | | | | | | | | | |
| 1 | | | | | | | | | | | | | | | | | | | |
| 2 | | | | | | | | | | | | | | | | | | | |
| 3 | | | | | | | | | | | | | | | | | | | |
| 4 | | | | | | | | | | | G | | | | | | | | |
| 5 | | | | | | | | | | | | | | | | | | | |
| 6 | | | | | | | | | | | | | | | | | | | |
| p53 -/- | | | | | | | | | | | | | | | | | | | |
| 1 | | | | | | | | | | | | | | | G | | | | |
| 2 | | | | | | | | | | | | | | | | | | | |
| 3 | | | | | | | | | L | | | | | | | | | | |
| 4 | | | | G | | | | | | | G | | | G | G | | | | |
| 5 | | | | G | | | | | | | | | | G | | | | | |
| 6 | | | | G | | | | | G | | | | | | | G | | | G |
| 7 | | | | | | | | | | | | | | | | | | | |
| MSH2 -/- p53+/- | | | | | | | | | | | | | | | | | | | |
| 1 | | | | | | | | | | | | | | | | | | | |
| 2 | | | | | | | | | | | | | | | | | | | |
| 3 | | | | | G | | | | G | | G | | | | | | | | |
| 4 | | | | | | | | | | | | | | | | | | | |
| 5 | | | | | | | | | | | | | | | | | | | |
| 6 | | | | | | | | | | | | | | | | | | | |
| 7 | | | | | | | | | | | | | | | | | | | |
| 8 | | | | | | | | | | | | | | | | | | | |
| MSH2 -/- p53 -/- | | | | | | | | | | | | | | | | | | | |
| 1 | | | | | | | | | | | | | | | | | | | |
| 2 | | | | | | | | | | | | | | | | | | | |
| 3 | | | | | | | | | | | | | | | | | | | |
| 4 | | | | | | | | | | | | | | | | | | | |
| 5 | | | | | | | | | | | | | | | | | | | |
| 6 | | | | | | | | | | | | L | | | G | | | | |

**Discussion**

All genotypic combinations of mutant *MSH2* / *p53* inter-crossed mice, including *MSH2* -/- *p53* -/- mice were viable with a normal phenotype initially. The successful generation of *MSH2* -/- *p53* -/- mice was not surprising since both *MSH2* -/- mice and *p53* -/- mice alone are viable. Data from the cohort of mutant *MSH2* / *p53* inter-crossed mice showed that the male / female ratio in *MSH2* -/- *p53* -/- was similar to the ratio observed in *MSH2* +/+ *p53* -/- mice. Hence, *p53* nullizygosity, irrespective of *MSH2* status, conferred a reduction (40%) in the number of live born female mice. This level of female embryonic lethality was identical to previous reports on the relative deficiency of female mice from *p53*-associated exencephaly and subsequent anencephaly observed in outbred crosses (Armstrong *et al.*, 1995). Thus, the combined effects of both *MSH2* and *p53* working in parallel did not affect viability or alter embryonic development significantly from *p53* -/- mice alone, demonstrating that dual *MSH2* and *p53* deficiency does not adversely affect embryogenesis. Furthermore, male and female *MSH2* -/- *p53* -/- mice were used in breeding pairs confirming that these mice are fertile, and proving that successful gametogenesis can occur in a background of combined *p53* and *MSH2* deficiency.

Previous studies have demonstrated that male mice bearing targeted inactivations of both *p53* and *MSH2* are viable, but succumb rapidly to lymphoma earlier than either *p53* or *MSH2* singly null mice (Cranston *et al.*, 1997). This study reported that all female mice nullizygous for both *p53* and *MSH2* underwent developmental arrest at 9.5 days and died *in utero* (Cranston *et al.*, 1997). In addition, Cranston *et al.* did not report a significant reduction in the number of female *p53* -/- mice from Mendelian ratios, although the authors state that this was probably due to their small cohort size (only seven *p53* -/- mice). Similarly, male mice generated in this thesis which were null for both *p53* and *MSH2* were also viable and succumbed to lymphoma at an equally early age, with a median age of death of 65 days. However, the results presented in this thesis differ substantially from the findings of Cranston *et al.* in the successful generation of 22 adult female mice nullizygous for both *p53* and *MSH2* which possess an identical phenotype to their male counterparts. Four possible explanations may account for the discrepancy between the data presented in this thesis

and the work of Cranston *et al.* (1997). First, the discrepancy may have resulted from different levels of environmental insult. However, as the colony used in this thesis was not maintained under barrier conditions this therefore seems unlikely. Second, the difference observed may have arisen through the use of different genetic backgrounds. Indeed, previous studies have documented the strain dependency of *p53*-related anencephaly (Armstrong *et al.*, 1995). Against this possibility is the fact that both groups of mice were generated from outbred crosses derived from a mixture of mouse strains and previous analysis has shown that different out-crossed strains possess similar levels of *p53*-related embryonic death (Armstrong *et al.*, 1995). Although the parental strains used to generate the mutant *MSH2 / p53* inter-crossed cohort in this thesis differed from those used by Cranston *et al.*, both have been well characterised previously (Donehower *et al.*, 1992; Clarke *et al.*, 1993; Reitmair *et al.*, 1995; de Wind *et al.*, 1995). In fact the mice used in this thesis segregated for 129/Ola, Balb-c and SWR genomes whereas the mice studied by Cranston *et al.* contained genomes derived from 129/Ola, 129/Sv, and C57BL/6J strains. More importantly, the single null *MSH2* and *p53* parental strains studied in this thesis possessed very similar reported phenotypes to those used by Cranston *et al.* (Donehower *et al.*, 1992; Purdie *et al.*, 1994; Reitmair *et al.*, 1995; de Wind *et al.*, 1995). Notwithstanding these observations it still remains possible that the female *MSH2*-related death observed by Cranston *et al.* was in fact strain dependent. Third, it is possible that the female embryonic lethality observed by Cranston *et al.* arose as a consequence of a second mutation which was co-segregating with one or other of the targeted alleles. The likelihood of such a linked mutation may perhaps have been increased if either of these cohorts had been derived from Embryonic Stem cells engineered over an extended period *in vitro* to carry multiple mutations, but this was not the case with either of the cohorts (Donehower *et al.*, 1992; Clarke *et al.*, 1993, de Wind *et al.*, 1995; Reitmair *et al.*, 1995). Finally, it is possible that the targeted events differed in some way either at the targeted locus itself or by the influence of the targeted locus upon neighbouring genes. Although it is impossible to confirm or refute any of the above explanations, it is clear from the data presented in this thesis that, at the very

least, the reported female embryonic lethality associated with *MSH2* and *p53* deficiency is not fully penetrant.

Wild-type and *MSH2* heterozygote mice were all viable up to the age of 240 days with no animals developing tumours, confirming previous studies by de Wind *et al.*, (1995) and Reitmair *et al.*, (1995 & 1996a). The median age of death of *MSH2* -/- mice in this thesis was 142 days which is in accordance with the published data of Reitmair *et al.* (1996a) of approximately 150 days. *p53* null mice used in this thesis succumbed at an average age of 121 days which is similar to that reported previously by Purdie *et al.* (1994). Combined nullizygosity for *MSH2* and *p53* decreased survival to a median of 65 days which is in concordance with the *MSH2* -/- *p53* -/- mice of Cranston *et al.* (1997) which had a median age of death of 73 days. Notwithstanding any minor differences in survival, both the Kaplan-Meier plots presented here and published by Cranston *et al.* are in complete agreement with *MSH2* -/- *p53* -/- mice succumbing first, followed by *p53* -/- mice and finally *MSH2* -/- mice displaying longer survival. Thus, despite differences in strain and targeting events between the various knockout mice, the survival data is closely similar.

In addition to possessing similar survival curves, the cohorts of mice in this thesis also developed the same spectrum of tumours reported by previous studies. All of the *MSH2* -/- mice developed lymphomas of T-cell origin together with adenomas and adenocarcinomas of both the small and large intestine, which were found only in mice over 140 days old. These findings are identical to those of de Wind *et al.*, (1995) and Reitmair *et al.* (1995 & 1996a) and confirm that both *MSH2* deficient strains possess a closely similar phenotype despite different targeting events and different genetic backgrounds. Furthermore, one of the *MSH2* -/- mice outwith the cohort group developed a keratoacanthoma analogous to the Muir-Torre syndrome as previously reported by Reitmair *et al.*, (1996a). *p53* null mice in this thesis developed the same range of tumours as reported by Purdie *et al.*, (1994), although the incidence of sarcoma reported in this thesis may be an underestimate since the carcasses were not X-rayed to detected osteosarcomas. The tumour spectrum observed in *MSH2* -/- *p53* -/- mice was similar to that of Cranston *et al.* although no sarcomas, histiocytomas, or intestinal adenomas were observed in this cohort. Indeed, only thymic T-cell

lymphomas were observed. The most likely explanation to account for the lack of any additional tumours in the *MSH2* -/- *p53* -/- mice in this thesis is that these tumours are rare and did not manifest themselves in the relatively small cohort examined (20 mice). Alternatively, subtle differences between the two stains of mice, highlighted above, may account for the lack of additional tumours.

*APC*$^{Min}$ heterozygosity on a *MSH2* -/- *p53* -/- background did not alter survival in mice, but modified the spectrum of tumours to include intestinal and pancreatic adenomas and adenocarcinomas. The development of intestinal tumours was not surprising since *APC* +/$^{Min}$ *MSH2* -/- mice develop numerous such lesions (Reitmair *et al.*, 1996b). The accelerated development of adenomas seen in *APC* +/$^{Min}$ *MSH2* -/- mice is thought to result from somatic mutation of the wild-type *APC* allele by *MSH2*-deficiency induced point mutation (Reitmair *et al.*, 1996b). It is unlikely that the appearance of intestinal lesions in *APC* +/$^{Min}$ *MSH2* -/- *p53* -/- mice is the result of *p53* nullizygosity since *APC* +/$^{Min}$ *p53* -/- do not show increased intestinal malignancy when compared to *Min* mice alone (Clarke *et al.*, 1995). Notwithstanding the above observations, it is remains possible that *MSH2* and *p53* can co-operate to accelerate gastrointestinal tract tumourigenesis, since no quantitative analysis of adenoma number was performed in the *APC* +/$^{Min}$ *MSH2* -/- *p53* -/- mice. The development of pancreatic adenomas and carcinomas in *APC* +/$^{Min}$ *MSH2* -/- *p53* -/- mice is consistent with previous studies on *APC* +/$^{Min}$ *p53* -/- mice by Clarke *et al.* (1995) which demonstrated that *p53* nullizygosity on a *Min* background leads to the appearance of pancreatic tumours. The *APC* +/$^{Min}$ *MSH2* -/- *p53* -/- mice generated therefore demonstrated no new tumour phenotype and instead displayed a combination of tumours already seen in *MSH2* -/- *p53* -/- mice, *APC* +/$^{Min}$ *MSH2* -/- mice, and *APC* +/$^{Min}$ *p53* -/- mice. Thus, *APC*$^{Min}$ heterozygosity does not accelerate lymphoma development or decrease survival in *MSH2* -/- *p53* -/- mice.

*MSH2* +/- *p53* -/- mice succumbed at similar age to *p53* -/- mice alone. Thus, *MSH2* heterozygosity on a *p53* null background does not accelerate tumourigenesis. This is not surprising since *MSH2* +/- cells do not show microsatellite instability, and are proficient in DNA mismatch repair (de Wind *et al,* 1995; Kolodner, 1995). However, it is possible that the remaining wild-type *MSH2* allele may act as a target for *p53*

null-induced mutation since deficiency of *p53* has been shown to cause genomic instability (Bouffler *et al.*, 1995; Levine, 1997), DNA amplification (Yin *et al.*, 1992) and elevations of *in vivo* mutation rates following high doses of DNA damage (Clarke *et al.*, 1997). Since *MSH2* +/- *p53* -/- mice survived to a similar age as *MSH2* +/+ *p53* -/- mice it suggests that this scenario does not occur, with *p53* null-induced tumours being unable to capitalise upon a single copy of *MSH2*. This can be reconciled by the observation that *p53* deficiency is only mutagenic at high levels of DNA damage, whereas in untreated intestinal cells *p53* deficiency does not alter the *in vivo* mutation rate (Clarke *et al.*, 1997). However, it is interesting to note that *MSH2* heterozygosity appears to alter the site of lymphoma development (i.e. outwith the thymus) and influences the site of sarcoma development. The reasons for these anomalies are unclear at present, although a shift in tumour phenotype was also observed in *APC* $+/^{Min}$ *p53* -/- mice (Clarke *et al.*, 1995).

In sharp contrast, *MSH2* -/- *p53* +/- mice succumbed at a significantly earlier age than *MSH2* null mice alone, with a median survival of only 99 days versus 142 days. Thus, *p53* heterozygosity accelerated tumour development in a *MSH2* -/- background, but did not alter the tumour spectrum. *MSH2* -/- cells show microsatellite instablility and possess elevated mutation rates (de Wind *et al.*, 1995, Eshelman *et al.*, 1995; Part IV of this thesis). One possible explanation for the acceleration in tumourigenesis seen in these mice is that *MSH2* deficiency may predispose the cell to covert a *p53* +/- cell to a *p53* null cell by point mutation of the remaining wild-type allele. This alone would explain an increased incidence in tumour development. In the nine thymic lymphomas examined, loss of the remaining untargeted *p53* allele was excluded by PCR. Sequencing data from three of these tumours demonstrated a single point mutation in only one of the tumours. However, this mutation was a G→A transition and occurred at codon 234 in the mouse. Such a base transition is characteristic of *MSH2* deficiency (Andrew *et al.*, 1997) and its site is located in a known mutational hot spot of *p53* occurring in the sequence-specific DNA-binding domain of the *p53* protein (Vogelstein & Kinzler, 1992; Levine, 1997). The absence of mutation in exons 5-9 of *p53* in the other two tumours sequenced does not exclude the possibility that *MSH2* deficiency induced point mutations in other exons of *p53* or the promoter of *p53*.

Notwithstanding the above observations, these results demonstrate that in one tumour at least, mutant *MSH2* can positively interact with heterozygous *p53* to enhance tumour development. However, a second explanation for the accelerated tumourigenesis seen in *MSH2* -/- *p53* +/- mice arises from the possibility that *p53* heterozygosity itself predisposes to tumourigenesis. Analysis of the status of the wild-type *p53* allele in tumours taken from *p53* +/- mice demonstrated that over 50% of the tumours examined retained an intact, and functional wild-type *p53* allele (L. Donehower, personal communication). This indicates that a mere reduction in *p53* levels is sufficient to cause tumours. Hence, accelerated tumour development observed in *MSH2* -/- *p53* +/- mice may result from mutation of the remaining *p53* allele or may simply reflect a reduction in *p53* protein levels in the heterozygous state. Which of these pathways predominate is unclear at present although this issue could be resolved by yeast analyses aimed at determining *p53* function (Flaman *et al.*, 1995). These results, together with the data of Reitmair *et al.* (1996b), demonstrate that *MSH2* deficiency combined with heterozygosity at another tumour suppressor locus (*APC*) leads to accelerated tumour development. The most likely mechanism for this phenomenon is that *MSH2* deficiency results in greater susceptibility to point mutations in the remaining wild-type allele and effectively converts that cell to a double null genotype.

Immunophenotyping of the thymic lymphomas arising in mutant *MSH2* / *p53* inter-crossed mice demonstrated a T-cell origin. Both singly null *MSH2* and *p53* mice are also known to develop T-cell lymphomas (Purdie *et al.*, 1994; de Wind *et al.*, 1995; Reitmair *et al.*, 1995). Tumours from *MSH2* -/- *p53* -/- mice retained surface molecules CD2, CD4, CD8, CD24, CD45 and Thy-1. In contrast, lymphoma cells from *MSH2* -/- *p53* +/- mice displayed lower levels of all the cell surface markers examined. Why should this occur? One possible explanation for this is that the cell of origin of the lymphomas is different between genotypes, with *MSH2* -/- *p53* -/- driven tumourigenesis affecting an earlier lineage of T-cell progenitors which express more surface markers (Godfrey & Zlotnik, 1993). Alternatively, differences in cell surface molecule expression may result from differences in genotype alone, although this is unlikely since neither *MSH2* nor *p53* is known to affect T-cell marker expression.

Furthermore, thymocyte development is normal in *MSH2* null mice (Reitmair *et al.*, 1995). Therefore, doubly null T-cells, since they possess two genome destabilising pathways may undergo malignant conversion earlier in T-cell ontogenesis with progenitor T-cells expressing high levels of cell surface proteins which the tumours retain. In contrast, *MSH2* -/- *p53* +/- T-cells become malignant later in the life of a mouse when T-cells are at a later stage of differentiation and are characterised by fewer surface markers (Godfrey & Zlotnik, 1993). Inconsistent patterns of antigen expression were observed in *MSH2* -/- and *p53* -/- tumours, and are in accordance with the previous findings of Reitmair *et al.* (1995) and Purdie *et al.* (1994). Both of the *p53* -/- and the *MSH2* -/- tumours were observed in mice significantly older than either *MSH2* -/- *p53* -/- or *MSH2* -/- *p53* +/- mice. Thus, the inconsistent pattern of expression seen in single null mice may reflect malignant conversion in T-cells after lineage commitment has occurred when the patterns of marker expression are different between different T-cell types.

Aneuploidy occurs frequently in colorectal and other cancers (Heim & Mitelman, 1987) and is often associated with a poor prognosis (Shackney *et al.*, 1989). Colorectal cancers without microsatellite instability demonstrate defects in chromosome segregation, which result in gains or losses in excess of one whole chromosome per hundred chromosomes replicated (Lengauer *et al.*, 1997). This form of karyotypic instability leads to the development of aneuploidy (Schlegel *et al.*, 1995; Lengauer *et al.*, 1997) which is positively correlated with *p53* mutation (Carder *et al.*, 1993). Furthermore, there is an inverse correlation between $RER^{+}$ status and *p53* mutation in colorectal cancer cell lines (Cottu *et al.*, 1996). Colorectal cancers therefore appear to exhibit two distinct forms of genomic instability, one through loss of MMR and the other through loss of *p53*. This thesis has already demonstrated that although distinct, these two pathways can co-operate at the level of the organism to accelerate tumourigenesis. Analysis of *MSH2* -/- tumour cells by both flow cytometry and CGH demonstrated no aneuploidy or chromosomal instability. In contrast, 29% of tumours from *p53* null mice were aneuploid with CGH analysis showing evidence of chromosomal instability in the form of DNA amplification. *MSH2* -/- *p53* -/- tumours displayed a diploid karyotype with no evidence of any chromosomal

instability being demonstrated either by flow cytometry or CGH. The absence of any form of gross chromosomal instability in these tumours is surprising given that *p53* deficiency exists. Three possible explanations may account for the absence of *p53*-associated genetic changes in these tumours despite the known co-operativity between the two genes. First, deficiency of *p53* may contribute to tumourigenesis by reducing genome stability at a nucleotide level, in a similar manner to *MSH2* deficiency. This is unlikely since the frequency of microsatellite instability in tumours from *MSH2* -/- *p53* -/- mice is not significantly different from that of *MSH2* -/- mice (Cranston *et al.*, 1997). Second, tumours arising in *MSH2* -/- *p53* -/- mice develop rapidly, perhaps before gross chromosomal changes occur or if they do occur are undetectable by flow cytometry or CGH. Third, *p53* deficiency may enhance lymphomagenesis, not through DNA instability, but through inhibition of apoptosis (Clarke *et al.*, 1993; Lowe *et al.*, 1993a).

The significance of these findings to malignancy is that combined *MSH2* and *p53* deficiency accelerates tumour development. In the case of colorectal cancer such a scenario rarely occurs (Cottu *et al.*, 1996). However, examples of combined microsatellite and chromosomal instability do exist (Lengauer *et al.*, 1997), showing that these pathways are not mutually exclusive. Indeed, the results presented in this thesis demonstrate that despite combined *MSH2* and *p53* deficiency *only* an *MSH2*-deficiency type pattern of genomic instability is detectable in tumour cells. In addition, the survival data from *MSH2* -/- *p53* +/- mice highlights the risk of being heterozygous at a tumour suppressor loci in the presence of *MSH2* deficiency.

# SUMMARY

**I** ***MSH2*** **plays a major role in coupling DNA mismatch type lesions to apoptosis efficiently in the murine small intestine.** ***MSH2*** **is specific for DNA mismatch type lesions with cells requiring only one copy of** ***MSH2*** **for induction of apoptosis.** ***MSH2*** **status does not alter the target population of cells exposed to methylating agents or Cisplatin.**

**II** ***p53*** **is required for the "immediate" apoptotic response in small intestinal cells following methylating agents or Cisplatin. Delayed** ***p53*****-independent apoptosis is observed following Temozolomide, and is entirely** ***MSH2*****-dependent. Both the crypt position and the morphology of apoptosis is altered in delayed** ***p53*****-independent apoptosis.**

**III** ***MSH2*** **status does not alter resting AGT levels within cells. AGT appeared to play no significant role in** ***MSH2*****-dependent apoptosis following DNA damage in the murine small intestine. Benzylguanine, a competitive inhibitor of AGT, prevents the metabolic activation of Dacarbazine probably through the inhibition of cytochrome P450 enzymes.**

**IV Absence of** ***MSH2*** **increases the spontaneous mutation frequency at the** ***Dlb-1*** **locus within cells of the murine small intestine six-fold. An** ***MSH2*****-dependent increase in mutation frequency is observed following exposure to MNNG and Temozolomide. In contrast,** ***MSH2*** **plays little or no role in the defence against Cisplatin-induced mutations.**

**V** ***MSH2*** **and** ***p53*** **can co-operate to accelerate tumourigenesis in the mouse. Examination of tumours from** ***MSH2*** **-/-** ***p53*** **-/- mice demonstrate that only** ***MSH2*****-type instability can be detected. This suggests that** ***p53*** **may accelerate malignancy through mechanisms other than gross chromosomal rearrangement.**

# MATERIALS & METHODS

# MATERIALS & METHODS

## Generation and maintenance of mouse colonies

All mice were maintained under non-barrier conditions, and given a standard diet and water *ad libitum*. From a single *MSH2* +/- male mouse (de Wind *et al.*, 1995) a large cohort of *MSH2* +/+, *MSH2* +/-, and *MSH2* -/- mice were generated on an outbred background segregating for a variety of genomes including 129/Ola, Balb-c, and SWR.

Interbreeding *MSH2* -/- mice to *p53* -/- mice (Clarke *et al.*, 1993) a colony of animals was generated which segregated for both mutant alleles. The background of this outbred colony included 129/Ola, Balb-c, and SWR genomes. Mice of the following genotypes were used for study or breeding: *MSH2* -/- *p53* +/+, *MSH2* +/+ *p53* -/-, *MSH2* -/- *p53* +/-, *MSH2* +/- *p53* -/-, *MSH2* -/- *p53* -/-.

By interbreeding *MSH2* -/- *p53* +/- to *Min* mice (Moser *et al.*, 1990, Su *et al.*, 1992) a cohort of mice with the genotype *APC* $+/^{Min}$ *MSH2* -/- *p53* -/- were generated.

By mating *MSH2* -/- male mice to wild-type C57BL/6J female mice the F1 progeny from this mating were designated Colony "A". Thus, Colony A mice were *MSH2* +/-, homozygous for the *Dlb-1* a allele (*Dlb-1* a/a), and 50% C57BL/6J (Winton *et al.*, 1988). A second cohort of mice was generated by mating *MSH2* +/- mice to wild-type C57BL/6J which were homozygous for the *Dlb-1* b allele (*Dlb-1* b/b) (Winton *et al.*, 1988). *MSH2* +/- progeny from this mating were back-crossed to C57BL/6J *Dlb-1* b/b mice. Four subsequent back-crosses to C57BL/6J *Dlb-1* b/b mice were performed, maintaining *MSH2* +/- status. *Dlb-1* status of the mice was determined by staining formalin fixed tail biopsies with *Dolichos biflorus* agglutinin peroxidase (Winton *et al.*, 1988). *MSH2* +/- *Dlb-1* b/b progeny from the final matings were designated Colony "B".

By crossing Colony "A" mice to Colony "B" mice the F1 progeny generated were all heterozygous at the *Dlb-1* locus (*Dlb-1* a/b) and also either *MSH2* +/+, or *MSH2* +/-, or *MSH2* -/-. These mice were used for the *in vivo* mutation frequency experiments.

**DNA extraction from mouse tails**

DNA was extracted from mouse tail biopsies using Puregene (Gentra Systems) as per protocol. Alternatively, DNA was extracted as follows: tail biopsies were digested overnight at 37°C in 500µl Phenol Lysis Buffer and 25µl Proteinase K (20mg/ml). 500µl of Phenol was added, mixed, and microfuged at 13 000 rpm for 2 minutes. The top layer was removed, an equal volume of Phenol/Chloroform added, mixed, and microfuged as before. The upper layer was then removed, an equal volume of Chloroform/Iso-amyl alcohol added, mixed, and microfuged as before. The top layer was again removed, and DNA precipitated with 250µl of 7.5M Ammonium Acetate and 3.75mls absolute ethanol. DNA was removed by pipette, air-dried for 10 minutes and resuspended in 500µl TE buffer. Samples which required only *MSH2* status were boiled in 500µl of MSH2-PCR Lysis Buffer for 15 minutes.

**Genotyping mice by PCR**

***MSH2***

As a large number of samples required genotyping for *MSH2* status, and the only method available was Southern Blotting (de Wind *et al.*, 1995), a specific PCR assay for *MSH2* status was designed. Studying the mouse genomic *MSH2* targeting event in de Wind *et al.* (1995) a three primer approach was identified with a sense primer in intron 11 of mouse *MSH2* (Primer 1), and two antisense primers, the first in the polyA tail of the targeting cassette to detect the targeted allele (Primer 2), and a second antisense primer in exon 12 downstream of the targeting event, to detect the wild-type allele (Primer 3). In order to design Primer 1 approximately 100 base pairs of intron 11 (the sequence of which was unpublished) was sequenced using Primer 3 and plasmid pHA224 (H. te Riele, unpublished) which contains a 12.5kb BamH1 fragment of mouse genomic *MSH2*. Sequencing was carried out using the dideoxy chain termination method using Sequenase 2.0 (Amersham) used as per manufacturer's protocol with 2pmoles Primer 3 and 5µg of plasmid pHA224 (1µl of Manganese buffer was added at the extension step). 2.5µl of reaction mixture was boiled for 5 minutes, loaded on to a 6% acrylamide gel, and run at 75 watts until the bromophenol

blue migrated to the bottom of the gel. The gel was fixed in 12% methanol / 10% acetic acid solution for 15 minutes and attached to Whatmann 3MM filter paper. The gel was covered with cling film, vacuum dried at 80°C for 1 hour then exposed to X-ray film (Biomax MR, Kodak) overnight at 4°C in a hypercassette. The film was developed using a Hyperprocessor (Amersham). The sequence identified was used to design Primer 1. A PCR reaction specific to *MSH2* was optimised and generated a 164 base pair product for the wild-type allele and 194 base pair product for the targeted event (Figure A).

The protocol was as follows: to a 50µl PCR reaction containing 5µl PCR Buffer, 2.5µl 1%WI, 2.5µl each primer (10pmoles per µl), 1µl dNTP (40mM), 2µl $MgCl_2$ (50mM), 30µl DDW and 1µl *Taq* (1.25U) (all components GibcoBrl), 1µl (100ng) of template DNA was added. The reaction mix was overlain with 50µl paraffin oil. Reaction conditions were 94°C 5min, 60°C 2min, 72°C 2min (X1); 94°C 1min, 60°C 2 min, 72°C 2 min (X30); 94°C 1min, 60°C 2min, 72°C 10min (X1) (OmniGene, Hybaid). 10µl of product was analysed on a 4% TBE agarose gel.

Primer 1 CGGCCTTGAGCTAAGTCTATTATAAGG
Primer 2 GGTGGGATTAGATAATGCCTGCTCT
Primer 3 CCAAGATGACTGGTCGTACATAAG

***p53* PCR**

*p53* status was determined by specific PCR reaction (Malcomson *et al.*, 1997). 2µl (200ng) of template DNA was added to a 50µl PCR reaction containing 5µl PCR Buffer, 2.5µl 1%WI, 2.5µl each primer (10pmoles per µl), 1µl dNTP (40mM), 2µl $MgCl_2$ (50mM), 2µl DMSO, 27µl DDW and 1µl *Taq* (1.25U) (all components GibcoBrl). The reaction mix was overlain with 50µl paraffin oil. Reaction conditions were 94°C 2min (X1); 94°C 1min, 62°C 1min, 72°C 1 min (X30); 72°C 10min (X1) (OmniGene, Hybaid). 20µl of product was analysed on a 2% TBE agarose gel.

## Figure A

UV-transilluminated, ethidium bromide stained 4% TBE agarose gel, showing *MSH2* specific PCR. **L** 1kb ladder molecular weight marker (sizes of bands in base pairs are arrowed); **WT** *MSH2* +/+, 164 base pair product; **HET** *MSH2* +/-, 164 and 194 base pair products; **HOM** *MSH2* -/-, 194 base pair product.

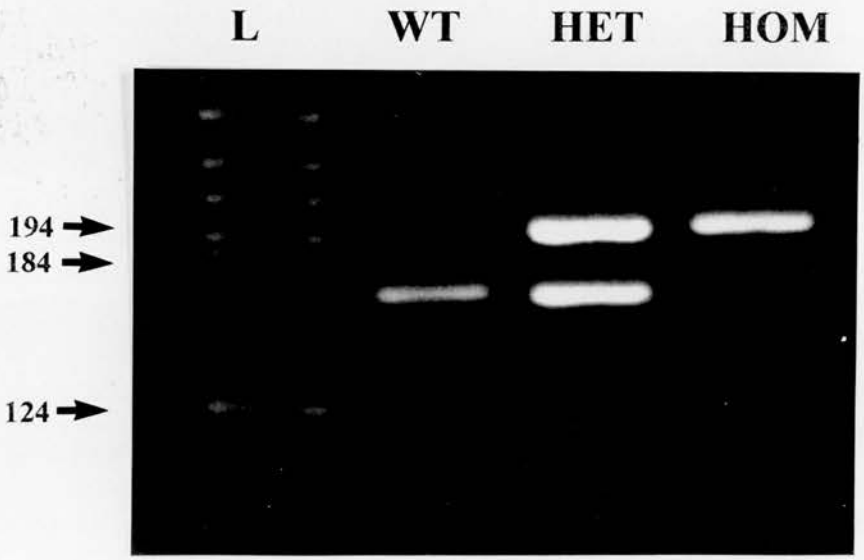
L
WT
HET
HOM
194
184
124

### *Min* PCR

*Min* status of mice was determined by the PCR reaction and HindIII digestion described by Luongo *et al.* (1994). 2µl (200ng) of template DNA was added to a 50µl PCR reaction containing 5µl PCR Buffer, 2.5µl each primer (10pmoles per µl), 1µl dNTP (40mM), 2.5 µl $MgCl_2$ (50mM), 33.5µl DDW and 1µl *Taq* (1.25U) (all components GibcoBrl). The reaction mix was overlain with 50µl paraffin oil. Reaction conditions were 94°C 2min (X1); 94°C 1min, 60°C 1min, 72°C 1 min (X30); 72°C 10min (X1) (OmniGene, Hybaid). 16µl of product digested with HindIII (GibcoBrl) for 1 hour at 37 °C. Digested product was analysed on a 4% TBE agarose gel.

### Reagent administration / irradiation of mice

Ten week old mice were given intraperitoneal (i.p.) injections of various doses of MNNG, Temozolomide, Cisplatin, or Benzylguanine. Doses of reagent was mg per kg body weight of mouse (mg/kg). The injection volume for all reagents was from 0.2 to 0.5ml per mouse. All drugs, except Cisplatin (David Bull Laboratories), were prepared fresh and first dissolved in DMSO (10% of the final volume) and made to a final concentration with PBS (Temozolomide & Benzylguanine) or corn oil (MNNG). Mice were exposed to γ-irradiation using a $^{137}$Caesium source at 0.27 Gray per minute for 15 minutes, so that each mouse received a total dose of 4 Gray.

### Quantitation of apoptosis

All experiments were initiated at the same time of day (10 00 hours a.m.) in order to control for the effects of diurnal changes in susceptibility to apoptosis, since a clear circadian rhythm has been shown to exist for the induction of apoptosis in the murine small intestine (Potten, 1990). At a specified time point following reagent injection or irradiation, a minimum of three mice were killed, their small intestines removed. A ten cm section proximal to the caecum was flushed with water, opened longitudinally and fixed overnight in methocarn. Samples were rolled into "swiss-rolls" and stored in 70% ethanol prior to staining. Haematoxylin and eosin (H&E) stained sections were made and apoptosis scored through the use of the Highly Optimised Microscopic

Environment (HOME) (Brugal *et al.*, 1992; Clarke *et al.*, 1994). Each slide was assigned an arbitrary reference number by a separate individual and data was therefore collected blind. A random section of slide displaying crypts cut in longitudinal plane was identified. Consecutive crypts were marked using the HOME microscope such that the same crypt was not counted twice. Running mean values were determined prior to counting and demonstrated that an accurate mean for murine apoptotic bodies was generated beyond approximately 40 half crypts. A minimum of fifty half-crypts were scored per animal. To address the possibility of intra-observer error sample slides were scored on three separate occasions. Counts obtained this way did not markedly differ from each other (the degree of error was always below 15%). To remove the possibility of inter-observer error sample slides were rechecked by an independent observer. This process was facilitated by the use of the HOME microscope as individual assessments of cell status were verified by the second observer. Some inter-experimental variation in the level of apoptosis was observed. Such differences in the prevalence of apoptosis between comparable experiments may arise from a number of possible variables: 1) small differences in mouse size 2) small inaccuracies in drug delivery 3) differences in sex ratio between experiments 4) difference in histological preparation of samples which may have influenced the ease of identification of apoptosis. Taken together these differences may well account for the observed inter-experimental variation, however, within individual experiments these factors were more closely controlled as sex ratios and the age of mice closely matched. In addition, the small intestines from each experiment were stained and sectioned as a single batch.

To determine the crypt position of cells undergoing apoptosis, cumulative counts of one hundred apoptotic bodies were performed on histological sections. In slides to be counted a random section of longitudinally cut crypts were identified and one hundred apoptotic bodies were counted in consecutive crypts progressing in the same direction around the "swiss-roll". Each apoptosis was assigned a crypt position from 1 to 22 as previously described (Potten, 1990; Clarke *et al.*, 1994), with position one at the base and twenty-two at the apex. Mean data was generated from three slides.

### $O^6$-Alkylguanine-DNA-alkyltransferase (AGT) assay

Mice were sacrificed, tissues of interest removed, snap frozen in liquid nitrogen, and stored at -70°C until assayed as described previously (Rafferty *et al.*, 1996).

### *Dlb-1* mutation assay

Ten week old *Dlb-1* a/b heterozygote mice generated from crossing Colony "A" to Colony "B" were injected i.p. with a single dose of MNNG, or Temozolomide, or Cisplatin. 21 days later the mice were killed, their small intestines removed, and flushed with water. Whole mount preparations of 15 cm of the intestine were stained with *Dolichos biflorus* agglutinin (DBA) peroxidase (Winton *et al.*, 1988). Villus ribbons not staining with the DBA-peroxidase conjugate were scored using Kyowa Stereo 200M microscope and the results presented as number of mutations per 10 000 villi.

### Mouse cohort survival and tumour incidence

Cohorts of mice with altered genotypes were maintained as separate colonies. The genotype and number of mice in each cohort were as follows: *MSH2* +/+ 29 mice, *MSH2* +/- 30 mice, *MSH2* -/- 28 mice, *MSH2* +/+ *p53* -/- 88 mice, *MSH2* +/- *p53* -/- 23 mice, *MSH2* -/- *p53* +/- 44 mice, *MSH2* -/- *p53* -/- 20 mice, *APC* $+/^{Min}$ *MSH2* -/- *p53* -/- 8 mice. For each mouse, a date of birth and date of death was recorded. Mice which were sick or moribund, were sacrificed, their age recorded, and a full autopsy performed. All organs, including any tumour, were fixed in 4% buffered formaldehyde and H&E histological sections made. Small intestine and colon were removed, flushed with water, and fixed overnight in methocarn. Histological sections of gut were made as described previously (Clarke *et al.*, 1994) and scored for adenomas and adenocarcinomas. Samples of tumour tissue were stored at -70°C for RNA extraction and Flow Cytometry. DNA was extracted from small pieces (3mm x 3mm) of tumour by digestion in 5ml Phenol Lysis Buffer and 150µl of Proteinase K (20mg/ml) for 48hours at 55°C. DNA was prepared from 500µl of sample by the Phenol/Chloroform method and resuspended in 500µl TE.

**Sequencing of wild-type *p53* allele in *MSH2* -/- *p53* +/- mice**

Total RNA was extracted from tumour tissue (5mm x 5mm) using 1ml Trizol (GibcoBrl), and aliquotted at a concentration of 1mg/ml in RNase-free DDW. 1µl of RNA was reverse transcribed into cDNA using oligo$(dT)_{15}$ primers and Expand Reverse Transcriptase (Boehringer Mannheim) as per protocol. PCR primers 33A and 21B (Ozbun *et al.*, 1993) were used to amplify a 686 base pair fragment of *p53* cDNA which included exons 5-9. A 100µl PCR reaction containing 250ng of primers 33A and 21B, 0.5µl cDNA template and 5U *Pfu* DNA polymerase (Stratagene) was performed using the thermocycling profile detailed in Ozbun *et al.* (1993). An aliquot (10µl) of each product was digested with HinfI (Boehringer Mannheim) to verify that amplification was from mRNA and not mouse *p53* pseudogene DNA. For each tumour cDNA three separate PCR reactions were performed. Each sample (90µl) was purified using Wizard PCR Preps DNA Purification System (Promega) prior to cloning. 100ng of purified PCR product was cloned into pCR-Script SK+ vector (Stratagene) as per manufacturer's protocol. 1µl of ligation mixture was used to transform Epicurian Coli XL2-blue Ultracompetent Cells (Stratagene) and a blue/white selection screen performed. White transformants were grown in 5ml of LB-Ampicillin for 8 hours. 1ml of each culture was used to inoculate 100mls of LB-Ampicillin. Cultures were grown overnight at 37°C in an orbital shaker. Plasmid DNA was extracted using a Plasmid Maxi Kit (Qiagen). 5µg of plasmid DNA was sequenced using a Fluorescent Automated DNA Sequencer (Licor). The *p53* cDNA insert was sequenced from both directions using T3 and T7 primers. Thus, exons 5-9 of *p53* in each tumour were amplified by PCR and sequenced by three separate and identical reactions. *p53* sequence data from each tumour was compared to that of published wild-type *p53* sequence (Arai *et al.*, 1986) using DNA alignment software available through Human Genome Mapping Project.

## Table 1

Table summarising the Primary and Secondary Antibodies used in the immunophenotyping of the murine lymphomas. For each antibody details of the species of origin, the manufacturer and the dilutions at which they were used are shown.

**Table 1**

| Primary Antibody | Origin | Source | Dilution |
|---|---|---|---|
| Anti-CD2 | rat | Pharmingen | 1:100 |
| Anti-CD45 | rat | Pharmingen | 1:100 |
| Anti-CD24 | rat | Pharmingen | 1:100 |
| Anti-IL2R | rat | Pharmingen | 1:100 |
| F4-80 | rat | ATCC | 1:10 |
| Anti-CD4 | rat | ECACC | 1:10 |
| Anti-CD8 | rat | ECACC | 1:10 |
| Anti-Thy-1 | rat | ECACC | 1:10 |
| Anti-mouse IgG | mouse | ECACC | 1:10 |
| | | | |
| Secondary Antibody | | | |
| Anti-rat IgG (FITC) | Rabbit | Sigma | 1:100 |
| Anti-mouse IgG (FITC) | Rabbit | Sigma | 1:100 |

**DNA flow cytometry**

DNA content of tumours was analysed by a modified Vindelov method (Vindelov *et al.*, 1983). Tumour tissue (5mm x 5mm) was forced through a 100μm sieve together with 500μl of Citrate Buffer to generate a single cell suspension. To 100μl of Citrate Buffer/Cell mixture, 450μl of Solution A was added and incubated for 10 minutes. 325μl of Solution B was then added for 10 minutes. Finally, 250μl of Solution C was added and the sample incubated on ice for a further 10 minutes. DNA content was analysed on a EPICS XL Flow Cytometer (Coulter) using Multicycle Software (Coulter).

**Immunophenotyping of tumours**

Fresh tumour tissue in PBS (GibcoBrl) was forced through a 100μm sieve and spun at 1800 rpm for 10 minutes. Cells were resuspended in 1ml Freezing Medium and frozen at -70°C overnight before transfer to liquid nitrogen. Prior to analysis samples were defrosted and lymphocytes isolated using Lympholyte M (Cedarlane Laboratories) as per protocol. Lymphocytes were resuspended in Flow Buffer to a concentration of 3 $x10^7$/ml. 100μl of cells were added to each well in a 96 well plate. The plate was spun at 800 rpm for 3 minutes and the supernatant removed. 25μl aliquots of Primary Antibody was added at various concentrations (Table 1) and incubated on ice for 1 hour. Cells were washed in 200μl of Flow Buffer, spun for 3 minutes at 800 rpm and supernatant removed. 25μl of the appropriate Secondary Antibody as added and incubated on ice for 1 hour (Table 1). 200μl of Flow Buffer was added, spun for 3 minutes at 800 rpm and supernatant removed. Cells were resuspended in 200μl of Flow Buffer before analysis on the EPICS XL Flow Cytometer (Coulter) using XL2 Software (Coulter).

Non-commercial antibodies were isolated from the supernatants of Hybridoma Cell Lines obtained from European Collection of Animal Cell Cultures (ECACC) or American Type Culture Collection (ATCC). Antibodies were purified using protein G columns (Sigma) as per manufacturer's instructions.

**Comparative genomic hybridisation**

[Performed by Lucy Curtis]

Normal metaphases for comparative genomic hybridisation (CGH) were obtained from cultured E14 mouse Embryonic Stem cells, which were originally derived from a 129/Ola cross (Hooper *et al.*, 1987). Cells were grown in CM5-5 medium in 75cm$^2$ flasks. Metaphase spreads were prepared by standard protocols.

Comparative genomic hybridisation was carried out using the modified method of Kallioniemi *et al.* (1993), with the substitution of 20µl mouse Cot-1 DNA for human. Analysis of hybridisations was carried out using the Apple MacIntosh based quantitative image analysis software (MacProbe, Perceptive Scientific Instruments). Karyotyping was performed manually. CGH analysis was carried out on a minimum of five metaphase spreads per tumour. Green/red ratios were scored and an average profile generated for each chromosome. Green/red cut-off points of 0.875 and 1.125 were chosen for scoring copy number changes which were equivalent to loss or gain of one chromosome in 25% of cells with a diploid karyotype.

# APPENDIX

**Solution A**

15μg/ml Trypsin

Diluted in Stock Solution

pH 7.6

**Solution B**

0.5mg/ml Trypsin Inhibitor

0.1mg/ml Ribonuclease A

Diluted in Stock Solution

pH 7.6

**Solution C**

0.42mg/ml Propidium Iodide

1mg/ml Spermine Tetrahydrochloride

Diluted in Stock Solution

pH 7.6

**Chloroform/Iso-amyl Alcohol**

24 parts Chloroform

1 part Iso-amyl alcohol

**Citrate Buffer**

250mM Sucrose

40mM Trisodium Citrate

5% DMSO

pH 7.6

**Flow Buffer**

1% Bovine Serum Albumin

1% Sodium Azide

**Freezing Medium**

10% DMSO

50% Heat-Inactivated Newborn Calf Serum (Sigma)

40% RPMI 1640 (GibcoBrl)

**LB-Ampicillin**

1% Bacto-trypone

0.5% Bacto-yeast extract

1% NaCl

Ampicillin (50mg/litre)

**Metaphase Fixitive**

3 parts methanol

1 part glacial acetic acid

**Methocarn**

4 parts methanol

2 parts chloroform

1 part glacial acetic acid

**MSH2-PCR Lysis Buffer**

100mM Tris-HCl pH 8.5

5mM EDTA

200mM NaCl

0.2% SDS

**Phenol Lysis Buffer**

500mM Tris-HCl pH 8

20mM EDTA

10mM NaCl

1% SDS

**Phenol/Chloroform**

1 part Phenol

1 part Choroform

**Stock Solution**

3mM Trisodium Citrate

0.5mM Tris

1% Nonidet P40

pH 7.6

**TBE**

89mM Tris

2mM EDTA pH 8

89mM Boric Acid

**TE**

10mM Tris pH 8

1mM EDTA

# BIBLIOGRAPHY

## BIBLIOGRAPHY


Aaltonen, L.A., Peltomaki, P., Leach, F.S., Sistonen, P., Pylkkanen, L., Mecklin, J.P., Jarvinen, H., Powell, S.M., Jen, J., Hamilton, S.R., Petersen, G.M., Kinzler, K.W., Vogelstein, B. & de la Chapelle, A. (1993). Clues to the pathogenesis of familial colorectal cancer. Science **260,** 812-816.

Aebi, S., Kurdi-Haidar, B., Gordon, R., Cenni, B., Zheng, H., Fink, D., Christen, R.D., Boland, C.R., Koi, M., Fishel, R., & Howell, S.B. (1996). Loss of DNA mismatch repair in acquired resistance to cisplatin. Cancer Res. **56,** 3087-3090.

Aebi S., Fink, D., Gordon, R., Kim, H.K., Zheng, H., Fink, L., & Howell, S.B. (1997). Resistance to cytotoxic drugs in DNA mismatch repair-deficient cells. Clin. Cancer Res. **3,** 1763-1767.

Andrew, S.E., Reitmair, A.H., Fox, J., Hsiao, L., Francis, A., McKinnon, M., Mak, T.W., & Jirik, F.R. (1997). Base transitions dominate the mutational spectrum of a transgenic reporter gene in MSH2 deficient mice. Oncogene **15,** 123-129.

Anthoney, D.A., McIlwrath, A.J., Gallagher, W.M., Edlin, A.R., & Brown, R. (1996). Microsatellite instability, apoptosis, and loss of p53 function in drug-resistant tumor cells. Cancer Res. **56,** 1374-1381.

Arai, N., Nomura, D., Yokota, K., Wolf, D., Brill, E., Shohat, O., & Rotter, V. (1986). Immunologically distinct p53 molecules generated by alternative splicing. Mol. Cell. Biol. **6,** 3232-3239.

Arends, M.J., Morris, R.G., & Wyllie, A.H. (1990). Apoptosis the role of the endonuclease. Am. J. Pathol. **136,** 593-608.

Arends, M.J. & Wyllie, A.H. (1991). Apoptosis: mechanisms and roles in pathology. Int. Rev. Exp. Pathol. **32,** 223-254.

Arends, M.J., McGregor, A.H., Toft, N.J., Brown, E.J., & Wyllie, A.H. (1993). Susceptibility to apoptosis is differentially regulated by c-myc and mutated Ha-ras oncogenes and is associated with endonuclease availability. Br. J. Cancer **68,** 1127-1133.

Arends, M.J., McGregor, A.H., & Wyllie, A.H. (1994). Apoptosis is inversely related to necrosis and determines net growth in tumors bearing constitutively expressed myc, ras, and HPV oncogenes. Am. J. Pathol. **144,** 1045-1057.

Arends, MJ. (1995). How do cancer cells die? Apoptosis and its role in neoplastic progression. In: The biology of gynaecological cancer. [Eds. Leake, R., Gore, M., & Ward, R.H.] RCOG Press, London, 73-91.

Armstrong, J.F., Kaufman, M.H., Harrison, D.J. & Clarke A.R. (1995). High-frequency developmental abnormalities in p53-deficient mice. Curr. Biol. **5**, 931-936.

Bean C.L., Bradt, C.I., Hill, R., Johnson, T.E., Stallworth, M. & Galloway, S.M. (1994). Chromosome aberrations: persistence of alkylation damage and modulation by $O^6$-alkylguanine-DNA-alkyltransferase. Mutat. Res. **307,** 67-81.

Bedi, A., Pasricha, P.J., Akhtar, A.J., Barber, J.P., Bedi, G.C., Giardiello, F.M., Zehnbauer, B.A., Hamilton, S.R., & Jones, R. (1995). Inhibition of apoptosis in the development of colorectal cancer. Cancer Res. **55,** 1811-1816.

Bellamy, C.O., Malcolmson, R.D., Harrison, D.J., & Wyllie, A.H. (1995). Cell death in health and disease: the biology and regulation of apoptosis. Semin. Cancer Biol. **6,** 3-16.

Bertrand, R., Sarang, M., Jenkin, J., Kerrigan, D., & Pommier, Y. (1991). Differential induction of secondary DNA fragmentation by topoisomerase II inhibitors in human tumor cell lines with amplified c-myc expression. Cancer Res. **51,** 6280-6285.

Bhattacharyya, N.P., Skandalis, A., Ganesh, A., Groden, J., & Meuth, M. (1994). Mutator phenotypes in human colorectal carcinoma cell lines. Proc. Natl. Acad. Sci. USA. **91,** 6319-6323.

Bhattacharyya, N.P., Ganesh, A., Phear, G., Richards, B., Skandalis, A., & Meuth, M. (1995). Molecular analysis of mutations in mutator colorectal carcinoma cell lines. Hum. Mol. Genet. **4,** 2057-2064.

Bingham, S.A., Pignatelli, B., Pollock, J.R., Ellul, A., Malaveille, C., Gross, G., Runswick, S., Cummings, J.H., & O'Neil, I.K. (1996). Does increased endogenous formation of N-nitroso compounds in the human colon explain the association between red meat and colon cancer? Carcinogenesis **17,** 515-523.

Bodmer, W., Bishop, T., & Karran, P. (1994). Genetic steps in colorectal cancer. Nature Genet. **6,** 217-219.

Bohr, V.A. (1991). Gene specific DNA repair. Carcinogenesis **12,** 1983-1992.

Bouffler, S.D., Kemp, C.J., Balmain, A., & Cox, R. (1995). Spontaneous and ionizing radiation-induced chromosomal abnormalities in p53-deficient mice. Cancer Res. **55,** 3883-3889.

Bowen I.D., & Bowen, S.M. (1990). Programmed cell death in tumours and tissues. Chapman and Hall, London.

Branch, P., Aquilina, G., Bignami, M., & Karran, P. (1993). Defective mismatch binding and a mutator phenotype in cells tolerant to DNA damage. Nature **362,** 652-654.

Branch, P., Hampson, R., & Karran, P. (1995). DNA mismatch binding defects, DNA damage tolerance, and mutator phenotypes in human colorectal carcinoma cell lines. Cancer Res. **55,** 2304-2309.

Bresalier, R.S. & Kim, Y.S. (1993). Malignant neoplasms of the large intestine. In: Gastrointestinal disease. [Eds. Sleisenger, M.H. & Fordtran, J.S.] W.B. Saunders, Philedelphia, 1149-1183.

Brugal, G., Dye, R., Krief, B., Chassey, J-M., Tanke, H., & Tucker, J.E. (1992). HOME: Highly Optimized Microscope Environment. Cytometry **13,** 109-116.

Bubb, V.J., Curtis, L.J., Cunningham, C., Dunlop, M.G., Carothers, A.D., Morris, R.G., White, S., Bird, C.C., & Wyllie, A.H. (1996). Microsatellite instability and the role of hMSH2 in sporadic colorectal cancer. Oncogene **12,** 2641-2649.

Bussey, H.J. (1978). Multiple adenomas and carcinomas. In: The pathogenesis of colorectal cancer. [Ed. Morson, B.C.] W.B. Saunders, Philadelphia, 72-86.

Caduff, R.F., Johnston, C.M., Svoboda-Newman, S.M., Poy, E.L., Merajver, S.D., & Frank, T.S. (1996). Clinical and pathological significance of microsatellite instability in sporadic endometrial carcinoma. Am. J. Pathol. **148,** 1671-1678.

Cancer Research Campaign (1997). Scientific Yearbook 1996-1997.

Cannon-Albright, L.A., Skolnick, M.H., Bishop, D.T., Lee, R.G., & Burt, R.W. (1988). Common inheritance of susceptibility to colonic adenomatous polyps and associated colorectal cancers. N. Engl. J. Med. **319,** 533-537.

Carder, P.J., Wyllie, A.H., Purdie, C.A., Morris, R.G., White, S., Piris, J., & Bird, C.C. (1993). Stabilised p53 facilitates aneuploid clonal divergence in colorectal cancer. Oncogene **8,** 1397-1401.

Carder, P.J., Cripps, K.J., Morris, R., Collins, S., White, S., Bird, C.C., & Wyllie, A.H. (1995). Mutation of the p53 gene precedes aneuploid clonal divergence in colorectal carcinoma. Br. J. Cancer **71,** 215-218.

Chang, F., Syrjanen, S., Kurvinen, K., & Syrjanen, K. (1993). The p53 tumour suppressor gene as a common cellular target in human carcinogenesis. Am. J. Gastroenterol. **88,** 174-186.

Chinnasamy, N., Rafferty, J.A., Hickson, I., Ashby, J., Tinwell, H. Margison, G.P., Dexter, T.M., & Fairbairn, L.J. (1997). $O^6$-Benzylguanine potentiates the in vivo toxicity and clastogenicity of temozolomide and BCNU in the mouse bone marrow. Blood **89,** 1566-1573.

Chung, D.C. & Rustgi, A.K. (1995). DNA mismatch repair and cancer. Gastroenterology **109,** 1685-1699.

Clarke, A.R., Maandag, E.R., van Roon, M., van der Lugt, N.M., van der Valk, M., Hooper, M.L., Berns, A., & te Riele, H. (1992). Requirement for a functional Rb-1 gene in murine development. Nature **359,** 328-330.

Clarke, A.R., Purdie, C.A., Harrison, D.J., Morris, R.G., Bird, C.C., Hooper, M.L., & Wyllie, A.H. (1993). Thymocyte apoptosis induced by p53-dependent and independent pathways. Nature **362,** 849-852.

Clarke, A.R., Gledhill, S., Hooper, M.L., Bird, C.C., & Wyllie, A.H. (1994). p53 dependence of early apoptotic and proliferative responses within the mouse intestinal epithelium following gamma-irradiation. Oncogene **9,** 1767-1773.

Clarke, A.R., Cummings, M.C., & Harrison, D.J. (1995). Interaction between murine germline mutations in p53 and APC predisposes to pancreatic neoplasia but not to increased intestinal malignancy. Oncogene **11,** 1913-1920.

Clarke, A.R., Howard, L.A., Harrison, D.J., & Winton, D.J. (1997). p53 mutation frequency and apoptosis in the murine small intestine. Oncogene **14,** 2015-2018.

Cohen, P.R., Kohn, S.R., & Kurzrock R. (1991). Association of sebaceous gland tumours and internal malignancy: The Muir-Torre syndrome. Am. J. Med. **90,** 606-613.

Cormier, R.T., Hong, K.H., Halberg, R.B., Hawkins, T.L., Richardson, P., Mulherkar, R., Dove, W.F., & Lander, E.S. (1997). Secretory phospholipase Pla2g2a confers resistance to intestinal tumorigenesis. Nature Genet. **17,** 88-91.

Cottrell, S., Bicknell, D., Kaklamanis, L., & Bodmer, W.F. (1992). Molecular analysis of APC mutations in familial adenomatous polyposis and sporadic colon carcinomas. Lancet **340,** 626-630.

Cottu, P.H., Muzeau, F., Estreicher, A., Flejou, J-F., Iggo, R., Thomas, G., & Hamelin, R. (1996). Inverse correlation between RER+ status and p53 mutation in colorectal cancer cell lines. Oncogene **13,** 2727-2730.

Cox, L.S., & Lane, D.P. (1995). Tumour suppressors, kinases and cell clamps: how p53 regulates the cell cycle in response to DNA damage. Bioessays **17,** 501-508.

Cranston, A., Bocker, T., Reitmair, A., Palazzo, J., Wilson, T., Mak, T., & Fishel, R. (1997). Female embryonic lethality in mice nullizygous for both Msh2 and p53. Nature Genet. **17**, 114-118.

Cross, S.M., Sanchez, C.A., Morgan, C.A., Schimke, M.K., Rammel, S., Idzerda, R.L., Rasking, W.H., & Reid, B.J. (1995). A p53-dependent mouse spindle checkpoint. Science **267,** 1353-1356.

Cunningham, C., & Dunlop, M.G. (1996). Molecular genetic basis of colorectal cancer susceptibility. Br. J. Surg. **83,** 321-329.

da Costa, L.T., Liu, B., El-Deiry, W., Hamilton, S.R., Kinzler, K.W., Vogelstein, B., Markowitz, S., Willson, J.K., de la Chapelle, A., Downey, K.M., & So, A.G. (1995). Polymerase delta variants in RER colorectal tumours. Nature Genet. **9,** 10-11.

Denny, B.J., Wheelhouse, R.T., Stevens, M.F., Tsang, L.L., & Slack, J.A. (1994). NMR and molecular modeling investigation of the mechanism of activation of the antitumor drug temozolomide and its interaction with DNA. Biochemistry **33,** 9045-9051.

de Wind, N., Dekker, M., Berns, A., Radman, M., & te Riele, H. (1995). Inactivation of the mouse Msh-2 gene results in mismatch repair deficiency, methylation tolerance, hyperrecombination and predisposition to cancer. Cell **82,** 321-330.

Dietrich, W.F., Lander, E.S., Smith, J.S., Moser, A.R., Gould, K.A., Luongo, C., Borenstein, N., & Dove, W. (1993). Genetic identification of Mom-1, a major modifier locus affecting Min-induced intestinal neoplasia in the mouse. Cell **75,** 631-639.

D'Incalci, M. (1994). Metabolism of triazine anticancer agents. In: International encyclopedia of pharmacology and therapeutics [Ed Powis, G.] Pergamon Press, Oxford, 157-165.

Dolan, M.E., Moschel, R.C., & Pegg, A.E. (1990). Depletion of mammalian $O^6$-alkylguanine-DNA-alkyltransferase activity by $O^6$-benzylguanine provides a means to evaluate the role of this protein in protection against carcinogenic and therapeutic alkylating agents. Proc. Natl. Acad. Sci. USA **87,** 5368-5372.

Dolan, M.E., Chae, M-Y., Pegg, A.E., Mullen, J.H. Friedman, H.S., & Moschel, R.C. (1994). Metabolism of $O^6$-benzylguanine, an inactivator of $O^6$-alkylguanine-DNA-alkyltransferase. Cancer Res. **54,** 6123-5130.

Dollery, C. (1991). Dacarbazine. In: Therapeutic drugs volume1 [Ed Dollery, C.] Churchill Livingstone, London, D1-D3.

Donehower, L.A., Harvey, M., Slagle, B.L., McArthur, M.J., Montgomery, C.A., Butel, J.S., & Bradley, A. (1992). Mice deficient for p53 are developmentally normal but susceptible to spontaneous tumours. Nature **356**, 215-221.

Dove, W.F., Luongo, C., Connelly, C.S., Gould, K.A., Shoemaker, A.R., Moser, A.R., & Gardner, R.L. (1994). The adenomatous polyposis coli gene of the mouse in development and neoplasia. Cold Spring Harb. Symp. Quant. Biol. **59,** 501-508.

Drummond, J.T., Li, G.M., Longley, M.J., & Modrich, P. (1995). Isolation of an hMSH2-p160 heterodimer that restores DNA mismatch repair to tumor cells. Science **268,** 1909-1912.

Drummond, J.T., Anthoney, A., Brown, R., & Modrich, P. (1996). Cisplatin and adriamycin resistance are associated with MutLα and mismatch repair deficiency in an ovarian tumour cell line. J. Biol. Chem. **271,** 19645-19648.

Duckett, D.R., Drummond, J.T., Murchie, A.I., Reardon, J.T, Sancar, A., Lilley, D.M., & Modrich, P. (1996). Human MutSα recognises damaged DNA base pairs containing $O^6$-methylguanine, $O^4$-methylthymine, or the cisplatin-d(GpG) adduct. Proc. Natl. Acad. Sci. USA. **93,** 6443-6447.

Dumenco, L.L., Allay, E., Norton, K., & Gerson, S.L. (1993). The prevention of thymic lymphomas in transgenic mice by human $O^6$-alkylguanine-DNA alkyltransferase. Science **259,** 219-222.

Eastman, A. (1983). Characterisation of the adducts produced in DNA by cis-diamminedichloroplatinum(II) and cis-dichloro(ethylenediamine)platinum. Biochemistry **22,** 3927-3933.

Edelmann, W., Yang, K., Umar, A., Heyer, J., Lau, K., Fan, K., Liedtke, W., Cohen, P.E., Kane, M.F., Lipford, J.R., Yu, N., Crouse, G.F., Pollard, J.W., Kunkel, T., Lipkin, M., Kolodner, R., & Kucherlapati, R. (1997). Mutation in the mismatch repair gene MSH6 causes cancer susceptibility. Cell **91,** 467-477.

Eshleman, J.R., Lang, E.Z., Bowerfind, G.K., Parsons, R., Vogelstein, B., Willson, J.K., Veigl, M.L., Sedwick, W.D., & Markowitz, S.D. (1995). Increased mutation rate at the hprt locus accompanies microsatellite instability in colon cancer. Oncogene **10,** 33-37.

Eshelman, J.R., & Markowitz, S.D. (1995). Microsatellite instability in inherited and sporadic neoplasms. Curr. Opin. Oncol. **7,** 83-89.
Eshleman, J.R., & Markowitz, S.D. (1996). Mismatch repair defects in human carcinogenesis. Hum. Mol. Genet. **5,** 1489-1494.

Evan, G.I., Wyllie, A.H., Gilbert, C.S., Littlewood, T.D., Land, H., Brooks, M., Waters, C.M., Penn, L.Z., & Hancock, D.C. (1992). Induction of apoptosis in fibroblasts by c-myc protein. Cell **69,** 119-128.

Fearon, E.R., & Vogelstein, B. (1990). A genetic model for colorectal tumorigenesis. Cell **61,** 759-767.

Fink, D., Zheng, H., Sibyelle, N., Norris, P.S., Aebi, S., Lin, T-P., Nehme, A., Christen, R.D., Haas, M., MacLeod, C.L. & Howell, S.B. (1997). In vitro and in vivo resistance to cisplatin in cells that have lost DNA mismatch repair. Cancer Res. **57,** 1841-1845.

Fishel, R., & Kolodner, R. (1995). Identification of the mismatch repair genes and their role in the development of cancer. Curr. Opin. Genet. Dev. **5,** 382-395.

Flaman, J-M., Frebourg, T., Moreau, V., Charbonnier, F., Martin, C., Chappuis, P., Sappino, A-P., Limacher, J-M., Bron, L., Benhattar, J., Tada, M., Van Meir, E.G., Estreicher, A., & Iggo R.D. (1995). A simple p53 functional assay for the screening cell lines, blood, and tumours. Proc. Natl. Acad. Sci. USA. **92,** 3963-3967.

Folkman, J. (1995). Angiogenesis in cancer, vascular, rheumatoid and other disease. Nature Med. **1,** 27-31.

Fukasawa, K., Choi, T., Kuriyama, R., Rulong, S., & Vande Woude, G.F. (1996). Abnormal centrosome amplification in the absence of p53. Science **271,** 1744-1747.

Funae,Y., & Imaoka, S. (1993). Cytochrome P450 in rodents. In: Handbook of experimental pathology: cytochrome P450. [Eds Schenkman, J.B & Greim, H.] Springer-Verlag, Berlin, 221-238.

Godfrey, D.I., & Zlotnik, A. (1993). Control points in early T-cell development. Immunol. Today **14,** 547-553.

Gorlin, R.J., & Chaudry, A.P. (1960). Multiple osteomatosis, fibromas, lipomas and fibrosarcomas of the skin and mesentry, epidemoid inclusion cysts of the skin, leiomyomas and multiple intestinal polyposis. N. Engl. J. Med. **263,** 1151-1158.

Gossen, J.A., de Leeuw, W.J., Verwest, A., Lohman, P.H., & Vijg, J. (1991). High somatic mutation frequencies in a LacZ transgene integrated on the mouse X-chromosome. Mutat. Res. **250,** 423-429.

Graeber, T., Peterson, J.F., Tsai, M., Monica, K., Fornace, A.J., & Giaccia, A.J. (1994). Hypoxia induces accumulation of p53 protein, but activation of a G1 phase checkpoint by low oxygen conditions is independent of p53 status. Mol. Cell. Biol. **14,** 6264-6277.

Graeber, T., Osmanian, C., Jacks, T., Houseman, D.E., Koch, C.J., Lowe, S.W., & Giaccia, A.J. (1996). Hypoxia-mediated selection of cells with diminished apoptotic potential in solid tumours. Nature **379,** 88-91.

Groden, J., Thliveris, A., Samowitz, W., Carlson, M., Gelbert, L., Albertson, H., Joslyn, G., Stevens, J., Spirio, L., Robertson, M., Sargeant, L., Krapcho, K., Wolff, E., Burt, R., Hughes, J.P., Warrington, J., McPherson, J., Wasmuth, J., Le Paslier, D., Abderrahim, H., Cohen, D., Leppert, M., & White, R. (1991). Identification and characterisation of the familial polyposis coli gene. Cell **66,** 589-600.

Guengerich, F.P. (1992). Characterisation of human cytochrome P450 enzymes. FASEB J. **6,** 745-748.

Gumbiner, B.M. (1995). Signal transduction of beta-catenin. Curr. Opin. Cell. Biol. **7,** 634-640.

Haffner, R., & Oren, M. (1995). Biochemical properties and biological effects of p53. Curr. Opin. Genet. Dev. **5,** 84-90.

Hall, C.N., Badawi, A.F., O'Connor, P.J., & Saffhill, R. (1991). The detection of alkylation damage in the DNA of human gastrointestinal tissues. Br. J. Cancer **64,** 59-63.

Han, H.J., Yanagisawa, A., Kato, Y., Park, J.G., & Nakamura, Y. (1993). Genetic instability in pancreatic cancer and poorly differentiated type of gastric cancer. Cancer Res. **53,** 5087-5089.

Harmon, B.V., Takano, Y.S., Winterford, C.M., & Potten, C.S. (1992). Cell death induced by vincristine in the intestinal crypts of mice and in a human Burkitts lymphoma cell line. Cell Prolif. **25,** 523-536.

Hartwell, L. (1992). Defects in a cell cycle checkpoint may be responsible for the genomic instability of cancer cells. Cell **71,** 543-546.

Hawn, M.T., Umar, A., Carethers, J.M., Marra, G., Kunkel, T.A., Boland, C.R., & Koi, M. (1995). Evidence for a connection between the mismatch repair system and the G2 cell cycle checkpoint. Cancer Res. **55,** 3721-3725.

Heim, S., & Mitelman, F. (1987). Cancer cytogenetics. Liss, New York.

Hockenbery, D., Nunez, G., Milliman, C., Schreiber, R.D., & Korsmeyer, S.J. (1990). Bcl-2 is an inner mitochondrial membrane protein that blocks programmed cell death. Nature **348,** 334-336.

Hollstein, M., Sidransky, D., Vogelstein, B., & Harris, C.C. (1991). p53 mutations in human cancers. Science **253,** 49-53.

Hollstein, M., Rice, K., Greenblatt, M.S., Soussi, T., Fuchs, R., Sorlie, T., Hovig, E., Smith-Sorensen, B., Montesano, R., & Harris, C.C. (1994). Database of p53 gene somatic mutations in human tumours and cell lines. Nucleic Acids Res. **22,** 3551-3555.

Hooper, M., Hardy, K., Handyside, A., Hunter, S., & Monk, M. (1987). HPRT-deficient (Lesch-Nyhan) mouse embryos derived from germline colonization by cultured cells. Nature **326,** 292-295.

Huang, J., Papadopoulos, N., McKinley, A.J., Farrington, S.M., Curtis, L.J., Wyllie, A.H., Zheug, S., Willson, J.K., Markowitz, S.D., Morin, P., Kinzler, K.W., Vogelstein, B., & Dunlop, M.G. (1996). APC mutations in colorectal tumours with mismatch repair deficiency. Proc. Natl. Acad. Sci. USA. **93,** 9049-9054.

Ichii, S., Horii, A., Nakatsuri, S., Furuyama, J., Utsunomiya, J. & Nakamura, Y. (1992). Inactivation of both APC alleles in an early stage of colon adenomas in a patient with a familial adenomatous polyposis (FAP). Hum. Mol. Genet. **1,** 387-390.

Ilyas, M., & Tomlinson, I.P. (1997). The interactions of APC, E-cadherin and β-catenin in tumour development and progression. J. Pathol. **182,** 128-137.

Jacks, T., Remington, L., Williams, B.O., Schmitt, E.M., Halamachi, S., Bronson, R.T., & Weinberg, R.A. (1994). Tumour spectrum analysis in p53-mutant mice. Curr. Biol. **4,** 1-7.

Jeffery, P.D., Gorina, S., & Pavletich, N.P. (1995). Crystal structure of the tetramerization domain of the p53 tumour suppressor at 1.7 angstroms. Science **267,** 1498-1502.

Kallioniemi, O.P., Kallioniemi, A., Sudar, D., Rutovitz, D., Gray, J.W., Waldman, F., & Pinkel, D. (1993). Comparative genomic hybridization: a rapid new method for detecting and mapping DNA amplification in tumours. Semin. Cancer Biol. **4,** 41-46.

Karran, P., & Bignami, M. (1992). Self-destruction and tolerance in resistance of mammalian cells to alkylation damage. Nucleic Acids Res. **20,** 2933-2940.

Karran, P., & Bignami, M. (1994). DNA damage tolerance, mismatch repair and genome instability. Bioessays **16,** 833-839.

Karran, P. (1996). Microsatellite instability and DNA mismatch repair in human cancer. Semin. Cancer Biol. **7,** 15-24.

Kaufmann, W.K., & Paules, R.S. (1996). DNA damage and cell cycle checkpoints. FASEB J. **10,** 238-247.

Kaur, P., & Potten, C.S. (1986). Cell migration velocities in the crypts after cytotoxic insult are not dependent on mitotic activity. Cell Tissue Kinet. **19,** 601-610.

Kemler, R. (1993). From cadherins to catenins: cytoplasmic protein interactions and regulation of cell adhesion. Trends Genet. **9,** 317-321.

Kerr, J.F., Wyllie, A.H., & Currie, A.R. (1972). Apoptosis: a basic biological phenomenon with wide-ranging implications in tissue kinetics. Br. J. Cancer **26,** 239-257.

Kerr, K.M., & Lamb, D. (1984). Actual growth rate and tumour cell proliferation in human pulmonary neoplasms. Br. J. Cancer **50,** 343-349.

Khine, K., Smith, D.R., & Goh, H-S. (1994). High frequency of allelic deletion on chromosome 17p in advanced colorectal cancer. Cancer **73,** 28-35

Kim, H., Jen, J., Vogelstein, B., & Hamilton, S.R. (1994). Clinical and pathological characteristics of sporadic colorectal carcinomas with DNA replication errors in microsatellite sequences. Am. J. Pathol. **145,** 148-156.

Kinzler, K.W., Nilbert, M.C., Vogelstein, B., Bryan, T.M., Levy, D.B., Smith, K.J., Preisinger, A.C., Hamilton, S.R., Hedge, P., Markham, A., Carlson, M., Joslyn, G., Grogen, J., White, R., Miki, Y., Miyoshi, Y., Nishisho, I., & Nakamura, Y. (1991). Identification of a gene located at chromosome 5q21 that is mutated in colorectal cancers. Science **251,** 1366-1370.

Kinzler, K.W., & Vogelstein, B. (1996). Lessons from hereditary colorectal cancer. Cell **87,** 159-170.

Knudson, A. (1985). Hereditary cancer, oncogenes, and antioncogenes. Cancer Res. **45,** 1437-1443.

Kobayashi, K., Matsushima, M., Koi, S., Saito, H., Sagae, S., Kudo, R., & Nakamura, Y. (1996). Mutational analysis of mismatch repair genes, hMLH1 and hMSH2, in sporadic endometrial carcinomas with microsatellite instability. Jpn. J. Cancer Res. **87,** 141-145.

Koc, O.N., Philips, W.P., Lee, K., Liu, L., Zaidi, N.H., Allay, J.A., & Gerson, S.L. (1996). Role of DNA repair in resistance to drugs that alkylate $O^6$ of guanine. Cancer Treat. Res. **87,** 123-146.

Koi, M., Umar, A., Chauhan, D.P., Cherian, S.P., Carethers, J.M., Kunkel, T.A., & Boland, C.R. (1994). Human chromosome 3 corrects mismatch repair deficiency and microsatellite instability and reduces N-methyl-N'-nitro-N-nitrosoguanidine tolerance in colon tumour cells with homozygous hMLH1 mutation. Cancer Res. **54,** 4308-4312.

Kolodner, R.D., Hall, N.R., Lipford, J., Kane, M.F., Rao, M.R., Morrison, P., Wirth, L., Finan, P.J., Burn, J., Chapman, P., Earabino, C., Merchant, E., & Bishop, T.D. (1994). Structure of the human MSH2 locus and analysis of two Muir-Torre kindreds for MSH2 mutations. Genomics **24,** 516-526.

Kolodner, R.D. (1995). Mismatch repair: mechanisms and relationship to cancer susceptibility. Trends Biochem. Sci. **20,** 397-401.

Konishi, M., Kikuchi-Yanoshita, R., Tanaka, K, Muraoka, M., Onda, A., Okumura, Y., Kishi, N., Iwama, T., Mori, T., Koike, M., Ushio, K., Chiba, M., Nomizu, S., Konishi, F., Utsunomiya, J., & Miyaki, M. (1996). Molecular nature of colon tumours in hereditary non-polyposis colon cancer, familial polyposis, and sporadic colon cancer. Gasteroenterology **111,** 307-317.

Kouri, M., Lassonen, A., Mecklin, J-P., Jarvinen, H., Franssila, K., & Pyrhonen, S. (1990). Diploid predominance in hereditary non-polyposis colorectal carcinoma evaluated by flow cytometry. Cancer **65,** 1825-1829.

Kurpad, S.N., Dolan, M.E., McLendon, R.E., Archer, G.E., Moschel, R.C., Pegg, A.E., Bigner, D.D., & Friedman, H.S. (1997). Intraarterial $O^6$-benzylguanine enables the specific therapy of nitrosourea-resistant intracranial human glioma xenografts in athymic rats with 1,3-bis(2-chlororthyl)-1-nitrososurea. Cancer. Chemother. Pharmacol. **39,** 307-316.

Lacal, P.M., D'Atri, S., Orlando, L., Bonmassar, E., & Graziani, G. (1996). In vitro inactivation of human $O^6$-alkyltransferase by antitumour triazene compounds. J. Pharmacol. Exp. Ther. **279,** 416-422.

Lane, D.P. (1992). p53, guardian of the genome. Nature **358,** 15-16.

Leach, F.S., Nicolaides, N.C., Papadopoulos, N., Liu, B., Jen, J., Parsons, R., Peltomaki, P., Sistonen, P., Aaltonen, L.A., Nystrom-Lahti, M., Guan, X-Y., Zhang, J., Meltzer, P.S., Yu, J.W., Kao, F-T., Chen, D.J., Cerosaletti, K.M., Fournier, R.E., Todd, S., Lewis, T., Leach, R.J., Naylor, S.L., Weissenbach, J., Mecklin, J-P., Jarvinen, H., Petersen, G.M., Hamilton, S.R., Green, J., Jass, J., Watson, P., Lynch, H.T., Trent, J.M., de la Chapelle, A., Kinzler, K.W., & Vogelstein, B. (1993). Mutations of a mutS homolog in hereditary non-polyposis colorectal cancer. Cell **75,** 1215-1225.

Leach, F.S., Polyak, K., Burrell, M., Johnson, K.A., Hill, D., Dunlop, M.G., Wyllie, A.H., Peltomaki, P., de la Chapelle, A., Hamilton, S.R., Kinzler, K.W., & Vogelstein, B. (1996). Expression of the human mismatch repair gene hMSH2 in normal and neoplastic tissues. Cancer Res. **56,** 235-240.

Lee, S., Elenbaas, B., Levine, A., & Griffith, J. (1995). p53 and its 14 kDa C-terminal domain recognise primary DNA damage in the form of insertion/deletion mismatches. Cell **81,** 1013-1020.

Lengauer, C., Kinzler, K.W., & Vogelstein, B. (1997). Genetic instability in colorectal cancers. Nature **386,** 623-627.

Levine, A.J. (1997). p53, the cellular gatekeeper for growth and division. Cell **88,** 323-331.

Levinson, G., & Gutman, G.A. (1987). High frequencies of short frameshifts in poly-CA/TG tandem repeats borne by bacteriophage M13 in Escherichia coli K-12. Nucleic Acids Res. **15,** 5323-5338.

Lewis, R.A., Crowder, W.E., Eierman, L.A., Nussbaum, R.L. & Ferrall, R.E. (1984). The Gardner syndrome - significance of ocular features. Opthalmology **91,** 916-925.

Li, F.P., & Fraumeni, J.F. (1969). Soft-tissue sarcomas, breast cancer and other neoplasms. A familial syndrome? Ann. Intern. Med. **71,** 747-752.

Lindblom, A., Tannergard, P., Werelius, B., & Nordenskjold, M. (1993). Genetic mapping of a second locus predisposing to hereditary non-polyposis colorectal cancer. Nature Genet. **5,** 279-282.

Linke, S.P., Clarkin, K.C., Di Leonardo, A., Tsou, A., & Whal, G.M. (1996). A reversible p53-dependent G0/G1 cell cycle arrest induced ribonucleotide depletion in the absence of detectable DNA damage. Genes Dev. **10,** 934-947.

Liu, B., Nicolaides, N.C., Markowitz, S., Willson, J.K., Parsons, R.E., Jen, J., Papadopoulos, N., Peltomaki, P., de la Chapelle, A., Hamilton, S.R., Vogelstein, B., & Kinzler, K.W. (1995). Mismatch repair gene defects in sporadic colorectal cancers with microsatellite instability. Nature Genet. **9,** 48-55.

Liu, B., Parsons, R., Papadopoulos, N., Nicolaides, N.C., Lynch, H.T., Watson, P., Jass, J.R., Dunlop, M., Wyllie, A.H., Peltomaki, P., de la Chapelle, A., Hamilton, S.R., Vogelstein, B., & Kinzler, K.W. (1996a). Analysis of mismatch repair genes in hereditary non-polyposis colorectal cancer patients. Nature Med. **2,** 169-174.

Liu, L., Markowitz, S., & Gerson, S.L. (1996b). Mismatch repair mutations override alkyltransferase in conferring resistance to temozolomide but not to 1,3-Bis(2-Chloroethyl)nitrosourea. Cancer Res. **56,** 5375-5379.

Liu, L., Lee, K., Markowitz, S., & Gerson, S.L. (1996c). Differential sensitivity of human and mouse alkyltransferase to $O^6$-benzylguanine using a transgenic model. Cancer Res. **56,** 1880-1885.

Livingstone, L.R., White, A., Sprouse, J., Livanos, E., Jacks, T., & Tlsty, T. (1992). Altered cell cycle arrest and gene amplification potential accompany loss of wild-type p53. Cell **70,** 923-935.

Lothe, R.A., Peltomaki, P., Meling, G.I., Aaltonen, L.A., Nystrom-Lahti, M., Pylkkanen, L., Heimdal, K., Andersen, T.I., Moller, P., Rognum, T.O., Fossa, S.D., Haldorsen, T., Langmark, F., Brogger, A., de la Chapelle, A., & Borresen, A-L. (1993). Genomic instability in colorectal cancer: relationship to clinicopathological variables and family history. Cancer Res. **53,** 5849-5852.

Lowe, S.W., Schmitt, E.M., Smith, S.W., Osborne, B.A., & Jacks, T. (1993a). p53 is required for radiation induced apoptosis in mouse thymocytes. Nature **362,** 847-849.

Lowe, S.W., Ruley, H.E., Jacks, T., & Houseman, D.E. (1993b). p53-dependent apoptosis modulates the cytotoxicity of anticancer agents. Cell **74,** 957-968.

Lukash, L.L., Boldt, J., Pegg, A.E., Dolan, M.E., Maher, V.M., & McCormick, J.J. (1991). Effect of $O^6$-alkylguanine-DNA-alkyltransferase on the frequency and spectrum of mutations induced by N-methyl-N-nitro-N-nitrosoguanidine in the HPRT gene of diploid human fibroblasts. Mutat. Res. **250,** 397-409.

Luongo, C., Moser, A.R., Gledhill, S., & Dove, W.F. (1994). Loss of Apc+ in intestinal adenomas from Min mice. Cancer Res **54,** 5947- 5952.

Lynch, H.T., Smyrk, T.C., Watson, P., Lanspa, S.J., Lynch, J.F., Lynch, P.M., Cavalieri, R.J., & Boland, C.R. (1993). Genetics, natural history, tumour spectrum, and pathology of hereditary non-polyposis colorectal cancer: an updated review. Gasteroenterology **104,** 1535-1549.

Lynch, H.T., Smyrk, T., & Lynch, J.F. (1996). Overview of the natural history, pathology, molecular genetics and management of HNPCC (Lynch syndrome). Int. J. Cancer **69,** 38-43.

Lyons, S.K. & Clarke, A.R. (1997). Apoptosis and carcinogenesis. Br. Med. Bull. **53,** 554-569.

MacGrogan, D., Pegram, M., Slamon, D., & Bookstein, R. (1997). Comparative mutational analysis of DPC4 (Smad4) in prostatic and colorectal carcinomas. Oncogene **15,** 1111-1114.

MacPhee, M., Chepenik, K.P., Liddell, R.A., Nelson, K.K., Siracusa, L.D. & Buchberg, A.M. (1995). The secretory phospholipase A2 gene is a candidate for the Mom1 locus, a major modifier of ApcMin-induced intestinal neoplasia. Cell **81,** 957-966.

Malcomson, R.D., Clarke A.R., Peter, A., Coutts, S.B., Howie, S.E., & Harrison, D.J. (1997). Apoptosis induced by γ-irradiation, but not CD4 ligation, of peripheral T lymphocytes in vivo is p53-dependent. Oncogene **181,** 166-171.

Malkhosyan, S., Rampino, N., Yamamoto, H., & Perucho, M. (1996). Frameshift mutator mutations. Nature **382,** 499-500.

Maltzman, W., & Czyzyk, L. (1984). UV irradiation stimulates levels of p53 cellular tumour antigen in nontransformed mouse cells. Mol. Cell. Biol. **4,** 1689-1694.

Markowitz, S., Wang, J., Myeroff, L., Parsons, R., Sun, L., Lutterbaugh, J., Fan, R.S., Zborowska, E., Kinzler, K.W., Vogelstein, B., Brattain, M., & Willson, J.K. (1995). Inactivation of the type II TGF-beta receptor in colon cancer cells with microsatellite instability. Science **268,** 1336-1338.

Meer, L., Janzer, R.C., Kleihues, P., & Kolar, G.F. (1986). In vivo metabolism and reaction of DNA with the cytostatic agent 5-(3,3-dimethyl-1-triazeno)imidazole-4-carboxamide (DITC). Biochem. Pharmacol. **35,** 3243-3247.

Merlo, A., Mabry, M., Gabrielson, E., Vollmer, R., Baylin, S.B., & Sidransky, D. (1994). Frequent microsatellite instability in primary small cell lung cancer. Cancer Res. **54,** 2098-2101.

Merritt, A.J., Potten, C.S., Kemp, C.J., Hickman, J.A., Balmain, A., Lane, D.P., & Hall, P.A. (1994). The role of p53 in spontaneous and radiation-induced apoptosis in the gastrointestinal tract of normal and p53-deficient mice. Cancer Res. **54,** 614-617.

Merritt, A.J., Potten, C.S., Watson, A.J., Loh, D.Y., Nakayama, K., & Hickman, J.A. (1995). Differential expression of bcl-2 in intestinal epithelia. Correlation with attenuation of apoptosis in colonic crypts and the incidence of colonic neoplasia. J. Cell Sci. **108,** 2261-2271.

Merritt, A.J., Allen, T.D., Potten, C.S., & Hickman, J.A. (1997). Apoptosis in small intestinal epithelia from p53-null mice: evidence for delayed, p53-independent G2/M-associated cell death after γ-irradiation. Oncogene **14,** 2759-2766

Miyaki, M., Konishi, M., Tanaka, K., Kikuchi-Yanoshita, R., Muraoka, M., Yasuno, M., Igari, T., Koike, M., Chiba, M., & Mori, T. (1997). Germline mutation of MSH6 as the cause of hereditary nonpolyposis colorectal cancer. Nature Genet. **17,** 271-272.

Miyashita, T., & Reed, J.C. (1995). Tumour suppressor p53 is a direct transcriptional activator of the human bax gene. Cell **80,** 293-299.

Moggs, J.G., Yarema, K.J., Essigmann, J.M., & Wood, R.D. (1996). Analysis of incision sites produced by human cell extracts and purified proteins during nucleotide excision repair of a 1,3-intrastrand d(GpTpG)-cisplatin adduct. J. Biol. Chem. **271,** 7177-7186.

Moore J.V. (1983). Cytotoxic injury to cell populations of solid tumors. In: Cytotoxic insult to tissue. [Eds. Potten, C.S., & Hendry, J.H.] Churchill Livingstone, Edinburgh, 368-404.

Moore J.V. (1987). Death of cells and necrosis of tumors. In: Perspectives in mammalian cell death. [Ed. Potten, C.S.] Oxford University Press, Oxford, 295-325.

Morin, P.J., Vogelstein, B., & Kinzler, K.W. (1996). Apoptosis and APC in colorectal tumourigenesis. Proc. Natl. Acad. Sci. USA. **93,** 7950-7954.

Moser, A.R., Pitot, H.C., & Dove, W.F. (1990). A dominant mutation that predisposes to multiple intestinal neoplasia in the mouse. Science **247,** 322-324.

Mudipalli, A., Nadadur, S.S., Maccubbin, A.E., & Gurtoo, H.L. (1995). Mutations induced by dacarbazine activated with cytochrome P-450. Mutat. Res. **327,** 113-120.

Munemitsu, S., Souza, B., Muller, O., Albert, I., Rubinfeld, B., & Polakis, P. (1994). The APC gene product associates with microtubules in vivo and promotes their assembly in vitro. Cancer Res. **54,** 3676-3681.

Nagase, H., & Nakamura, Y. (1993). Mutations of the APC (adenomatous polyposis coli) gene. Hum Mutat. **2,** 425-433.

Nebert, D.W., & Weber, W.W. (1990). Pharmacogenetics In: Principles of drug action: the basis of pharmacology. [Eds Pratt, W.B. & Taylor, P.] Churchill Livingstone, New York, 469-531.

Nelson, W.G., & Kastan, M.B. (1994). DNA strand breaks: the DNA template alterations that trigger p53-dependent DNA damage response pathways. Mol. Cell Biol. **14,** 1815-1823.

Newell, D., Gescher, A., Harland, S., Ross, D. & Rutty, C. (1987). N-Methyl antitumour agents: a distinct class of anticancer drugs? Cancer Chemother. Pharmacol. **19,** 91-102.

Nishino, H., Knoll, A., Buettner, V.L., Frisk, C.S., Maruta, Y., Haavik, J., & Sommer, S.S. (1995). p53 wild-type and p53 nullizygous big blue transgenic mice have similar frequencies and patterns of observed mutation in the liver, spleen and brain. Oncogene **11,** 263-270.

Ozbun, M.A., Jerry, J., Kittrell, F.S., Medina. D., & Butel, J.S. (1993). p53 mutations selected in vivo when mouse mammary epithelial cells form hyperplastic outgrowths are not necessary for establishment of mammary cell lines in vitro. Cancer Res. **53,** 1646-1652.

Palombo, F., Iccarino, I., Nakajima, E., Ikejima, M., Shimada, T., & Jiriony, J. (1996). hMutSβ, a heterodimer of hMSH2 and hMSH3, binds to insertion/deletion loops in DNA. Curr. Biol. **6,** 1181-1184.

Papadopoulos, N., Nicolaides, N.C., Wei, Y-F., Ruben, S.M., Carter, K.C., Rosen, C.A., Haseltine, W.A., Fleischmann, R.D., Fraser, C.M., Adams, M.D., Venter, J.C., Hamilton, S.R., Petersen, G.M., Watson, P., Lynch, H.T., Peltomaki, P., Mecklin, J-P., de la Chapelle, A., Kinzler, K.W., & Vogelstein, B. (1994). Mutation of a mutL homolog in hereditary colon cancer. Science **263,** 1625-1629.

Papadopoulos, N., Nicolaides, N.C., Liu, B., Parsons, R., Lengauer, C., Palombo, F., D'Arrigo, A., Markowitz, S., Willson, J.K., Kinzler, K.W., Jiricny, J., & Vogelstein, B. (1995). Mutations of GTBP in genetically unstable cells. Science **268,** 1915-1917.

Pegg, A.E. (1990). Mammalian $O^6$-alkylguanine-DNA-alkyltransferase: regulation and importance in response to alkylating carcinogenic and therapeutic agents. Cancer Res. **50,** 6119-6129.

Pegg, A.E., & Byers, T.L. (1992). Repair of DNA containing $O^6$-alkylguanine. FASEB J. **6,** 2302-2310.

Pegg, A.E., Boosalis, M., Samson, L., Moschel, R.C., Byers, T.L., Sween, K., & Dolan, M.E. (1993). Mechanism of inactivation of $O^6$-alkylguanine-DNA alkyltransferase by $O^6$-benzylguanine. Biochemistry **32,** 11998-12006.

Peifer, M. (1997). β-Catenin as oncogene: the smoking gun. Science **275,** 1752-1753.

Peltomaki, P., Aaltonen, L.A., Sistonen, P., Pylkkanen, L., Mecklin, J.P., Jarvinen, H., Green, J.S., Jass, J.R., Weber, J.L., Leach, F.S., Petersen, G.M., Hamilton, S.R., de la Chapelle, A., & Vogelstein, B. (1993a). Genetic mapping of a locus predisposing to human colorectal cancer. Science **260,** 810-812.

Peltomaki, P., Lothe, R.A., Aaltonen, L.A., Pylkkanen, L., Nystrom-Lathi, M., Seruca, R., David, L., Holm, R., Ryberg, D., Haugen, A., Brogger, A., Borresen, A-L., & de la Chapelle, A. (1993b). Microsatellite instability is associated with tumors that characterise the hereditary non-polyposis colorectal cancer syndrome. Cancer Res. **53,** 5853-5855.

Perucho, M. (1996). Microsatelllite instability: the mutator that mutates the other mutator. Nature Med. **2,** 630-631.

Polakis, P. (1995). Mutations in the APC gene and their implications for protein structure and function. Curr. Opin. Genet. Dev. **5,** 66-71.

Potten, C.S. (1990). A comprehensive study of the radiobiological response of the murine (BDF1) small intestine. Int. J. Rad. Biol. **58,** 925-973.

Potten, C.S., Li, Y.Q., O'Connor, P.J. & Winton, D.J. (1992). A possible explanation for the differential cancer incidence in the intestine based on distribution of the cytotoxic effects of carcinogens in the murine large bowel. Carcinogenesis **13,** 2305-2312.

Potten, C.S., Wilson, J.W., & Booth, C. (1997). Regulation and significance of apoptosis in the stem cells of the gastrointestinal epithelium. Stem Cells **15,** 82-93.

Prescott, S.M., & White, R.L. (1996). Self-promotion? Intimate connections between APC and prostaglandin H synthase-2. Cell **87,** 783-786.

Preuss, I., Thust, R., & Kaina, B. (1996). Protective effect of $O^6$-methylguanine-DNA methyltransferase (MGMT) on the cytotoxic and recombinogenic activity of different antineoplastic drugs. Int. J. Cancer **65,** 506-512.

Provost, G.S., & Short, J.M. (1994). Characterization of mutations induced by ethylnitrosourea in seminiferous tubule germ cells of transgenic B6C3F1 mice. Proc. Natl. Acad. Sci. USA. **91,** 6564-6568.

Puju, S., Shuker, D.E., Bishop, W.W., Falchuk, K.R., Tannenbaum, S.R., & Thilly, W.G. (1982). Mutagenicity of N-nitroso bile acid conjugates in samonella typhimurium and diploid lymphoblasts. Cancer Res. **42,** 2601-2604.

Purdie, C.A., Harrison, D.J., Peter, A., Dobbie, L., White, S., Howie, S.E., Salter, D.M., Bird, C.C., Wyllie, A.H., & Hooper, M.L. (1994). Tumour incidence, spectrum and ploidy in mice with a large deletion in the p53 gene. Oncogene **9,** 603-609.

Rafferty J.A., Clarke, A.R., Sellappan, D., Koref, M.S., Frayling, I.M., & Margison, G.P. (1996). Induction of murine $O^6$-alkylguanine-DNA-alkyltransferase in response to ionising radiation is p53 gene dose dependent. Oncogene **12,** 693-697.

Reddy, B.S., & Wynder, E.L. (1973). Bowel carcinogenesis: fecal constituents of poulations with diverse incidence rates of colon cancer. J. Natl. Cancer Inst. **50,** 1437-1442.

Reichmann, A., Martin, P., & Levin, B. (1981). Chromosome banding patterns in human large bowel cancer. Int. J. Cancer **28,** 431-440.

Reitmair, A.H., Schmits, R., Ewel, A., Bapat, B., Redston, M., Mitri, A., Waterhouse, P., Mittrucker, H.W., Wakeham, A., Liu, B., Thomason, A., Griesser, H., Gallinger, S., Ballhausen, W.G., Fishel, R., & Mak, T.W. (1995). MSH2 deficient mice are viable and susceptible to lymphoid tumours. Nature Genet. **11,** 64-70.

Reitmair, A.H., Redston, M., Cai, J.C., Chuang, T.C., Bjerknes, M., Cheng, H., Hay, K., Gallinger, S., Bapat, B., & Mak, T.W. (1996a). Spontaneous intestinal carcinomas and skin neoplasms in Msh2-deficient mice. Cancer Res. **56,** 3842-3849.

Reitmair, A.H., Cai, J.C., Bjerknes, M., Redston, M., Cheng, H., Pind, M.T., Hay, K., Mitri, A., Bapat, B.V., Mak, T.W., & Gallinger, S. (1996b). MSH2 deficiency contributes to accelerated APC-mediated intestinal tumorigenesis. Cancer Res. **56,** 2922-2926.

Reitmair, A.H., Risely, R., Bristow, R.G., Wilson, T., Ganesh, A., Jang, A., Peacock, J., Benchimol, S., Hill, R., Mak, T., Fishel, R., & Meuth, M. (1997). Mutator phenotype in Msh2-deficient murine embryonic fibroblasts. Cancer Res. **57,** 3765-3771.

Risinger, J.I., Berchuck, A., Kohler, M.F., Watson, P., Lynch, H.T., & Boyd, J. (1993). Genetic instability of microsatellites in endometrial cancer. Cancer Res. **53,** 5100-5103.

Risinger, J.I., Umar, A., Boyd, J., Berchuck, A., Kunkel, T.A., & Barret, J.C. (1996). Mutation of MSH3 in endometrial cancer and evidence for its functional role in heteroduplex repair. Nature Genet. **14,** 102-105.

Rubinfeld, B., Souza, B., Albert, I., Muller, O., Chamberlain, S.H., Masiarz, F.R., Munemitsu, S., & Polakis, P. (1993) Association of the APC gene with beta-catenin. Science **262,** 1731-1734.

Rubinfeld, B., Albert, I., Porfini, E., Fiol, C., Munemitsu, S., & Polakis, P. (1996). Binding of GSK3-beta to the APC-beta-catenin complex and regulation of complex assembly. Science **272,** 1023-1025.

Sah, V.P., Attardi, L.D., Mulligan, G.J., Williams, B.O., Bronson, R.T., & Jacks, T. (1995). A subset of p53-deficient embryos exhibit exencephaly. Nature Genet. **10,** 175-180.

Sarraf, C.E., & Bowen, I.D. (1986). Kinetic studies on a murine sarcoma and an analysis of apoptosis. Br. J. Cancer **54,** 989-998.

Sarraf, C.E., & Bowen, I.D. (1988). Proportions of mitotic and apoptotic cells in a range of untreated experimental tumours. Cell Tissue Kinet. **21,** 45-49.

Schlegel, J., Stumm, G., Scherthan, H., Bocker, T., Zirngibl, H., Ruschoff, J., & Hofstader, F. (1995). Comparative genomic in situ hybridization of colon carcinomas with replication error. Cancer Res. **55,** 6002-6005.

Shackney, S.E., Smith, C.A., Miller, B.W., Burholt, D.R., Murtha, K., Giles, H.R., Ketterer, D.M., & Pollice, A.A. (1989). Model for the genetic evolution of human solid tumours. Cancer Res. **49,** 3344-3354.

Shibata, D., Schaeffer, J., Li, Z.H., Capella, G., & Perucho, M. (1993). Genetic heterogeneity of the c-K-ras locus in colorectal adenomas but not in adenocarcinomas. J. Natl. Cancer Inst. **85,** 1058-1063.

Shibata, D. (1996). Loss of DNA mismatch repair: life in the fast lane? Gastroenterology **111,** 519-528.

Shimada, T., El-Bayoumy, K., Upadhyaya, P., Sutter, T.R., Guengerich, F. P., & Yamazaki, H. (1997). Inhibition of human cytochrome P450-catalysed oxidations of xenobiotics and procarcinogens by synthetic organoselenium componds. Cancer Res. **57,** 4757-4764.

Shuker, D.E., Tannenbaum, S.R., & Wishnok, J.S. (1981). N-nitroso bile acid conjugates. 1. Synthesis, chemical reactivity, and mutagenic activity. J. Org. Chem. **46,** 2092-2096.

Smith, K.J., Levy, D.B., Maupin, P., Pollard, T.D., Vogelstein, B., & Kinzler, K.W. (1994). Wild-type but not mutant APC associates with the microtubule cytoskeleton. Cancer. Res. **54,** 3672-3675.

Steel, C.G. (1977). Growth kinetics of tumors. Oxford University Press, Oxford.

Stevens, M.F., Hickman, J.A., Langdon, S.P., Chubb, D., Vickers, L., Stone, R., Baig, G., Goddard, C., Gibson, N.W., Slack, J.A., Newton, C., Lunt, E., Fizames, C., & Lavelle, F. (1987). Antitumour activity and pharmacokinetics in mice of 8-carbamoyl-3-methyl-imidazo[5,1-d]-1,2,3,5-tetrazin-4(3H)-one (CCRG 81045; M&B 39831), a novel drug with potential as a alternative to dacarbazine. Cancer Res. **47,** 5846-5852.

Su, L.K., Kinzler, K.W., Vogelstein, B., Preisinger, A.C., Moser, A.R., Luongo, C., Gould, K.A., & Dove, W.F. (1992). Multiple intestinal neoplasia caused by a mutation in the murine homologue of the APC gene. Science **256,** 668-670.

Swann, P.F. (1990). Why do $O^6$-alkylguanine and $O^4$-alkylthymine miscode? The relationship between the structure of DNA containing $O^6$-alkylguanine and $O^4$-alkylthymine and the mutagenic properties of these bases. Mutat. Res. **233,** 81-94.

Thibodeau, S.N., Bren, G., & Schaid, D. (1993). Microsatellite instability in cancer of the proximal colon. Science **260,** 816-819.

Thomlinson, R.H., & Gray, L.H. (1955). The histological structure of some human lung cancers and the possible implications for radiotherapy. Br. J. Cancer **9,** 539-549.

Tlsty, T.D. (1997). Genomic instability and its role in neoplasia. Curr. Top. Microbiol. Immunol. **221,** 37-46.

Uchida, T., Wada, C., Wang, C., Egawa, S., Ohtani, H., & Koshiba, K. (1994). Genomic instability of microsatellite repeats and mutations of H-, K-, and N-ras, and p53 genes in renal cell carcinoma. Cancer Res. **54,** 3682-3685.

Uchida, T., Wada, C., Wang, C., Ishida, H., Egawa, S., Yokoyama, E., Ohtani, H., & Koshiba, K. (1995). Microsatellite instability in prostate cancer. Oncogene **10,** 1019-1022.

Vasen, H.F., Mecklin, J-P., Meera-Khan, P.M., & Lynch, H.T. (1991). The international collaborative group on hereditary non-polyposis colorectal cancer (ICG-HNPCC). Dis. Colon. Rectum **34,** 424-425.

Vasen, H.F., Nagenhast, F.M., Meera-Khan, P. (1995). Interval cancers in hereditary non-polyposis colorectal cancer (Lynch Syndrome). Lancet **345,** 1183-1184.

Vindelov, L.L., Christensen, I.J., & Nissen N.I. (1983). A detergent-trypsin method for the preparation of nuclei for flow cytometric DNA analysis. Cytometry **3,** 323-327.

Vogelstein, B., & Kinzler, K.W. (1992). p53 function and dysfunction. Cell **70,** 523-526.

Vogelstein, B., & Kinzler, K.W. (1993). The multistep nature of cancer. Trends Genet. **9,** 138-141.

von Hofe, E., & Kennedy, A.R. (1988). In vitro induction of $O^6$-methylguanine-DNA methyltransferase in C3H/10T1/2 cells by X-rays is inhibited by nitrogen. Carcinogenesis **9,** 679-681.

Wang L., & Setlow, R.B. (1989). Inactivation of $O^6$-alkylguanine-DNA-alkyltransferase in HeLa cells by cisplatin. Carcinogenesis **10,** 1681-1684.

Wedge, S.R. & Newlands, E.S. (1996). $O^6$-Benzylguanine enhances the sensitivity of a glioma xenograft with low $O^6$-alkylguanine-DNA-alkyltransferase activity to temozolomide and BCNU. Br. J. Cancer **73,** 1049-1052.

Wedge, S.R., Porteous, J.K., & Newlands, E.S. (1996). 3-aminobenzamide and /or $O^6$-benzylguanine evaluated as an adjuvant to temozolomide or BCNU treatment in cell lines of variable mismatch repair status and $O^6$-alkylguanine-DNA-alkyltransferase activity. Br. J. Cancer **74,** 1030-1036.

White, E. (1996). Life, death, and the pursuit of apoptosis. Genes Dev. **10,** 1-15.

Wijnen, J.T., Vasen, H.F., Meera Khan, P., Zwinderman, A.H., van der Klift, H., Mulder, A., Tops, C., Moller, P., & Fodde, R. (1998). Clinical findings with implications for genetic testing in families with clustering of colorectal cancer. N. Engl. J. Med. **339,** 511-518.

Winton, D., Blount, M.A., & Ponder, B.A. (1988). A clonal marker induced by mutation in mouse intestinal epithelium. Nature **333,** 463-466.

Wyllie, A.H. (1980). Glucocorticoid-induced thymocyte apoptosis is associated with endogenous endonuclease activation. Nature **284,** 555-556.

Wyllie, A.H., Kerr, J.F., & Currie, A.R. (1980). Cell death: the significance of apoptosis. Int. Rev. Cytol. **68,** 251-306.

Wyllie, A.H. (1981). Cell death: a new classification separating apoptosis from necrosis. In: Cell death in biology and pathology. [Eds. Bowen, I.D., & Lockshin, R.A.] Chapman and Hall Press, London, 9-34.

Wyllie, A.H., Morris, R.G., Smith, A.L., & Dunlop, D. (1984). Chromatin cleavage in apoptosis: association with condensed chromatin morphology and dependence on macromolecular synthesis. J. Pathol. **142,** 76-77.

Wyllie, A.H. (1985). The biology of cell death in tumours. Anticancer Res. **5,**131-136.

Wyllie, A.H. (1987). Apoptosis: cell death under homeostatic control. Arch. Toxicol. **11,** 3-10.

Wyllie, A.H., Carder, P.J., Clarke, A.R., Cripps, K.J., Gledhill, S., Greaves, M.F., Griffiths, S., Harrison, D.J., Hooper, M.L., Morris, R.G., Purdie, C.A., & Bird, C.C. (1994). Apoptosis in carcinogenesis: the role of p53. Cold Spring Harb. Symp. Quant. Biol. **59,** 403-409.

Yamada, M., O'Regan, E., Brown, R., & Karran, P. (1997). Selective recognition of a cisplatin-DNA adduct by human mismatch repair proteins. Nucleic Acids Res. **25,** 491-495.

Yin, Y., Tainsky, M.A., Bischoff, F.Z., Strong, L.C., & Wahl, G.M. (1992). Wild-type p53 restores cell cycle control and inhibits gene amplification in cells with mutant p53 alleles. Cell **70,** 937-948.

Zhan, Q., Carrier, F., & Fornace, A.J. (1993). Induction of cellular p53 activity by DNA-damaging agents and growth arrest. Mol. Cell Biol. **13,** 4242-4250.

*V.v.H. and N.D.H. are International Scholars of the Howard Hughes Medical Institute.*

**Kiyoshi Miyagawa[1,6], Jill Kent[1], Adrian Moore[1], Jean-Paul Charlieu[1], Melissa H. Little[1], Kathleen A. Williamson[1], Anna Kelsey[2], Keith W. Brown[3], Shabbir Hassam[4], Jakob Briner[4], Yasuhide Hayashi[5], Hisamaru Hirai[6], Yoshio Yazaki[6], Veronica van Heyningen[1] & Nicholas D. Hastie[1]**

*[1]MRC Human Genetics Unit, Western General Hospital, Crewe Road, Edinburgh EH4 2XU, UK. [2]Department of Pathology, Royal Manchester Children's Hospital, Pendlebury, Manchester M27 1HA, UK. [3]CLIC Research Unit, Department of Pathology and Microbiology, School of Medical Sciences, University Walk, Bristol BS8 1TD, UK. [4]Departement Pathologie der Universitat, Institut fur Klinische Pathologie, Universitätsspital Zürich, Schmelzbergstrasse 12, CH-8091 Zurich, Switzerland. [5]Department of Paediatrics and [6]Third Department of Internal Medicine, University of Tokyo, 7-3-1 Hongo, Bunkyo-ku, Tokyo 113, Japan. Correspondence should be addressed to N.D.H.*
*e-mail: oldnick@hgu.mrc.ac.uk*

1. Hastie, N.D. *Annu. Rev. Genet.* **28**, 523–558 (1994).
2. Call, K.M. *et al. Cell* **60**, 509–520 (1990).
3. Gessler, M. *et al. Nature* **343**, 774–778 (1990).
4. Drummond, I.A. *et al. Science* **257**, 674–678 (1992).
5. Larsson, S.H. *et al. Cell* **81**, 392–401 (1995).
6. Weintraub, H. *Cell* **75**, 1241–1244 (1993).
7. Olson, E.N. & Klein, W.H. *Genes Dev.* **8**, 1–8 (1994).
8. Little, M.H. *et al. Hum. Mol. Genet.* **2**, 259–264 (1993).
9. Brown, K.W. *et al. Oncogene* **7**, 763–768 (1992).
10. Bickmore, W.A. *et al. Science* **257**, 235–237 (1992).

# No female embryonic lethality in mice nullizygous for *Msh2* and *p53*

Recently, it has been reported that male mice bearing targeted inactivations of both *p53* and *Msh2* are viable, but rapidly succumb to lymphoma earlier than either *p53* or *Msh2* single mutants. In contrast, it was reported that all female mice lacking *p53* and *Msh2* underwent developmental arrest at 9.5 days and died *in utero*[1]. The published study did not report a significant reduction in the number of female $p53^{-/-}$ animals, although the authors state that this is probably due to their small cohort size. We have also generated male mice lacking *p53* and *Msh2* which are viable and succumb to lymphoma at a similarly early age (t½ is 65 days). However, our results differ from the data of Cranston *et al.* in that we have successfully generated 22 adult female mice nullizygous for both *p53* and *Msh2*. The parental strains used to generate our cohort differ from those used by Cranston *et al.*, but both have been well characterized previously[2,3]. Importantly, the single mutant *Msh2* and *p53* parental strains used in our cohort possess very similar reported phenotypes to those used by Cranston *et al.*[2–5]. Data from our cohort show the male to female ratio in $Msh2^{-/-}$ $p53^{-/-}$ mice is similar to the ratio observed in $Msh2^{+/+}$ $p53^{-/-}$ mice (Table 1). Thus, in our cohort *Msh2* plays no detectable role in female development with the reduction in female mice in our $Msh2^{-/-}$ $p53^{-/-}$ cohort from expected Mendelian ratios being accounted for by *p53*-associated exencephaly and subsequent anencephaly[6]. We observed an identical phenotype for female $Msh2^{-/-}$ $p53^{-/-}$ mice as for their male counterparts, dying from lymphoma at a similar age. We have used male $Msh2^{-/-}$ $p53^{-/-}$ mice in successful breeding pairs, confirming that these mice are fertile.

**Table 1 • Male to female ratio in live born mice**

| | $p53^{+/+}$ | $p53^{-/-}$ |
|---|---|---|
| $Msh2^{+/+}$ male/female | 262/254 (-2%) | 26/12 (-37%) |
| $Msh2^{+/-}$ | 118/94 (-11%) | 52/21 (-42%) |
| $Msh2^{-/-}$ | 166/177 (+3%) | 61/22 (-47%) |

Sex ratio of mice for each genotype group together with the percentage deviation from the expected 1:1 male to female ratio shown in brackets. The observed reduction in female mice doubly null for *Msh2* and *p53* is not significantly different from that related to *p53* deficiency alone ($\chi 2$ test). In this data set homozygosity for lack of *p53*, irrespective of *Msh2* status, confers a significant reduction in the number of female progeny ($p < 0.01$, $\chi 2$ test).

We suggest four possible explanations for the difference between our own data and the work of Cranston *et al.* First, the discrepancy may result from different levels of environmental insult. However, our colony is not maintained under barrier conditions and we therefore consider this unlikely. Second, this difference may arise through the use of different genetic backgrounds. Indeed, we have previously documented the strain dependency of *p53*-related anencephaly[6]. Against this possibility argues the fact that both groups of mice were generated from outbred crosses derived from a mixture of mouse strains (our animals segregate for 129/Ola, Balb-c and SWR genomes) and further, that our previous analysis showed different outcrossed strains to possess similar levels of *p53*-related embryonic death[6]. Notwithstanding these observations, it remains possible that the observed *Msh2*-related death is strain dependent, and we are currently carrying out appropriate backcrosses to address this point. Third, it is possible that the phenotype observed by Cranston *et al.* is arising as a consequence of a second mutation which is linked to one or other of the targeted alleles. The likelihood of such a linked mutation would perhaps be increased if either of these cohorts had been derived from ES cells engineered over an extended period *in vitro* to carry multiple mutations, but this was not the case[1–5]. Finally, it is possible that the targetted events differ in some way, either at the targetted locus itself or by the influence of the targeted locus upon neighbouring genes. Although we cannot at present confirm or refute any of the above explanations, it is clear from our data that, at the very least, the reported female embryonic lethality associated with *Msh2* and *p53* deficiency is not fully penetrant.

**Acknowledgements**

*We thank H. te Riele for supply of mice. A.R.C. is a Royal Society University Research Fellow.*

**Neil J. Toft, Mark J. Arends, Andrew H. Wyllie & Alan R. Clarke**

*Cancer Research Campaign Laboratories, Department of Pathology, University Medical School, Edinburgh, EH8 9AG, UK. Correspondence should be addressed to A.R.C.*

1. Cranston, A. *et al. Nature Genet.* **17**, 114–118 (1997).
2. de Wind, N. *et al. Cell* **82**, 321–330 (1995).
3. Clarke, A.R. *et al. Nature* **362**, 849–852 (1993).
4. Donehower, L.A. *et al. Nature* **356**, 215–221(1992).
5. Reitmair, A.H. *et al. Nature Genet.* **11**, 64–69 (1995).
6. Armstrong, J.F., Kaufman, M.H., Harrison, D.J. & Clarke A.R. *Curr. Biol.* **5**, 931–936 (1996).